

Aus der Klinik für Allgemeine, Unfall- und Wiederherstellungschirurgie

Klinik der Universität München

Direktor: Prof. Dr. med. Wolfgang Böcker

Experimentelle Chirurgie und Regenerative Medizin

Prof. Dr. med. Matthias Schieker

A platform for oxygen-controlled cultivation and investigation of 3-dimensional cell cultures for bone tissue engineering

Dissertation

zum Erwerb des Doktorgrades der Humanbiologie

an der Medizinischen Fakultät der

Ludwig-Maximilians-Universität zu München

vorgelegt von

Jakob Schmid

aus

Tübingen

2020

Mit Genehmigung der Medizinischen Fakultät der Universität München

Berichterstatter: Prof. Dr. med. Matthias Schieker

Mitberichterstatter: Prof. Dr. med. Peter Müller

PD Dr. med. Jörg Hausdorf

Prof. Dr. med. Andreas Dendorfer

Mitbetreuung durch den

promovierten Mitarbeiter: Prof. Dr. Robert Huber

Dekan: Prof. Dr. med. dent. Reinhard Hickel

Tag der mündlichen Prüfung: 27.07.2020

Das schönste Glück des denkenden Menschen ist,
das Erforschliche erforscht zu haben und das
Unerforschliche ruhig zu verehren

Johann Wolfgang von Goethe

Für Stefanie

Eidesstattliche Versicherung

Schmid, Jakob

Name, Vorname

Ich erkläre hiermit an Eides statt,
dass ich die vorliegende Dissertation mit dem Thema

**„A platform for oxygen-controlled cultivation and investigation of
3-dimensional cell cultures for bone tissue engineering“**

selbstständig verfasst, mich außer der angegebenen keiner weiteren Hilfsmittel bedient und alle Erkenntnisse, die aus dem Schrifttum ganz oder annähernd übernommen sind, als solche kenntlich gemacht und nach ihrer Herkunft und Bezeichnung der Fundstelle einzeln nachgewiesen habe.

Ich erkläre des Weiteren, dass die hier vorgelegte Dissertation nicht in gleicher oder ähnlicher Form bei einer anderen Stelle zur Erlangung eines akademischen Grades eingereicht wurde.

München, 29.07.2020

Ort, Datum

Jakob Schmid

Unterschrift

Table of contents

| | |
|---|------------------------------------|
| TABLE OF CONTENTS | I |
| ABBREVIATIONS..... | II |
| LIST OF PUBLICATIONS | III |
| 1. INTRODUCTION | 1 |
| 1.1. BONE TISSUE ENGINEERING..... | 2 |
| 1.1.1. ARTIFICIAL SCAFFOLDS FOR BONE TISSUE ENGINEERING | 2 |
| 1.1.2. SHEET-BASED SCAFFOLDS FOR BONE TISSUE ENGINEERING | 4 |
| 1.2. IMPACT OF OXYGEN CONCENTRATION ON BONE TISSUE ENGINEERING..... | 5 |
| 1.3. BIOREACTOR SYSTEMS FOR BONE TISSUE ENGINEERING | 6 |
| 1.4. AIMS OF THE THESIS | 10 |
| 1.5. OWN CONTRIBUTION TO THIS PROJECT | 11 |
| 2. SUMMARY | 12 |
| 3. ZUSAMMENFASSUNG | 16 |
| 4. BIBLIOGRAPHY | 21 |
| PAPER I | 30 |
| PAPER II..... | 42 |
| ACKNOWLEDGMENT | 54 |
| CURRICULUM VITAE | FEHLER! TEXTMARKE NICHT DEFINIERT. |

Abbreviations

| | |
|---------------|-----------------------------------|
| μL | Microliter |
| 3D | Three-dimensional |
| BMP | Bone morphogenetic protein |
| BTE | Bone tissue engineering |
| CFD | Computational fluid dynamics |
| CS | Cell sheet |
| CST | Compressive strength |
| ECM | Extracellular matrix |
| FDM | Fused deposition modeling |
| HA | Hydroxyapatite |
| HIF | Hypoxia-inducible factor |
| hMSC | Human mesenchymal stem cell |
| min | Minute |
| OC | Oxygen concentration |
| PCL | Polycaprolactone |
| PGA | Polyglycolic acid |
| PLA | Polylactic acid |
| $p\text{O}_2$ | Dissolved oxygen partial pressure |
| SSC | Sheet-based scaffold |
| SL | Stereolithography |
| TCP | Tricalcium phosphate |
| TE | Tissue engineering |
| YM | Young's modulus |

List of publications

This thesis is based on the following publications:

- 1 - *A Perfusion Bioreactor System for Cell Seeding and Oxygen-Controlled Cultivation of Three-Dimensional Cell Cultures*

Jakob Schmid, Sascha Schwarz, Robert Meier-Staude, Stefanie Sudhop, Hauke Clausen-Schaumann, Matthias Schieker, and Robert Huber

Tissue Eng Part C Methods (2018), doi: 10.1089/ten.TEC.2018.0204

- 2 - *A laser-cutting based manufacturing process for the generation of 3-D scaffolds for tissue engineering using Polycaprolactone/Hydroxyapatite composite polymer*

Jakob Schmid, Sascha Schwarz, Martina Fischer, Stefanie Sudhop, Hauke Clausen-Schaumann, Matthias Schieker, and Robert Huber

Journal of Tissue Engineering (2019), doi: 10.1177/2041731419859157

1. Introduction

Tissue engineering (TE) – the generation of artificial tissue, tailored to the specific need of a patient – has a high potential to successfully treat a variety of defects, irrespective of whether they are caused by trauma, organ failure, congenital malformations or tumors. By using artificial tissue, damaged tissue can be restored, replaced or improved in its function, without taking the risk of immunological rejection [1, 2, 3, 4].

The general principle of manufacturing artificial tissue is based on the application of autologous stem cells. The cells are extracted from a patient, multiplied and seeded on a biocompatible support structure, which provides a structural template. Subsequently, the seeded constructs are cultivated *in vitro*. During the cultivation, a functional tissue construct is created by differentiating the seeded cells to the desired cell type. Thereafter, the manufactured tissue construct is ready for implantation (Fig. 1).

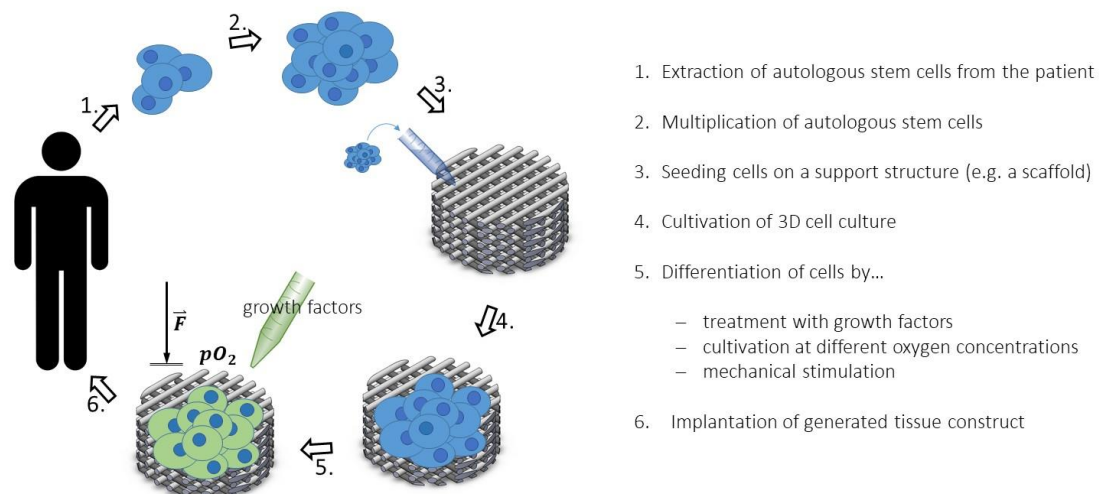


Figure 1: Principle of tissue engineering

Scheme describing the general principle of tissue engineering approaches. Stem cells (blue) are isolated from a patient, multiplied and subsequently cultivated on a support structure. Stems cells are differentiated to functional tissue cells (green). Afterward, the generated tissue construct is implanted into the patient.

To effectively create functional tissue, stem cells are commonly treated with growth factors and cytokines [2, 5, 6]. However, to make the whole biological potential of the cells available, the physiologic milieu, in which stem cells differentiate to the desired cell-type *in vivo*, has to be mimicked as well as possible [7]. Accordingly, all environmental factors, which may affect cell differentiation must be considered in this biomimetic approach. Consequently, a cell culture has to be provided, for instance, with the proper oxygen concentration [8, 9, 10], mechanical [11, 12] or electrical [13] stimuli. Also, the support structure on which the cells are growing has to be manufactured according to the mechanical properties of the engineered tissue.

1.1. Bone tissue engineering

The tissue engineering of bone (BTE) aims to provide substitute materials for the treatment of bone defects. To generate an artificial bone graft, human mesenchymal stem cells (hMSCs) or other osteoblast progenitor cells are seeded on biocompatible support structures and differentiated to osteoblasts.

In contrast to tissue engineering of soft tissues, where hydrogels are most commonly used, solid scaffolds are more beneficial for BTE approaches, since they provide mechanical stability and an interconnecting pore structure, which is required for cell infiltration [7, 14]. The differentiation of hMSCs to osteoblasts is performed by treating the cells with cytokines and growth factors such as bone morphogenetic proteins (BMPs) [1, 15, 16, 17]. To provide a biomimetic environment, to efficiently create a functional bone graft, the application of mechanical stimuli [18, 19], as well as the cultivation at proper oxygen concentrations [20] have also to be considered.

1.1.1. Artificial scaffolds for bone tissue engineering

The current gold standard for the treatment of traumatic bone injuries is the use of bone substitutes harvested from the patient's body (autografts) or a donor (allografts). Since these implants are essentially healthy bone, they meet all biological requirements for a bone substitute: viable osteogenic bone cells, an osteoconductive matrix for bone cell attachment, osteoinductive factors, biocompatibility, and mechanical stability. However, both methods have major drawbacks: harvesting an autograft requires a second operation and may result in donor-site morbidity. If allografts are used, there is a risk of disease transmission. [14, 21, 22]

An alternative to auto- or allografts is the use of natural scaffolds such as xenogenic decellularized bone grafts (e.g. bovine femur spongiosa) as scaffolds, which can be seeded with osteoblast progenitor cells to generate a bone tissue equivalent. However, xenogenic materials inherit the risk of immune rejection and pathogen transfer [23, 24].

The use of artificial scaffolds can circumvent these drawbacks. However, several aspects must be considered to create a scaffold, which meets the biological requirements and provides a biomimetic environment:

Biocompatibility:

Cells should adhere and proliferate on the scaffold and should maintain their *in vivo* cellular activity. Furthermore, the scaffold's material should not trigger inflammatory reactions or release toxic substances. [14, 25, 26]

Osteoconductivity:

Cells growing on the scaffold should produce their own extracellular matrix (ECM), to allow for bone cell migration and new bone cell attachment [27, 28].

Osteoinductivity:

The scaffold should allow for the recruitment of stem cells and other progenitor cells and induce the differentiation to osteogenic cells [27, 28].

Mechanical stability:

The scaffold should provide mechanical support and should cope with mechanical loading *in vivo* at the site of implantation. This is a major issue since both Young's modulus (YM) and compressive strength (CST) vary considerably when cortical bone and cancellous bone are compared. While the YM for cortical bone is 15 – 20 GPa, the YM of cancellous bone is significantly lower at 0.1 – 2 GPa. The CST of cortical bone is at 100 – 200 MPa, the CST of cancellous bone is at 2 – 20 MPa, respectively. Consequently, the mechanical properties of scaffolds have to be optimized with regard to the site of implantation. [14, 26, 28]

Pore size and porosity:

For a scaffold for bone tissue engineering an interconnecting pore network with sufficient pore sizes is required, since both affect the nutrient transfer, cell migration, and angiogenesis. In closed pore structures, the nutrient transfer is significantly reduced. Thus, cells will not migrate into closed pores, resulting in cell-free structures and a less viable engineered tissue. This is also the case if pore diameters are significantly smaller than 100 μm . For optimum bone ingrowth, pore diameters within the range of 250 – 300 μm were found to yield the best results. It must be taken into consideration that if pores are significantly larger, the mechanical stability of the scaffold may be impaired. However, the main factor affecting the mechanical stability of a scaffold is the overall porosity. [14, 21, 26, 29]

Degradation *in vivo*:

To fully restore the function of a defective bone, the foreign scaffold material of the tissue-engineered bone must be replaced by host bone tissue. Artificial scaffold materials cannot be assimilated in the natural bone remodeling cycle. Consequently, the scaffold must degrade *in vivo*, so that space is provided in which new bone tissue can grow. These degradation processes, whether driven by macromolecular degradation or hydrolysis, should preferably occur at controllable resorption rates between 3 – 9 months. Thereby, degradation behavior can be adapted to different applications. [14, 25, 26, 30, 31]

Apart from pore size and porosity, which are dependent on the design and the manufacturing technique, these requirements are mainly a function of the processed material. Consequently, several biomaterials have been researched for their use in bone tissue engineering in recent years.

Synthetic polymers:

Because of their excellent properties in regard of degradability, biocompatibility, and mechanical stability, synthetic polymer materials such as polylactic acid (PLA), polyglycolic acid (PGA) and polycaprolactone (PCL) have been widely used for BTE applications. Out of these polymers, PCL is the most commonly used material. PCL offers both osteoconductivity and osteoinductivity [25, 26]. Furthermore, its thermoplastic properties and its solubility in common organic solvents make it easily processable and accessible for up-to-date rapid prototyping manufacturing techniques [32, 33, 34]. Like other synthetic polymers, PCL degrades *in vivo* by hydrolysis, with degradation times of approximately one year, which is significantly slower than PLA and PGA. Consequently, PCL maintains its mechanical stability over a longer period of time [21]. However, the degradation of synthetic polymers may result in the release of acidic by-products, which locally creates an acidic environment if by-products are not eliminated fast enough. Naturally, this can result in tissue responses such as inflammatory reactions [14, 25, 35, 36, 37].

Bioceramics:

Bioceramics such as hydroxyapatite (HA) or tricalcium phosphate (TCP) can be used as an alternative to synthetic polymers. Since HA is of the same chemical composition of the inorganic phase of natural bone, it naturally provides both osteoconductivity and osteoinductivity [38, 39]. Compared to synthetic polymers, bioceramics offer superior mechanical stability with regard to CST. However, the CST of ceramic scaffolds can exceed the CST of natural bone, which can result in stress shielding at the implantation site [40]. Also, the brittleness of ceramic scaffolds results in an inferior fracture toughness, which carries the risk of failure if loading limits are reached. Consequently, ceramic scaffolds are not suitable for load-bearing applications [21, 25, 41].

Composite materials:

To minimize the drawbacks of synthetic polymers and bioceramics while maintaining their advantageous properties, polymers and bioceramics can be combined in a polymer-ceramic composite material. Consequently, composites can offer both the fracture toughness of a polymer and the compressive strength of the bioceramic, while offering great osteoconductivity and osteoinductivity, thus creating a matrix with mechanical and biological properties close to natural bone [25, 42, 43]. Furthermore, the acidification of the environment by by-products of the degradation of synthetic polymers can be buffered by basic resorption products of bioceramics such as HA [26, 44, 45].

1.1.2. Sheet-based scaffolds for bone tissue engineering

A main quality aspect of an engineered tissue is an even cell distribution of viable and functionally differentiated cells. However, for solid scaffolds, complex dynamic cell seeding methods must be applied to achieve even cell distributions and to avoid low initial cell densities [46, 47, 48, 49]. Furthermore, the assessment of cell fate after the cultivation of cells on a solid scaffold requires complex equipment [50] or cryosectioning of the scaffold and recompilation of the single images to a 3-dimensional (3D) image. Cryosectioning naturally includes fixation of the cells. As a result, the scaffolds cannot be used for further applications after analysis [49, 51]. To circumvent these drawbacks a sheet based-scaffold (SSC) concepts can be used.

The SSC concept derives from the scaffold-free cell sheet (CS) technology. This technology is based on thermo-responsive tissue culture dishes, which allow for the non-invasive harvest of confluent growing cells as monolayers with intact ECM. These monolayers can be stacked to form a scaffold-free 3D tissue equivalent [52, 53, 54, 55]. By using this approach, the problem of creating an engineered tissue with uniform cell distribution is addressed. Furthermore, the analysis of cell fate is facilitated, since no solid structures impede imaging even in deeper layers [53, 56]. However, the lack of solid structures results in inferior mechanical stability. Thus, the application of CS in BTE is limited to non-load-bearing, small bone defects [57]. However, cell sheets can be cultivated on solid scaffold structures, to generate a mechanical stable engineered bone [58, 59].

To provide mechanical stability, while maintaining the advantages of the CS technology, sheet-based scaffold (SSC) concepts were developed in recent years. These concepts are based on the manufacturing of single solid sheets, which are inoculated and subsequently stacked to form a 3D-cell culture (Fig. 2) [60, 61, 62].

SSCs offer the opportunity to create solid scaffolds with even cell distributions since the distribution of cells can be assessed on every single sheet prior to assembling. Also, the analysis of cell fate is

facilitated, since the SSC can be disassembled after cultivation. Accordingly, the 3D cell culture can be analyzed sheet by sheet. Furthermore, it is possible to create complex engineered tissues, which contain more than one cell type in defined areas, when sheets inoculated with different cell-types are stacked or combined with hydrogel layers [63, 64].

The manufacturing of current SSCs is mostly based on electrospinning of composite materials. However, electrospinning requires complex manufacturing setups. Also, the pore size of the manufactured grafts cannot be controlled easily and is limited to smaller pore sizes [65, 66]. Thus, cell migration can be lowered [60]. Also, the fine structures of electrospun grafts can result in inferior mechanical stability [65]. Both can hamper the generation of functional bone tissue equivalents significantly.

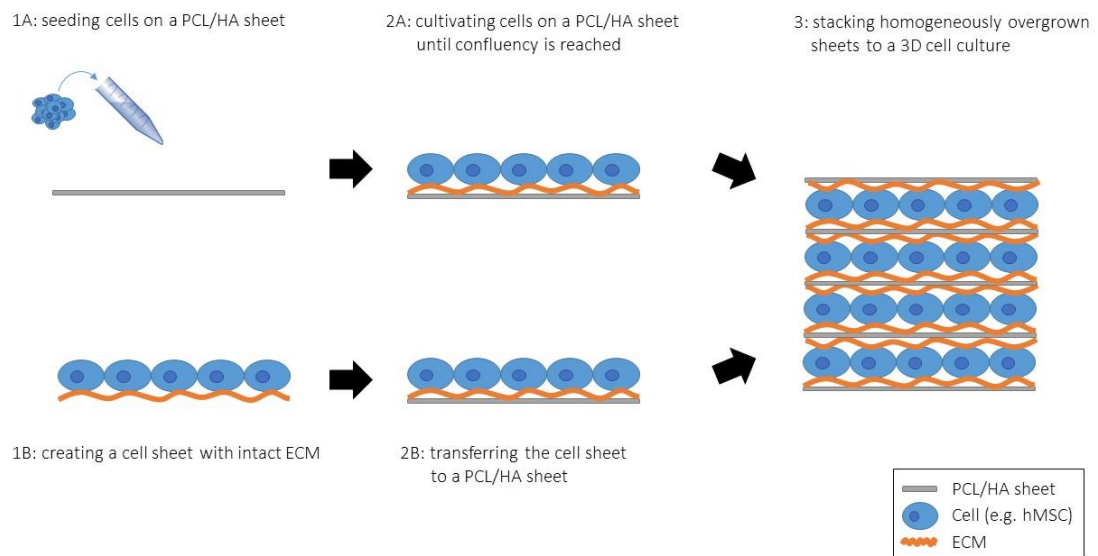


Figure 2: Sheet-based scaffold concept

The principle of sheet-based scaffold concepts, shown exemplarily for sheets manufactured of a PCL/HA composite material: Option A (1A, 2A): A cell suspension is seeded on a single PCL/HA sheet and cultivated until the sheet is homogeneously overgrown. Option B (1B, 2B): A cell sheet with intact ECM is created and transferred to a PCL/HA sheet. 3: Homogeneously overgrown sheets are stacked to a 3D cell culture.

1.2. Impact of oxygen concentration on bone tissue engineering

The generation of a biomimetic environment is of crucial importance for successful tissue engineering. An important factor, which must be considered for this approach, is the oxygen concentration (OC). Cells have to be supplied with sufficient levels of oxygen, since oxygen is one of the most critical parameters for cell survival. However, the OC does affect not only cell survival, but also cell differentiation [20, 67].

In vivo, cells are supplied with oxygen via both convection through the vascular network and diffusion. Since the diffusion of oxygen in tissue is limited, the distance between cells and capillaries rarely exceeds 200 μm [68, 69]. In native bone, a shortage of oxygen results in the accumulation of hypoxia-inducible factors (HIFs) in the cells. Among other things, these factors promote

angiogenesis by inducing the expression of the vascular endothelial growth factor, which results in neovascularization and thus the retrieval of a sufficient oxygen supply [20, 70].

However, HIFs also affect the differentiation potential of osteogenic precursor cells such as hMSCs. If hMSCs are exposed to hypoxic conditions, and HIFs accumulate within the cells, their continuance in the undifferentiated state is highly promoted [20, 67, 71, 72]. This is due to the impact of HIFs on the expression level of many genes, including pluripotency-related genes like the Yamanaka factors SOX2, OCT3/4, KLF4 and c-MYC, and other stemness-related transcription factors [67, 73, 74]. However, if normoxic conditions are restored, HIFs such as HIF-1 are inactivated by oxygen-dependent degradation, and the differentiation potential of the stem cells is restored. This demonstrates the relationship between sufficient supply with oxygen and osteogenesis [75, 76]. Consequently, hypoxic conditions must be avoided in a tissue engineering graft if the differentiation of hMSCs to functional osteocytes is desired.

Static cultivation methods are commonly used in conventional tissue engineering approaches. In doing so, the tissue-engineered graft is immersed in culture medium. Naturally, in a static cultivation setup, oxygen transport is solely dependent on passive diffusion. Due to the oxygen consumption of cells growing on the surface of a 3D-cell culture, and due to the limited oxygen diffusion, the OC will decline from the surface to the center of the 3D-cell culture. These oxygen gradients can possibly result in a hypoxic environment in the center of the tissue engineered graft [20, 77, 78]. Consequently, the size of a 3D-cell culture is highly limited for static cultivation approaches, if hypoxic conditions are to be avoided.

However, the limitation of size and the generation of a hypoxic environment can be circumvented by cultivating the engineered tissue under dynamic conditions using a bioreactor system [79, 80, 81].

1.3. Bioreactor systems for bone tissue engineering

In static cultivation, poor mass transport of oxygen, nutrients and waste products can result in insufficient nutrient supply and in the generation of an unfavorable environment for both cell survival and differentiation [20, 82, 83]. Furthermore, static conditions do not represent *in vivo* conditions. Consequently, a bioreactor system must be used for the manufacturing of native-like tissue, since it can provide a flow of cell culture media through a porous 3D-cell culture, in order to mimic the *in vivo* scenario of nutrient transport through blood vessels. In doing so, bioreactor systems cope with the limitations of static cultivation by improving the supply with nutrients and oxygen significantly [80, 83, 84]. Furthermore, bioreactor systems can be used for dynamic cell seeding procedures in order to facilitate the generation of a homogeneous initial cell distribution within a 3D-cell culture [85, 86, 87]. Besides the presence of viable and functional cells, even cell distributions are crucial for uniform tissue generation and thus critical for the quality of engineered tissue equivalents [5, 88].

To provide proper mass transport, several bioreactor systems have been developed in recent years [89, 90, 91, 92, 93]. Even though all of these bioreactor systems mitigate diffusional limitations, perfusion bioreactor systems (Fig. 3) have the highest potential to provide optimal nutrient and oxygen supply for the cultivation of 3D-cell cultures [81, 94, 95, 96]. Furthermore, perfusion bioreactors can be used to stimulate cells mechanically. By perfusing a 3D-cell culture, laminar shear stress is applied to the cultivated cells, while the amount of shear stress can be adjusted and

controlled by perfusing the 3D-cell culture at different flow velocities [19, 97]. This is a critical factor to be considered in BTE applications since the application of mechanical forces such as laminar shear stress is known to affect the differentiation behavior of hMSCs [19, 31, 98].

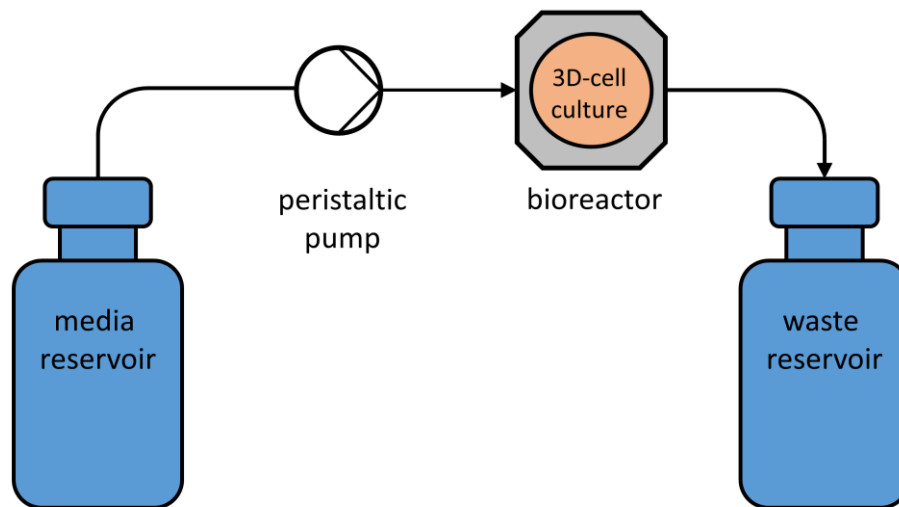


Figure 3: Schematic build of a perfusion bioreactor system

The bioreactor and thus the inserted 3D cell culture is directly perfused by culture medium with the help of a pump system (e.g. a peristaltic pump). Consequently, improved mass transport and mechanical stimulation of the cells due to laminar shear forces are provided.

Conventional bioreactors for suspension cell culture (e.g. stirred tank bioreactors) naturally provide the possibility to monitor and control crucial physiochemical conditions such as dissolved oxygen (pO_2) or pH [99]. However, this is not the case for available perfusion bioreactor systems for 3D-cell cultures. While this may not be critical in case of pH – continuous perfusion and chemical buffering of cell culture media avoid pH shifts, due to metabolic waste products [79] – the lack of pO_2 measurement [91, 92, 93] and/or control instrumentation [100, 101] is a crucial drawback of currently available bioreactor systems for 3D-cell culture [102, 103].

A bioreactor system with integrated pO_2 measurement instrumentation and control offers the possibility for the investigation of cell fate in an oxygen controlled environment, to determine optimal oxygen concentrations for different applications. Furthermore, the production of implants for clinical use in an oxygen controlled environment could allow for the production of homogeneously overgrown and highly viable tissue equivalents [104]. This is because optimal oxygen concentrations for cell growth and differentiation can be granted throughout the whole cultivation period. Also, the oxygen signals can be processed (e.g. calculation of oxygen consumption rates) and used for on-line quality assessments [105, 106].

Design considerations for the development of bioreactor systems for tissue engineering in research and clinical applications:

Bioreactor systems are a key technology for the investigation and manufacturing of engineered tissues *in vitro* since they offer the possibility to control environmental parameters and allow for automated and thus reproducible cultivation processes. For the development of a functional bioreactor system for tissue engineering approaches, whether for research or clinical applications,

the system must be designed to be safe, versatile, easy to use, to offer a biomimetic environment with real-time sensing and to operate reproducibly in an automated way. Furthermore, parallelization and compactness in size need to be considered (Table 1) [5, 83, 96, 98, 102, 107].

Bioreactor safety is directly linked to sterile long-term operation. Consequently, the bioreactor should be manufactured using a bio-inert and non-corrosive material which can be sterilized by autoclaving (re-usable devices) or by gamma-sterilization (single-use devices), to guarantee sterility. Also, a tight sealing mechanism is required to prevent leakage or contamination [5, 83, 96, 98].

For clinical applications, versatility is mainly necessary in terms of the shape and size of a 3D-cell culture. If the bioreactor is adjustable to differently shaped 3D-cell cultures, an artificial bone tissue could, for instance, be manufactured with the exact shape of a patient's defect, to further comply with the needs of personalized medicine. However, for research purposes, bioreactor systems which are also capable of cultivating different cell types are beneficial to investigate a multitude of different 3D-cell cultures [83, 102, 107].

The generation of a biomimetic environment is naturally the most crucial function of a bioreactor system. Therefore, mechanical stimuli (e.g. laminar shear forces), as well as biochemical factors such as proper oxygen concentrations, must be provided and maintained during cultivation. Furthermore, the bioreactor should provide even flow distribution, so that local gradients (e.g. of nutrients or shear forces) are avoided [5, 83, 102].

Computational fluid dynamics (CFD) can be used to simulate streamlines within a bioreactor, and to optimize the geometry of the cultivation chamber to provide even flow distribution [19, 81]. However, it must be taken into consideration that these simulations must be performed for each 3D-cell culture individually since every scaffold has an individual permeability (dependent on pore size, porosity, and size) [108, 109] which affects the flow distribution within the tissue-engineered graft. Furthermore, CFD can be used to simulate shear forces and shear force distributions [108, 110] and is thus a very useful tool for the development and optimization of bioreactors for tissue engineering.

To observe and maintain parameters like pO_2 or pH at the desired level, the integration of measurement instrumentation is required. For the measurement of pO_2 and pH, the use of fluorescence-based, non-invasive sensors is beneficial, since they circumvent the drawbacks of direct, invasive electrochemical probes (e.g. risk of contamination, analyte-consumption) [111, 112]. Furthermore, acquired data of oxygen probes can be used to evaluate the viability – and thus the quality – of a manufactured tissue, since oxygen consumption can be directly linked to metabolic activity and cell viability [105, 106]. Thus, the assessment of engineered tissue, e.g. by (cryo)sectioning and staining may be circumvented, which minimizes the risk of contamination or cell death during the assessment period.

To keep relevant parameters at an optimal level, the measurement instrumentation must be accompanied by an automated feedback mechanism, since automatization allows for higher reproducibility, better controllability and overall higher efficiency of the bioreactor system, which is a major criterion for clinical applications [5, 79, 83, 113].

Another factor of ever-increasing importance is the possibility for multiplexing. A parallel set-up allows for high experimental throughput, which provides faster results, as well as time and cost savings. To investigate different parameters in a single run, or to display the variation between equally treated samples, the bioreactors of a parallelized system should operate independently.

This is especially the case if environmental parameters are to be controlled since this requires individual adjustments for every single bioreactor [5, 83, 113].

Having a bench-top system allows for a system which can be placed in a commercially available incubator system for temperature and CO₂ atmosphere control [19, 81, 83]. Compact systems are also logistically easier to handle. This is especially important for clinical applications. The gold standard for tissue transport today is transportation at low temperatures [114], even though the properties of e.g. hMSCs can be impaired by this freeze-thaw process [115]. Also, cells are cut off from nutrient and oxygen supply during the transportation period, resulting in less viable implants. Consequently, bioreactor systems should not only be used for cultivation but also as transportation devices [104]. By using bioreactor systems for the transportation of engineered tissue grafts under optimal conditions, implants of the highest quality can be provided for clinical use. Thus, for both research and clinical applications, the size of a bioreactor system must be reasonably small.

All these criteria, as well as their importance for research or clinical set-ups, are summarized in the table below (Table 1):

Table 1: Design considerations for bioreactor systems for tissue engineering (adapted from [83])

| Criteria | Key elements | Purpose | Research | Clinical |
|-------------------------------|--|---|----------|----------|
| <i>Modeling</i> | Modeling and prediction of key parameters | Characterize microenvironment | +++ | +++ |
| <i>System set-up</i> | Selection of chamber material | Bio-inert, non-corrosive | +++ | +++ |
| | Tight sealing mechanism | Prevent leakage and contamination | +++ | +++ |
| | Versatile design | Accommodate various scaffold configurations and cell types | +++ | +++ |
| | Autoclavable/single-use accessories | Prevent contamination | + | +++ |
| <i>System size</i> | Smaller system | Save resources, logistically easier in case of transport | +++ | +++ |
| | Multiple independent-operating parallel systems | Study of multiple parameters or samples | +++ | ++ |
| | Bench-top | Easier to handle | +++ | +++ |
| <i>Flow regime</i> | Appropriate level of laminar shear stress | Increase mass transport, stimulate cells without wash off or damage | +++ | +++ |
| <i>Environmental control</i> | Control of oxygen levels, pH, temperature, gas levels, and flow rate | Maintain optimal cell growth and differentiation conditions | +++ | +++ |
| <i>Mechanical stimulation</i> | Specific mechanical stimulation of scaffold for biomimetic <i>in vitro</i> cultivation | Mimic physiological loading, control cell fate processes | +++ | +++ |
| <i>Sensors</i> | Dissolved oxygen, pH, temperature | Investigate environmental parameters | +++ | +++ |
| | Media sampling for metabolites | Understand metabolic requirements | + | +++ |
| | Media sampling for contaminations | Assess sterility of cell culture media | ++ | +++ |
| <i>Imaging</i> | Imaging facility integrated into the bioreactor chamber | Evaluation of scaffolds, cells, cell viability, tissue growth, and dynamics | + | +++ |
| <i>Feedback</i> | Sensor/imaging-based control mechanism | Maintain optimal conditions | + | +++ |

'+' indicates the level of importance in research or clinical set-ups; '+++' represents high importance

1.4. Aims of the thesis

The oxygen concentration is a key factor for cell growth and differentiation. However, the oxygen concentration is neglected in many experimental setups. Available bioreactor systems lack oxygen measurement instrumentation and/or the ability to control oxygen levels within a 3D-cell culture. Also, most parallelized setups do not provide independently operating bioreactors.

To generate a platform, which allows for the cultivation and optimization of 3D-cell cultures in an oxygen-controlled environment as well as for the facile assessment of cell fate in 3D-cell cultures, we aimed to develop:

1. A modular, parallelizable microbioreactor system, with integrated oxygen measurement instrumentation and the possibility to control the oxygen concentration in each microbioreactor individually. Furthermore, size and weight were considered.

The following working packages were defined:

- a) Design, construction, characterization, and manufacturing of a perfusion microbioreactor
 - b) Integration of measurement instrumentation
 - c) Coding of a user interface and implementation of a feedback-control mechanism
 - d) Development of a sterility concept
 - e) Proof-of-concept experiments
2. A sheet-based scaffold concept manufactured of a biocompatible, osteoinductive and osteoconductive polycaprolactone/hydroxyapatite composite material. To avoid drawbacks of electrospun SSCs, the sheet manufacturing protocol should be based on laser-cutting. The scaffold concept should allow for controllable pore size and porosity, facile generation of homogeneously overgrown scaffolds and should be able to be disassembled for facile analysis of cell fate.

The following working packages were defined:

- a) Investigation of suitable settings for the manufacturing of PLC/HA sheets by laser-cutting
- b) Determination of the accuracy and the limits of the manufacturing process
- c) Characterization of the manufactured sheets (mechanical properties, element analysis)
- d) Assessment of growth and differentiation of hMSCs growing on PCL/HA sheets
- e) Proof-of-concept experiments

1.5. Own contribution to this project

Paper I:

A Perfusion Bioreactor System for Cell Seeding and Oxygen-Controlled Cultivation of Three-Dimensional Cell Cultures

I performed the bioreactor design and optimization, except of CFD modeling. I coded the control software in LabView and optimized the control mechanism. I tested and established a functioning concept for sterilization. I conducted all the experiments and analyses. I wrote the manuscript with help from Robert Huber.

Paper II:

A Laser-Cutting based Manufacturing Process for the Generation of Three-Dimensional Scaffolds for Tissue Engineering using Polycaprolactone/Hydroxyapatite composite polymer

I performed the optimization of the laser-cutting process, cell culture experiments, image processing, and statistical analyses. Mechanical testing was performed with the help of Sascha Schwarz, SEM, and EDX with the help of Dr. Constanze Eulenkamp. I wrote the manuscript with help from Robert Huber.

2. Summary

There is an increasing need for bioreactor systems for tissue engineering applications that meet the needs of clinics. These are biomimicry, high reproducibility, safety, effectiveness, automatization, and transportability. For bone tissue engineering approaches, a biomimetic environment includes providing growth factors such as bone morphogenetic proteins and mechanical stimulation. Both can be provided by perfusion bioreactors, which mitigate diffusional limits by active mass transport. Also, the cell culture media flow provides mechanical stimulation by laminar shear forces. Furthermore, proper oxygen concentrations must be provided. However, the oxygen concentration is – even though known to be a critical factor for cell fate – neglected in most commercially available and tailor-made bioreactor systems.

In order to develop a bioreactor system which fulfils these requirements, and to facilitate the research of cell fate in bone tissue engineering approaches, we aimed to develop a functional platform consisting of an automated oxygen-controlled perfusion bioreactor system and an innovative sheet-based scaffold concept.

A parallelized perfusion microbioreactor system for automated, dynamic cell seeding and oxygen-controlled cultivation of 3D-cell cultures

The bioreactor system was developed according to the design considerations specified in section 1.3.1, to fulfill the needs of both research laboratories and clinics. To provide maximal flexibility towards the design of the bioreactor and the corresponding cultivation chamber, the bioreactor system was manufactured using the rapid manufacturing techniques fused deposition modeling (FDM) and stereolithography (SL). The processed materials (PLA for FDM, and DentalSG resin for SL) were selected according to their approval as biocompatible by the Food and Drug Administration, to avoid toxic effects on the cultivated cells. To guarantee impermeability and thus long-term contamination-free cultivation, bioreactor parts, which are in contact with fluids, were manufactured by SL.

The bioreactor consists of two main parts. The bottom part inherits the cell culture medium inlet and the cultivation chamber. The upper part inherits the cell culture medium outlet and a sensor port. The cultivation chamber for the 3D-cell culture is created by silicon casting and can be inserted into the bottom part of the bioreactor. By using silicon casting, the cultivation chamber can be adjusted to the shape of a 3D-cell culture. Consequently, the bioreactor is capable of preventing leakage flow around an inserted scaffold, regardless of its shape.

By having the medium inlet in the bottom part of the bioreactor, the medium flow is directed upwards, which facilitates bubble-free operation. This is of high importance since entrapped air bubbles can hamper the distribution of cell culture medium within the 3D-cell culture and could thus result in less viable engineered tissue grafts. Also, air bubbles are a major obstacle to reliable oxygen measurements.

CFD simulations were conducted to prove the bioreactor's capability of providing even flow velocities within an inserted spongy bone scaffold at perfusion speeds between 10 – 250 $\mu\text{L}/\text{min}$.

Even flow distributions are of high importance for homogeneous mass transportation. Furthermore, shear force gradients are avoided, thus an equal mechanical stimulation is provided for each cell growing within a 3D-cell culture.

To enable oxygen measurements, needle-type oxygen microsensors are used. When connected to the sensor port of the bioreactor, they enable the measurement of oxygen concentrations in the geometric center of the cultivated tissue-engineered graft. The oxygen concentration measurement allows for the determination of the oxygen consumption rate of the 3D-cell culture, which can indicate cell viability, growth, and differentiation status. However, the on-line interpretation of oxygen consumption rates is not integrated into the systems software yet. To minimize the risk of incorrect oxygen measurements, a PT100 thermocouple is used to determine the exact temperature of the inflowing cell culture medium, in order to compensate for temperature changes. This is of high importance since the solubility of oxygen is massively dependent on the temperature of the fluid.

To control the oxygen concentration in the bioreactor, a proportional controller was used to link the signal of the oxygen sensor to the flow rate of the peristaltic pump used for perfusion. Using the established control algorithm, the perfusion speed is increased if the oxygen concentration drops below a pre-set level. This increase in medium flow naturally increases the oxygen mass transfer towards the 3D-cell culture to compensate for the oxygen consumption of the cells. Consequently, the oxygen concentration in the geometrical center of the cultivated construct is kept at a constant level. By using the developed control algorithm, the oxygen concentration can be kept at 'set-point \pm 0.5 %' over a time period of several days. To keep shear forces at a reasonable level, the flow rate increase is capped at 250 μ L/min, while the base flow rate is at 20 μ L/min.

In order to automate the control mechanism and to facilitate the overall handling of the bioreactor system, a software program was coded using LabView. The software is based on a while loop, which performs the following operations in each iteration: 1. request and process the oxygen sensor data, 2. examine deviations between the measured oxygen concentration and the pre-set oxygen level, 3. calculate and adjust the perfusion velocity according to the control algorithm (if necessary), 4. display the current oxygen concentration and flow rate, and 5. write the acquired data to a log-file. After the cultivation process, the software provides a quality assessment report, which summarizes time periods in which the oxygen concentration dropped below the pre-set level (feature not depicted in the published paper). This is of high importance for clinical applications for cases in which surgeons want to assess the engineered tissue quality based on oxygen data prior to implantation.

An automated, dynamic cell seeding procedure was developed and incorporated in the bioreactor's software to further improve the functionality of the bioreactor system, to conduct highly reproducible experiments, and to fully automate cultivations of 3D-cell cultures. To distribute a cell solution evenly on a scaffold inside of the bioreactor, the peristaltic pump of the bioreactor system is used to perform an oscillating flow profile. The oscillating flow is followed by a short period of static incubation to allow for cell adherence. Subsequently, the oxygen-controlled dynamic cultivation procedure is started. By using the automated, dynamic cell seeding procedure, even initial cell distributions can be achieved reproducibly, which is of high importance for the generation of tissue-engineered grafts of high quality.

To provide the option of multiplexing, a peristaltic pump with four individually movable channels was used to set up the bioreactor system. Accordingly, the bioreactor system can be used with up to four independently operating bioreactors. Nevertheless, the size of the bioreactor system was kept reasonably small. Consequently, the whole system can be set up in a bench-top incubator system – which can be used for temperature control, and to set up a CO₂-atmosphere if necessary. Due to its compactness, the bioreactor system is also logistically easy to handle and therefore could offer the option of tissue transport under cultivation conditions.

The following table sums up the implemented design considerations (according to section 1.3.1.) in the developed microbioreactor system (Table 2):

Table 2: Implemented design considerations (according to section 1.3.1.) in the developed microbioreactor system

| Criteria | Key elements | Developed microbioreactor system |
|-------------------------------|--|--|
| <i>Modeling</i> | Modeling and prediction of key parameters | CFD modeling of flow distributions within a spongy bone scaffold |
| <i>System set-up</i> | Selection of chamber material | DentalSG resin, approved by FDA as biocompatible |
| | Tight sealing mechanism | Tight sealing using silicon gaskets |
| | Versatile design | Flexibility towards the shape of the 3D-cell culture, due to a silicon-casted cultivation chamber |
| <i>System size</i> | Autoclavable/single-use accessories | DentalSG resin, sterilizable by autoclaving |
| | Smaller system | Compact system, which can be set up in a bench-top incubator. System size could allow for transport under cultivation conditions |
| <i>Flow regime</i> | Multiple independent-operating parallel systems | Up to 4 independently-operating microbioreactors |
| | Appropriate level of laminar shear stress | Perfusion bioreactor provides mechanical stimulation by laminar shear forces. Flowrate is capped at 250 µL/min to keep mechanical stimulation at a reasonable level |
| <i>Environmental control</i> | Control of oxygen levels, pH, temperature, gas levels, and flow rate | Oxygen control, as well as temperature and flow rate control, are provided |
| <i>Mechanical stimulation</i> | Specific mechanical stimulation of scaffold for biomimetic <i>in vitro</i> cultivation | Mechanical stimulation is provided by the perfusion bioreactor. However, the flow rate is adjusted during the cultivation period. Thus the mechanical stimulation cannot be designated as specific |
| <i>Sensors</i> | Dissolved oxygen, pH, temperature | Oxygen and temperature sensors are provided |
| | Media sampling for metabolites | Possible but not implemented |
| | Media sampling for contaminations | Possible but not implemented |
| <i>Imaging</i> | Imaging facility integrated into the bioreactor chamber | Oxygen data can be used to calculate oxygen consumption rates, which can be linked to cell fate |
| <i>Feedback</i> | Sensor/imaging-based control mechanism | Feedback mechanism based on oxygen sensor data |

A sheet-based polycaprolactone/hydroxyapatite composite scaffold concept for facile generation of artificial bone tissue grafts and assessment of cell fate

The scaffold concept is based on the manufacturing of single sheets, which are stacked to form a scaffold with an interconnecting pore structure. The concept was developed according to the requirements of scaffolds for bone tissue engineering specified in section 1.1.1.

In order to provide osteoinductivity, osteoconductivity, appropriate mechanical properties, and processability, a PCL/HA composite material was used. To manufacture the sheets for the scaffold production, a PCL/HA foil of 200 µm thickness was produced using an aluminum mold. The foil was subsequently processed by laser-cutting.

The laser-cutting procedure was optimized to guarantee high accuracy and reproducibility. By using a continuous wave CO₂ laser at 6 W laser power, the reproducibility of the manufacturing process is very high, with variations lower than 20 µm between equal structures. However, it must be noted,

that the laser-cutting process results in deviations between the cutting template and the resulting sheet due to material removal. For a cutting process at 6 W, these deviations are about 50 μm . Laser-cutting provides very high flexibility with regards to pore size and design. The only limitations are the following: resulting structures thinner than 125 μm are not reliably stable, and the smallest possible section which can be cut in a reliable way is approximately 40 μm in diameter.

Since laser-cutting is a manufacturing technique, which has not been used for the generation of scaffolds for tissue engineering yet, the question of whether the manufacturing process alters the properties of the PCL/HA material in an unfavorable way has been the object of research. Therefore cell growth and differentiation experiments were conducted. Furthermore, element analysis was performed by SEM to investigate if residual aluminum particles can be found on the manufactured sheets. It was found that both the manufacturing, as well as the processing of the PCL/HA foil by laser-cutting does not interfere with the advantageous properties of the composite material. Aluminum particles could not be detected on the PCL/HA sheets, and both cell growth of hMSCs as well as the differentiation of hMSCs to osteoblasts were not impeded on PCL/HA materials processed by laser-cutting.

To investigate if the manufactured sheets can be used to create 3D-cell cultures of high quality, single PCL/HA sheets were inoculated with hMSCs and stacked to a scaffold consisting of 50 sheets – resulting in a cylindrical scaffold with 10 mm in diameter and height. To guarantee for sufficient oxygen and nutrient supply, the SSC was cultivated under oxygen-controlled conditions using the developed microbioreactor system. Subsequently, the scaffold was disassembled and analyzed. Due to the oxygen control, the cells grew and remained viable throughout the whole scaffold. Also, the cells intergrew between stacked sheets, building a coherent 3D-cell culture. Consequently, the developed SSC concept is suitable for the generation of functional scaffolds for BTE.

The developed sheet-based scaffold concept allows for several applications: 1. Cell seeding of single sheets individually prior to stacking to a scaffold. This way, the initial cell distribution is easier to assess and even cell distributions within the scaffold are easier to obtain. 2. Creation of hybrid 3D-cell cultures, for example by incorporating hydrogel or cell sheets in-between PCL/HA sheets. By creating hybrid 3D-cell cultures, different cell types could be introduced in a 3D-cell culture in a very controlled way. This is especially interesting for vascularization approaches. 3. The assessment of cell fate after the cultivation period is facilitated to a great extent by the sheet-based design. Scaffolds can be disassembled easily and cell distribution, viability, and differentiation status can be assessed sheet by sheet without the need for sectioning techniques.

Summarizing, the 'platform for oxygen-controlled cultivation and investigation of 3-dimensional cell cultures for bone tissue engineering' consists of a novel bioreactor system and an innovative scaffold concept. The developed platform allows for the rapid investigation and assessment of 3D-cell cultures in an oxygen-controlled environment, which is of high interest for tissue engineering laboratories. Furthermore, it facilitates the generation of tissue equivalents of high quality, while offering an on-line assessment of tissue quality by the determination of the oxygen consumption of the cultivated 3D-cell culture. Also, the compact size of the system makes it logistically easy to handle.

Ultimately, the developed platform can contribute to a faster advancement of engineering 3D-cell cultures in BTE applications for both research and clinic.

3. Zusammenfassung

Es gibt einen stetig steigenden Bedarf an Bioreaktorsystemen für verschiedene Anwendungen im *tissue engineering* (TE), welche auch den Anforderungen eines klinischen Umfelds gerecht werden. Folgende Punkte müssen dabei in Betracht gezogen werden: Eine hohe Reproduzierbarkeit, Sicherheit, Automatisierbarkeit, Transportabilität und die Bereitstellung einer biomimetischen Umgebung. Für Letzteres muss, im Fall des *tissue engineering* von Knochen (BTE), die Zellkultur mit Wachstumsfaktoren, wie beispielsweise knochenmorphogenetischen Proteinen, behandelt werden. Zusätzlich müssen die Zellen mechanisch stimuliert werden. Dies kann von Perfusions-Bioreaktoren geleistet werden. Der aktive Massentransport des Perfusions-Bioreaktors minimiert nicht nur den Einfluss von Diffusionslimits, der Flüssigkeitsstrom durch den Reaktor übt auch laminare Scherkräfte auf die Zellen aus. Darüber hinaus muss die Zellkultur mit der optimalen Sauerstoffkonzentration versorgt werden. Die meisten Bioreaktorsysteme – sowohl kommerziell verfügbare, als auch Laboraufbauten – sind jedoch nicht in der Lage Sauerstoffkonzentrationen zu messen, zu regeln oder für weitere Analysen zu prozessieren.

Um ein Kultivierungs-System zu entwickeln, welches die Anforderungen des klinischen Umfelds erfüllt und um neue Anwendungen, wie die einfache Analyse von *scaffolds* im Bereich des BTE zu ermöglichen, wurde eine funktionelle Plattform entwickelt, welche aus einem automatisierten, Sauerstoff-kontrollierten Perfusions-Bioreaktorsystem und einem innovativem *sheet*-basierten *scaffold*-Konzepts besteht.

Ein parallelisiertes Perfusions-Mikrobioreaktorsystem für die automatisierte, dynamische Besiedelung und die Sauerstoff-kontrollierte Kultivierung von 3D-Zellkulturen

Das Bioreaktorsystem wurde unter Berücksichtigung der in Kapitel 1.3.1. aufgeführten Voraussetzungen entwickelt, um sowohl die Anforderungen von forschenden Einrichtungen, als auch die Anforderungen des klinischen Umfelds zu bedienen. Um die größtmögliche Flexibilität bei der Gestaltung des Bioreaktors und dessen Kultivierungskammer zu haben, wurden die Bioreaktoren mit den 3D-Druck-Technologien Schmelzschichtung (englisch: fused deposition modeling, FDM) und Stereolithografie gefertigt. Dabei wurden ausschließlich Materialien verwendet, welche von der ‚Food & Drug Administration‘ als biokompatibel zugelassen wurden, um toxische Effekte auf die kultivierten Zellen zu vermeiden. Um das Eindringen von Flüssigkeit in die gefertigten Teile zu verhindern – und somit einen kontaminationsfreien Betrieb zu gewährleisten – wurden Teile, welche mit Flüssigkeit in Kontakt kommen, mittels Stereolithographie gefertigt.

Der entwickelte Bioreaktor besteht aus zwei Hauptkomponenten. In das Unterteil wird die Kultivierungskammer eingesetzt. Zudem befindet sich dort das Inlet für das Zellkulturmedium. Im Oberteil befindet sich entsprechend das Medien-Outlet, sowie eine Anschlussmöglichkeit für einen Sensor. Die Kultivierungskammer selbst wird aus einem 2-Komponenten-Silikon gegossen. Somit kann sie optimal auf die Geometrie der eingesetzten 3D-Zellkultur angepasst werden. Das ermöglicht die optimale Versorgung von 3D-Zellkulturen unterschiedlicher Formen, da ein Medien-Leckstrom um die eingesetzte 3D-Kultur – unabhängig von deren Form – effektiv verhindert wird.

Die gewählte Anordnung der Anschlüsse für die Medienversorgung resultiert in einem aufwärts gerichteten Fluss durch den Bioreaktor. Dieser aufwärtsgerichtete Strom transportiert Luftblasen effektiv aus der Kultivierungskammer und erleichtert so einen Luftblasen-freien Betrieb. Dies ist wichtig, um eine verlässliche Messung der Sauerstoffkonzentration in der 3D-Zellkultur zu garantieren. Zudem können eingeschlossene Luftblasen Poren in der 3D-Zellkultur blockieren. Einzelne Bereiche werden dadurch von der Versorgung abgeschnitten, was entsprechend zu Zell-freien Regionen und damit zu einem Gewebestück von minderer Qualität führt.

Ein homogenes Strömungsfeld durch eine 3D-Zellkultur gewährleistet zweierlei. Erstens, eine gleichmäßige Versorgung der gesamten Kultur mit Nährstoffen und zweitens, eine vergleichbare mechanische Stimulation aller Zellen in der Kultur. Somit ist ein homogenes Strömungsfeld ein Muss für einen funktionellen Perfusions-Bioreaktor. Mittels CFD Simulationen wurde gezeigt, dass in dem entwickelten Bioreaktor eine homogene Strömungsverteilung entsteht. Dafür wurden die Strömungsgeschwindigkeiten in einem eingesetzten Knochen-*scaffold* bei Perfusionsraten zwischen 10 und 250 $\mu\text{L}/\text{min}$ simuliert.

Die Messung von Sauerstoffkonzentrationen im geometrischen Zentrum des Bioreaktors – und damit in dem der eingesetzten 3D-Zellkultur – wird durch Sauerstoff-Nadelsensoren ermöglicht. Die Sauerstoffmessung ermöglicht auch die Bestimmung der Sauerstoffverbrauchsrate der Kultur. Diese kann genutzt werden um Zellwachstum, Viabilität und den Differenzierungsstatus der Kultur abzuschätzen. Allerdings ist die echtzeit-Auswertung der Sauerstoffverbrauchsrate noch nicht in das momentane Bioreaktorsystem implementiert. Da die Sauerstoffmessung stark temperaturabhängig ist, wurde ein PT100-Thermoelement in das System integriert. So werden Temperaturschwankungen kompensiert, und eine korrekte Messung der Sauerstoffkonzentration garantiert.

Für die Regelung der Sauerstoffkonzentration in der 3D-Zellkultur wurde ein Proportional-Regler genutzt und für den Bioreaktor optimiert. Dieser Proportional-Regler fungiert als Rückkopplung zwischen der gemessenen Sauerstoffkonzentration und der Perfusionsrate des Bioreaktors. Entsprechend des entwickelten Algorithmus wird somit der Massentransport von Sauerstoff in die 3D-Kultur angepasst, um einer zunehmenden Sauerstoffverbrauchsrate entgegen zu wirken. So kann die Sauerstoffkonzentration im geometrischen Zentrum der 3D-Zellkultur über mehrere Tage konstant auf einem voreingestellten Level ($\pm 0.5\%$) gehalten werden. Um die wirkenden Scherkräfte unter einem kritischen Level zu halten, wurde die maximale Perfusionsrate auf 250 $\mu\text{L}/\text{min}$ festgesetzt, wobei die minimale Flussrate 20 $\mu\text{L}/\text{min}$ beträgt.

Zur Automatisierung des Regelalgorithmus, wurde dieser in eine Software eingebettet, welche in LabView programmiert wurde. Die Software basiert auf eine *while*-Schleife welche in jeder Iteration die folgenden Aufgaben ausführt: 1. Anfordern und Prozessieren der Daten des Sauerstoffsensors, 2. Bestimmen der Abweichung zwischen Sollwert und Istwert der Sauerstoffkonzentration, 3. Berechnung der notwendigen Perfusionsrate und (wenn nötig) Anpassen der Perfusionsrate entsprechend des Regelalgorithmus, 4. Darstellung der Prozessvariablen Sauerstoffkonzentration, Sauerstoffverbrauchsrate und Perfusionsrate im Verlauf der Kultivierung in einem Diagramm, 5. Schreiben der Prozessvariablen in ein Logbuch zur Dokumentation und Analyse der Daten. Nach der Kultivierung kann zudem ein Bericht abgerufen werden. Dieser Bericht führt Zeitintervalle, in welchen die Sauerstoffkonzentration unter den Sollwert gefallen ist (nicht in der Publikation

beschrieben). Diese Funktion ermöglicht es einem Chirurgen die Qualität des erhaltenen Gewebestücks vor der Implantation anhand der Sauerstoffdaten abzuschätzen.

Neben der Sauerstoffmessung wurde auch ein Verfahren zur dynamischen Besiedelung von *scaffolds* in dem Bioreaktor entwickelt. Hierfür wird die Peristaltikpumpe – welche im Normalfall für die Perfusion des Bioreaktors zuständig ist – genutzt, um einen oszillierenden Fluss an den Bioreaktor anzulegen. Über dieses Flussprofil wird eine Zellkultur-Lösung gleichmäßig auf einem *scaffold* verteilt. Anschließend wird die Kultur für eine kurze Zeit statisch inkubiert, damit die Zellen an das *scaffold* adhären können. Um die Funktionalität des Bioreaktorsystems zu erhöhen, die Reproduzierbarkeit zu steigern und um vollautomatisierte Kultivierungsprozesse zu ermöglichen, wurde dieses Verfahren in die Software des Bioreaktorsystems integriert. So können automatisiert homogene Zellverteilungen erreicht werden, was von großer Bedeutung für die Herstellung von hochqualitativen Gewebestücken ist.

Um mehrere Bioreaktoren in einem parallelisierten Setup betreiben zu können wurde eine Peristaltikpumpe mit vier unabhängigen Kanälen verwendet. Entsprechend können bis zu vier individuell regelbare Bioreaktoren gleichzeitig genutzt werden. Dabei wurde darauf geachtet, auch das parallelisierte Setup möglichst kompakt zu halten. So kann das gesamte System in einem handelsüblichen Tisch-Inkubator betrieben werden, wobei der Inkubator zur Temperaturregelung – und wenn nötig zur Einregelung einer CO₂-Atmosphäre – genutzt wird. Aufgrund seiner kompakten Maße könnte das System auch als Option für den Transport von Gewebe unter Kultivierungsbedingungen in Frage kommen.

Die folgende Tabelle fasst zusammen, wie die Anforderungen an ein Bioreaktorsystem für TE (entsprechend Kapitel 1.3.1.) in dem neu entwickelten System umgesetzt wurden (Tabelle 3):

Tabelle 3: Umgesetzte Anforderungen (entsprechend Kapitel 1.3.1) in dem neu entwickelten Bioreaktorsystem

| Anforderung | Hauptelemente | Umsetzung im entwickelten Bioreaktorsystem |
|--------------------------------|--|---|
| <i>Modellierung</i> | Modellierung von zentralen Merkmalen | CFD-Simulation der Verteilung der Fließgeschwindigkeiten in einem Knochen- <i>scaffold</i> |
| <i>Aufbau des Systems</i> | Material Dichtungsmechanismus Flexibles Design | DentalSG-Harz, von der FDA als biokompatibel zugelassen Dichtungsringe aus Silikon garantieren dichten Verschluss Fertigung der Kultivierungskammer aus 2-Komponenten-Silikon ermöglicht hohe Flexibilität bezüglich der Form der 3D-Zellkultur |
| | Autoklavierbar / Einwegartikel | DentalSG-Harz ist autoklavierbar |
| <i>Größe des Systems</i> | Möglichst klein | Kompaktes System, welches in einem Tisch-Inkubator aufgebaut werden kann. Größe ermöglicht den einfachen Transport des Systems |
| | Parallelisierter Aufbau | Bis zu vier Bioreaktoren, welche unabhängig voneinander arbeiten |
| <i>Strömungsform</i> | Mechanische Stimulation durch laminare Scherkräfte | Über den angelegten Fluss ist der Perfusionsbioreaktor in der Lage Zellen mechanisch zu stimulieren. Um die Scherkräfte unter einem kritischen Level zu halten ist die Flussrate auf maximal 250 µL/min beschränkt. |
| <i>Kultivierungsparameter</i> | Kontrolle von Sauerstoffkonzentration, pH, Temperatur und Flussrate | Die Sauerstoffkonzentration, die Temperatur und die Flussrate können im Bioreaktor kontrolliert werden |
| <i>Mechanische Stimulation</i> | Spezifische mechanische Stimulation der 3D-Zellkultur für biomimetische <i>in vitro</i> Kultivierung | Der Perfusionsbioreaktor stimuliert die Zellen durch den angelegten Fluss. Die Intensität der Stimulation variiert über den Verlauf der Kultivierung, da die Flussrate im Rahmen der Sauerstoffregelung angepasst wird |
| <i>Sensorik</i> | Sauerstoffkonzentration, pH, Temperatur Medienbeprobung | Sauerstoff- und Temperatur-Sensoren sind integriert Möglich, aber nicht umgesetzt |
| <i>Echtzeit-Analyse</i> | Echtzeit-Analyse der 3D-Zellkultur durch Sensorik oder bildgebende Verfahren | Sauerstoffmessung kann genutzt werden, um die Sauerstoffverbrauchsrate zu berechnen. Diese korreliert mit dem Zustand der Zellkultur (Viabilität,...) |
| <i>Regelung</i> | Sensor-basierte Regelung der Kultur | Anpassung der Perfusionsrate basierend auf die Sauerstoffmessung |

Ein *sheet*-basiertes Polycaprolacton/Hydroxyapatit *scaffold*-Konzept für die vereinfachte Herstellung und Untersuchung von künstlichem Knochengewebe

Das *scaffold*-Konzept basiert auf die Herstellung von einzelnen, flachen *sheets*. Diese werden aufeinandergestapelt, um ein dreidimensionales *scaffold* mit einer zusammenhängenden Porenstruktur zu generieren. Bei der Entwicklung des Konzepts wurden die in Kapitel 1.1.1. aufgeführten Anforderungen an ein funktionelles *scaffold* für die Herstellung von künstlichem Knochengewebe berücksichtigt.

Bei der Wahl des Materials wurde auf ein Kompositmaterial aus Polycaprolacton und Hydroxyapatit gesetzt, da dieses Material sowohl osteokonduktiv, als auch osteoinduktiv ist. Des Weiteren hat PCL/HA geeignete mechanische Eigenschaften und lässt sich leicht verarbeiten. Um die *sheets* herzustellen, wurde eine 200 µm dicke PCL/HA Folie mithilfe einer Gussform aus Aluminium gefertigt. Die *sheets* wurden im Anschluss mit einem Laserschneider aus der Folie geschnitten.

Das Laserschneiden wurde im Hinblick auf Genauigkeit und Reproduzierbarkeit optimiert. Der kontinuierliche CO₂-Laser des Laserschneiders wurde entsprechend bei einer Leistung von 6 W eingesetzt. Bei dieser Einstellung konnten die Variationen zwischen gleichen Strukturen unter 20 µm gehalten werden. Im Allgemeinen bietet Laserschneiden höchste Flexibilität in Bezug auf das Design der *sheets*. Dabei müssen jedoch die folgenden Grenzen des Prozesses berücksichtigt werden: Solide Strukturen sind unter einer Breite von 125 µm nicht zuverlässig stabil und die kleinsten reproduzierbar realisierbaren Porenstrukturen haben einen Durchmesser von ungefähr 40 µm. Bei dem Erstellen der Vorlagen muss zudem beachtet werden, dass der Materialabtrag durch das Laserschneiden zu Abweichungen zwischen der Vorlage und dem resultierenden *sheet* führt (bei 6 W ungefähr 50 µm).

Laserschneiden ist ein Herstellungsverfahren, welches noch nicht für die Herstellung von *scaffolds* für künstliches Knochengewebe genutzt wurde. Daher wurde überprüft, ob das Laserschneiden die Eigenschaften des prozessierten Materials negativ verändert. Entsprechend wurden das Zellwachstum und die Differenzierung von Zellen auf dem prozessierten Material untersucht. Darüber hinaus wurde eine Elementanalyse durchgeführt, um zu analysieren ob Aluminiumpartikel nach dem Herstellungsprozess auf den *sheets* verbleiben. Es konnte gezeigt werden, dass sich sowohl die Herstellung der PCL/HA-Folie, als auch die Verarbeitung derselben nicht negativ auf die hervorragenden Eigenschaften des Kompositmaterials auswirkt. Weder konnten Aluminiumpartikel nachgewiesen werden, noch wurde das Wachstum oder die Differenzierung von hMSCs durch die Verarbeitung verhindert.

Um zu zeigen, dass sich die *sheets* verwenden lassen um qualitativ hochwertige 3D-Zellkulturen herzustellen, wurden 50 runde *sheets* mit hMSCs besiedelt und zu einem zylindrischen *scaffold* mit einer Höhe und einem Durchmesser von 10 mm gestapelt. Anschließend wurde die 3D-Zellkultur in dem entwickelten Bioreaktorsystem unter Sauerstoff-kontrollierten Bedingungen kultiviert, um eine ausreichende Versorgung der Zellen zu gewährleisten. Anschließend wurde das *scaffold* auseinandergenommen und *sheet* für *sheet* analysiert. Durch die gute Sauerstoff- und Nährstoffversorgung in dem entwickelten Bioreaktor konnte eine homogene Verteilung viable Zellen über das gesamte *scaffold* erreicht werden. Dabei konnte auch gezeigt werden, dass die Zellen auf den einzelnen *sheets* miteinander verwachsen und so eine kohärente 3D-Zellkultur

bildeten. Entsprechend ist das entwickelte Konzept gut für die Herstellung von funktionellen *scaffolds* geeignet.

Das entwickelte *scaffold*-Konzept kann entsprechend für verschiedene Anwendungen genutzt werden: 1. Für die vereinfachte Herstellung homogen überwachsender 3D-Zellkulturen, durch die Besiedelung von einzelnen *sheets*, bevor diese zu einem *scaffold* gestapelt werden. So kann die initiale Zellverteilung besser kontrolliert werden. 2. Für die Herstellung von hybriden 3D-Zellkulturen, welche über die Kombination von soliden *sheets* mit Hydrogel-Schichten oder Zell-*sheets* gefertigt werden können. So können komplexe Gewebestrukturen hergestellt werden, die sich aus verschiedenen Zelltypen zusammensetzen. Dies ist beispielsweise für die Herstellung von vaskularisiertem Gewebe von großem Interesse. 3. Für die vereinfachte Analyse der 3D-Zellkulturen nach der Kultivierung. Dadurch, dass das *scaffold* auseinandergenommen und *sheet* für *sheet* untersucht werden kann, können Zellwachstum, Zellverteilung und Differenzierungsstatus analysiert werden ohne die Kultur aufwändig zu schneiden.

Zusammenfassend besteht die entwickelte Plattform aus einem neuartigen Bioreaktorsystem und einem innovativen *scaffold*-Konzept. Die Plattform ermöglicht die schnelle Untersuchung von 3D-Zellkulturen in einer Sauerstoff-kontrollierten Umgebung. Dies ist von großem Interesse für Labors, welche die Herstellung von künstlichem Gewebe untersuchen. Die Plattform vereinfacht die Herstellung von qualitativ hochwertigem Gewebe und ist darüber hinaus in der Lage die Qualität des Gewebes über die bereitgestellten Sauerstoffdaten (genauer Sauerstoffverbrauchsraten) zu beurteilen. Des Weiteren sind die kompakten Dimensionen des Systems ein großer Vorteil, in Bezug auf die Mobilität des Bioreaktors.

Durch diese Eigenschaften kann die entwickelte Plattform maßgeblich zu Fortschritten in der Entwicklung und Herstellung von künstlichem Knochengewebe beitragen – sowohl in forschenden Einrichtungen als auch im klinischen Umfeld.

4. Bibliography

- [1] Schieker, M., „Bone Substitutes,“ *Unfallchirurg 111*, p. 613, 2008.
- [2] Langer, R., and Vacanti, J.P., „Tissue Engineering,“ *Science 260*, pp. 920 - 926, 1993.
- [3] Shafiee, A., and Atala, A., „Tissue Engineering: Toward a New Era of Medicine,“ *Annu Rev Med 68*, pp. 29 - 40, 2017.
- [4] Wood, K.J., and Goto, R., „Mechanisms of rejection: Current perspectives,“ *Transplantation 93*, pp. 1 - 10, 2012.
- [5] Martin, I., Wendt, D., and Heberer, M., „The role of bioreactors in tissue engineering,“ *Trends Biotechnol 22*, pp. 80 - 86, 2004.
- [6] Frantz, C., Steward, K.M., and Weaver, V.M., „The extracellular matrix at a glance,“ *J Cell Sci 123*, pp. 4195 - 4200, 2010.
- [7] Grayson, W.L., Martens, T.P., Eng, G.M., Radisic, M., and Vunjak-Novakovic, G., „Biomimetic Approach to Tissue Engineering,“ *Semin Cell Dev Biol 20*, pp. 665 - 673, 2009.
- [8] Burke, D.P., and Kelly, D.J., „Substrate Stiffness and Oxygen as Regulators of Stem Cell Differentiation during Skeletal Tissue Regeneration: A Mechanobiological Model,“ *PLoS One 7*, p. e40737, 2012.
- [9] Horie, N., So, K., Moriya, T., Kitagawa, N., Tsutsumi, K., Nagata, I., and Shinohara, K., „Effects of oxygen concentration on the proliferation and differentiation of mouse neural stem cells in vitro,“ *Cell Mol Neurobiol 28*, pp. 833 - 845, 2008.
- [10] Redshaw, Z., and Loughna, P.T., „Oxygen concentration modulates the differentiation of muscle stem cells toward myogenic and adipogenic fates,“ *Differentiation 84*, pp. 193 - 202, 2012.
- [11] Altman, G., Horan, R., Martin, I., Farhardi, J., Stark, P., Volloch, V., Vunjak-Novakovic, G., Richmond, J., and Kaplan, D.L., „Cell differentiation by mechanical stress,“ *FASEB J 16*, pp. 270 - 272, 2002.
- [12] Clause, K.C., Liu, L.J., and Tobita, K., „Directed stem cell differentiation: the role of physical forces,“ *Cell Commun Adhes 17*, pp. 48 - 54, 2010.
- [13] Radisic, M., Park, H., Shing, H., Consi, T., Schoen, F.J., and Langer, R., „Functional assembly of engineered myocardium by electrical stimulation of cardiac myocytes cultured on scaffolds,“ *Proc Natl Acad Sci USA 101*, pp. 18129 - 18134, 2004.
- [14] Bose, S., Roy, M., and Bandyopadhyay, A., „Recent advances in bone tissue engineering scaffolds,“ *Trends Biotechnol 30*, pp. 546 - 554, 2012.
- [15] Vacanti, C.A., Bonassar, L.J., Vacanti, M.P., and Shufflebarger, J., „Replacement of an avulsed phalanx with tissue-engineered bone,“ *N Engl J Med 344*, pp. 1511 - 1514, 2001.

- [16] Heiss, C., Schieker, M., and Schnettler, R., „Implantation of bone substitutes for tibial head fractures,” *Unfallchirurg* 111, pp. 621 - 627, 2008.
- [17] Drosse, I., Volkmer, E., Capana, R., De Biase, P., Murschler, W., and Schieker, M., „Tissue engineering for bone defect healing: an update on a multi-component approach,” *Injury* 39, pp. 9 - 20, 2008.
- [18] Ignatius, A., Blessing, H., Liedert, A., Schmidt, C., Neidlinger-Wilke, C., Kaspar, D., Friement, B., and Claes, L., „Tissue engineering of bone: effects of mechanical strain on osteoblastic cells in type I collagen matrices,” *Biomaterials* 26, pp. 311 - 318, 2005.
- [19] Egger, D., Spitz, S., Fischer, M., Handschuh, S., Glösmann, M., Friemert, B., Egerbacher M., and Kasper, C., „Application of a Parallelizable Perfusion Bioreactor for Physiologic 3D Cell Culture,” *Cells Tissue Organs* 203, pp. 316 - 326, 2017.
- [20] Malda, J., Klein, T.J., and Upton, Z., „The Roles of Hypoxia in the in vitro Engineering of Tissues,” *Tissue Eng* 13, pp. 2153 - 2162, 2007.
- [21] Khan, Y., Yaszemski, M.J., Mikos, A.G., Laurencin, C.T., „Tissue Engineering of Bone: Material and Matrix Considerations,” *J Bone Joint Surg* 90, pp. 36 - 42, 2008.
- [22] Fleming, J.E., Cornell, C.N., and Muschler, G.F., „Bone cells and matrices in orthopedic tissue engineering,” *Orthop Clin North* 31, pp. 357 - 374, 2000.
- [23] Petrovic, J., Schlegel, A.K., Schultze-Mosgau, S., and Wiltfang, J., „Different Substitute Biomaterials as Potential Scaffolds in Tissue Engineering,” *Int J Oral Maxillofac Implants* 21, pp. 225 - 231, 2006.
- [24] Badylak, S.F., and Gilbert, T.W., „Immune response to biologic scaffolds materials,” *Seminars Immunol* 20, pp. 109 - 116, 2008.
- [25] Ghassemi, T., Shahroodi, A., Ebrahimzadeh, M.H., Mousavian, A., Movaffagh, J., and Moradi, A., „Current Concepts in Scaffolding for Bone Tissue Engineering,” *Arch Bone Jt Surg* 6, pp. 90 - 99, 2018.
- [26] Hutmacher, D.W., „Scaffolds in tissue engineering bone and cartilage,” *Biomaterials* 21, pp. 2529 - 2543, 2000.
- [27] Perry, C.R., „Bone repair techniques, bone graft, and bone graft substitutes,” *Clin Orthop Relat Res* 360, pp. 71 - 86, 1999.
- [28] Olszta, M.J. et al., „Bone structure and formation: A new perspective,” *Mater Sci Eng R: Rep* 58, pp. 77 - 116, 2007.
- [29] Murphy, C.M., et al., „The effect of pore size on cell attachment, proliferation and migration in collagen-glycosaminoglycan scaffolds for bone tissue engineering,” *Biomaterials* 31, pp. 461 - 466, 2010.
- [30] Vert, M., Li, M.S., Spenlehauer, G., and Guerin, P., „Bioresorbability and biocompatibility of aliphatic polyesters,” *J Mater Sci* 3, pp. 432 - 446, 1992.

- [31] Williams, D.F., „On the mechanisms of biocompatibility,“ *Biomaterials* 29, pp. 2941 - 2953, 2008.
- [32] Ma, P.X., „Scaffolds for tissue fabrication,“ *Mater Today* 7, pp. 30 - 40, 2004.
- [33] Moradi, A., Dalilottojari, A., Pigguan-Murphy, B. and Djordevic, I., „Fabrication and characterization of elastomeric scaffolds comprised of a citric acid-based polyester/hydroxyapatite microcomposite,“ *Mater Design* 50, pp. 446 - 450, 2013.
- [34] Chuenjitkuntaworn, B., Inrung, W., Damrongsri, D., Mekaapiruk, K., Supaphol, P., and Pavasant, P., „Polycaprolactone/Hydroxyapatite composite scaffolds: Preparation, characterization, and in vitro and in vivo biological responses of human primary bone cells,“ *J Biomed Mater Res Part A* 94, pp. 241 - 251, 2010.
- [35] Cheung, H.Y., Lau, K.T., Lu, T.P. and Hui, D., „A critical review on polymer-based bio-engineered materials for scaffold development,“ *Composites Part B* 38, pp. 291 - 300, 2007.
- [36] Bergsma, E.J., Bruijn, W., Rozema, F.R., Bos, R.M. and Boering, G., „Late tissue response to poly(L-lactide) bone plates and screws,“ *Biomaterials* 16, pp. 25 - 31, 1995.
- [37] Bergsma, E.J., Rozema, F.R., Bos, R.M., and Bruijn, W., „Foreign body reactions to resorbable poly(L-lactide) bone plates and screws used for the fixation of unstable zygomatic fractures,“ *J Maxillofac Surg* 51, pp. 666 - 670, 1993.
- [38] Biltz, R.M., and Pellegrino, E.D., „The chemical anatomy of bone. I. A comparative study of bone composition in sixteen vertebrates,“ *J Bone Joint Surg Am* 51, pp. 456 - 466, 1969.
- [39] Ducheyne, P. and Qiu, Q., „Bioactive ceramics: the effect of surface reactivity on bone formation and bone cell function,“ *Biomaterials* 20, pp. 2287 - 2303, 1999.
- [40] Athanasiou, K.A., Zhu, C., Lanctot, D.R., Agrawal, C.M., and Wang, X., „Fundamentals of biomechanics in tissue engineering of bone,“ *Tissue Eng* 6, pp. 361 - 381, 2000.
- [41] Kokubu, T., Kim, H.M., and Kawashita, M., „Novel bioactive materials with different mechanical properties,“ *Biomaterials* 24, pp. 2161 - 2175, 2003.
- [42] Wang, M., „Developing bioactive composite materials for tissue replacement,“ *Biomaterials* 24, pp. 2133 - 2151, 2003.
- [43] Stevens, M.M., „Biomaterials for bone tissue engineering,“ *Mater today* 11, pp. 18 - 25, 2008.
- [44] Agrawal, C.M., and Athanasiou K.A., „Techniques to control pH in vicinity of biodegrading PLA-PGA implants,“ *J Biomed Mater Res Appl Biomater* 38, pp. 105 - 114, 1997.
- [45] Shikinami, Y., and Okuno, M., „Bioresorbable devices made of forged composites of hydroxyapatite (HA) particles and poly-L-lactide (PLLA): part I. Basic characteristics,“ *Biomaterials* 20, pp. 857 - 877, 1998.

- [46] Vunjak-Novakovic, G., Obradovic, B., Martin, I., Bursac, P.M., Langer, R., and Freed L.E., „Dynamic Cell Seeding of Polymer Scaffolds for Cartilage Tissue Engineering,” *Biotechnol Prog* 14, pp. 193 - 202, 1998.
- [47] Melchels, F.P., Barradas, A.M., van Blitterswijk, C.A., de Boer, J., Feijen, J., and Grijpma, D.W., „Effects of the architecture of tissue engineering scaffolds on cell seeding and culturing,” *Acta Biomater* 6, pp. 4208 - 4217, 2010.
- [48] Alvarez-Barreto, J.F., Lineham, S.M., Shambaugh, R.L., and Sikavitsas, V.I., „Flow Perfusion Improves Seeding of Tissue Engineering Scaffolds with Different Architectures,” *Ann Biomed Eng* 25, pp. 429 - 442, 2007.
- [49] Wendt, D., Marasano, A., Jakob, M., Heberer, M., and Martin, I., „Oscillating Perfusion of Cell Suspensions Through Three-Dimensional Scaffolds Enhances Cell Seeding Efficiency and Uniformity,” *Biotechnol Bioeng* 84, pp. 205 - 214, 2003.
- [50] Tang, Q., Piard, C., Lin, J., Nan, K., Guo, T., Caccamese, J., Fisher, J., and Chen, Y., „Imaging stem cell distribution, growth, migration, and differentiation in 3-D scaffolds for bone tissue engineering using mesoscopic fluorescence tomography,” *Biotechnol Bioeng* 115, pp. 257 - 265, 2018.
- [51] Thevenot, P., Nair, A., Dey, J., Yang, J., and Tang, L., „Method to Analyze Three-Dimensional Cell Distribution and Infiltration in Degradable Scaffolds,” *Tissue Eng Part C* 14, pp. 319 - 331, 2008.
- [52] Moschouris, N., Firoozi, N., and Kang, Y., „The application of cell sheet engineering in the vascularization of tissue regeneration,” *Regen Med* 11, pp. 559 - 570, 2016.
- [53] Matsuda, N., Shimizu, T., and Yamato, M., „Tissue Engineering Based on Cell Sheet Technology,” *Adv Mater* 19, pp. 3089 - 3099, 2007.
- [54] Kim, H., Kim, Y., Park, J., Hwang, N.S., Lee, Y.K., and Hwang, Y., „Recent Advances in Engineered Stem Cell-Derived Cell Sheets for Tissue Regeneration,” *Polymers* 11, p. polym11020209, 2019.
- [55] Yang, J., Yamato, M., and Kohno, C., „Cell sheet engineering: recreating tissues without biodegradable scaffolds,” *Biomaterials* 26, pp. 6415 - 6422, 2005.
- [56] Asakawa, N., Shimizu, T., Tuda, Y., Sekiya, S., Sasagawa, T., Yamato, M., Fukai, F., and Okano, T., „Pre-vascularization of in vitro three-dimensional tissues created by cell sheet engineering,” *Biomaterials* 31, pp. 3903 - 3909, 2010.
- [57] Pirraco, R.P., Obokata, H., Iwata, T., Marques, A.P., Tsuneda, S., Yamato, M., Reis, R.L., and Okano, T., „Development of Osteogenic Cell Sheets for Bone Tissue Engineering Applications,” *Tissue Eng Part A*, pp. 1507 - 1515, 2011.
- [58] Gao, Z., Chen, F., Zhang, J., He, L., Cheng, X., and Ma, Q., „Vitalisation of tubular coral scaffolds with cell sheets for regeneration of long bones: a preliminary study in nude mice,” *Br J Oral Maxillofac Surg* 47, pp. 116 - 122, 2009.

- [59] Zhou, Y., Chen, F., Ho, S.T., Woodruff, M.A., Lim, T.M., and Hutmacher, D.W., „Combined marrow stromal cell-sheet techniques and high-strength biodegradable composite scaffolds for engineered functional bone grafts,” *Biomaterials* 28, pp. 814 - 824, 2007 .
- [60] Salifu, A.A., Lekakou, C., and Labeed, F., „Multilayer cellular stacks of gelatin-hydroxyapatite fiber scaffolds for bone tissue engineering,” *J Biomed Mater Res A* 105A, pp. 779 - 789, 2017.
- [61] Paşcu, E.I., Cahill, P.A., Stokes, J., and McGuinness, G.B., „Toward functional 3D-stacked electrospun composite scaffolds of PHBV, silk fibroin and nanohydroxyapatite: Mechanical properties and surface osteogenic differentiation,” *J Biomater Appl* 30, pp. 1334 - 1349, 2016.
- [62] He, F.L., Li, D.W., He, J., Liu, Y.Y., Ahmad, F., Liu, Y.L., Deng, X., Ye, Y.J., and Yin, D.C., „A novel layer-structured scaffold with large pore sizes suitable for 3D cell culture prepared by near-field electrospinning,” *Mat Sci and Eng C* 86, pp. 18 - 27, 2017.
- [63] Oviskanow, A., Khademhosseini, A., and Mironov, V., „The synergy of scaffold-based and scaffold-free tissue engineering strategies,” *Trends Biotechnol* 36, pp. 348 - 357, 2018.
- [64] Igwe, J.C., Mikael, P.E., and Nukavarapu, S.P., „Design, fabrication and in vitro evaluation of a novel polymer-hydrogel hybrid scaffold for bone tissue engineering,” *J Tissue Eng Regen Med* 8, pp. 131 - 142, 2014.
- [65] Trachtenberg, J.E., Kasper, F.K., and Mikos, A.G., „Chapter 22: Polymer Scaffold Fabrication,” in *Lanza, R., Langer, R., and Vacanti, J.: Principles of Tissue Engineering, 4th Ed.*, Burlington, MA, Academic Press, 2017, pp. 423 - 440.
- [66] Khorshidi, S., Solouk, A., Mirzadeh, H., Mazinani, S., Lagaron, J.M., Sharifi, S., and Ramakrishna, S., „A review of key challenges of electrospun scaffolds for tissue-engineering applications,” *J Tissue Eng Regen Med* 10, pp. 715 - 738, 2016.
- [67] Mas-Bargues, C., Sanz-Ros, J., Román-Domínguez, A., Inglés, M., Gimeno-Mallench, L., El Alami, M., Viña-Almunia, J., Gambini, J., Viña, J., and Borrás, C., „Relevance of Oxygen Concentration in Stem Cell Culture for Regenerative Medicine,” *Int J Mol Sci* 20, p. 1995, 2019.
- [68] Muschler, G.F., Nakamoto, C., and Griffith, L.G., „Engineering principles of clinical cell-based tissue engineering,” *J Bone Joint Surg Am* 86, pp. 1541 - 1558, 2004.
- [69] Lovett, M., Kyongbum, L., Edwards, A., and Kaplan, D.L., „Vascularization Strategies for Tissue Engineering,” *Tissue Eng Part B Rev*, pp. 353 - 370, 2009.
- [70] Huang, L.E., Gu, J., Schau, M., and Bunn, H.F., „Regulation of hypoxia-inducible factor 1 α is mediated by an O₂-dependent degradation domain via the ubiquitin-proteasome pathway,” *Proc Natl Acad Sci USA* 95, pp. 7987 - 7992, 1998.
- [71] Park, I.H., Kim, K.H., Choi, H.K., Shim, J.S., Whang, S.Y., Hahn, S.J., Kwon, O.J., and Oh, I.H., „Constitutive stabilization of hypoxia-inducible factor α selectively promotes the self-

- renewal of mesenchymal progenitors and maintains mesenchymal stromal cells in an undifferentiated state," *Exp Mol Med* 45, p. e44, 2013.
- [72] Basciano, L., Nemos, C., Foliguet, B., de Isla, N., de Carvalho, M., Tran, N., and Dalloul, A., „Long term culture of mesenchymal stem cells in hypoxia promotes a genetic program maintaining their undifferentiated and multipotent status," *BMC Cell Biol* 12, p. 12, 2011.
- [73] Forristal, C.E., Wright, K.L., Hanley, N.A., Oreffo, R.O., and Houghton, F.D., „Hypoxia-inducible factors regulate pluripotency and proliferation in human embryonic stem cells cultured at reduced oxygen tensions," *Reproduction* 139, pp. 85 - 97, 2010.
- [74] Koshiki, M., Kageyama, Y., Pete, E.A., Horikawa, I., Barrett, J.C., and Huang, L.E., „HIF-1alpha induces cell cycle arrest by functionally counteracting Myc," *EMBO J* 23, pp. 1949 - 1956, 2004.
- [75] Grosso, A., Burger, M.G., Lunger, A., Schaefer, D.J., Banfi, A., and Di Maggio, N., „It Takes Two to Tango: Coupling of Angiogenesis and Osteogenesis for Bone Regeneration," *Font Bioeng Biotechnol* 5, p. 68, 2017.
- [76] Street, J., Bao, M., de Guzman, L., Bunting, S., and Peale, F.V.Jr., „Vascular endothelial growth factor stimulates bone repair by promoting angiogenesis and bone turnover," *Proc Natl Acad Sci USA* 99, pp. 9656 - 9661, 2002.
- [77] Radisic, M., Malda, J., Epping, E., Geng, W., Langer, R., and Vunjak-Novakovic, G., „Oxygen gradients correlate with cell density and cell viability in engineered cardiac tissue," *Biotechnol Bioeng* 93, pp. 332 - 343, 2006.
- [78] Kellner, K., Liebsch, G., Klimant, I., Wolfbeis, O., Blunk, T., Schulz, M., and Gopferich, A., „Determination of oxygen gradients in engineered tissue using a fluorescent sensor," *Biotechnol Bioeng* 80, pp. 73 - 83, 2003.
- [79] Volkmer, E., Otto, S., Polzer, H., Saller, M., Trappendreher, D., Zagar, D., Hamisch, S., Ziegler, G., Wilhelmi, A., Mutschler, W., and Schieker, M., „Overcoming hypoxia in 3D culture systems for tissue engineering of bone in vitro using an automated, oxygen-triggered feedback loop," *J Mater Sci Mater Med* 23, pp. 2793 - 2801, 2012.
- [80] Volkmer, E., Drosse, I., Otto, S., Stangelmayer, A., Stengele, M., Cherian, B., Mutschler, W., and Schieker, M., „Hypoxia in Static and Dynamic 3D Culture Systems for Tissue Engineering of Bone," *Tissue Eng Part A* 14, pp. 1331 - 1340, 2008.
- [81] Schmid, J., Schwarz, S., Meier-Staude, R., Sudhop, S., Clausen-Schaumann, H., Schieker, M., and Huber, R., „A Perfusion Bioreactor System for Cell Seeding and Oxygen-Controlled Cultivation of Three-Dimensional Cell Cultures," *Tissue Eng Part C Methods* 24, pp. 585 - 595, 2018.
- [82] Liu, Y., Chan, J.K., and Teoh, S.H., „Review of vascularized bone tissue-engineering strategies with a focus on co-culture systems," *J Tissue Eng Regen Med* 9, pp. 85 - 105, 2015.

- [83] Ravichandran, A., Liu, Y., and Teoh, S.H., „Review: bioreactor design toward generation of relevant engineered tissues: focus on clinical translation,“ *J Tissue Eng Regen Med* 12, pp. e7 - e22, 2018.
- [84] Rouwkema, J., Rivron, N.C., and van Blitterswijk, C.A., „Vascularization in tissue engineering,“ *Trens Biotechnol* 26, pp. 434 - 441, 2008.
- [85] Ding, C.M., Henriksen, S.S., Wendt, D., and Overgaard, S., „An automated perfusion bioreactor for the streamlined production of engineered osteogenic grafts,“ *J Biomed Mater Res B Appl Biomater* 104, pp. 532 - 537, 2016.
- [86] Du, D., Furukawa, K., and Ushida, T., „Oscillatory perfusion seeding and culturing of osteoblast-like cells on porous beta-tricalcium phosphate scaffolds,“ *J Biomed Mater Res Part A* 86A, pp. 796 - 803, 2008.
- [87] Koch, M.A., Vrij, E.J., Engel, E., Planell, J.A., and Lacroix, D., „Perfusion cell seeding on large porous PLA/calcium phosphate composite scaffolds in a perfusion bioreactor system under varying perfusion parameters,“ *J Biomed Mater Res Part A* 95A, pp. 1011 - 1018, 2010.
- [88] Holy, C.E. et al., „Engineering three-dimensional bone tissue in vitro using biodegradable scaffolds: investigating initial cell-seeding density and cultivation parameters,“ *J Biomed Mater Res* 51, pp. 376 - 382, 2000.
- [89] Sikavitsas, V.I., Bancroft, G.N., and Mikos, A.G., „Formation of three-dimensional cell/polymer constructs for bone tissue engineering in a spinner flask and a rotating wall vessel bioreactor,“ *J Biomed Mater Res* 62, pp. 136 - 148, 2002.
- [90] Nishi, M., Matsumoto, R., Dong, J., and Uemura, T., „Engineered bone tissue associated with vascularization utilizing a rotating wall vessel bioreactor,“ *J Biomed Mater Res A* 101, pp. 421 - 427, 2013.
- [91] Bouet, G., Cruel, M., Laurent, C., Vico, L., Malaval, L., and Marchat, D., „Validation of an in vitro 3D bone culture model with perfused and mechanically stressed ceramic scaffold,“ *Eur Cell Mater* 29, pp. 250 - 266, 2015.
- [92] Piola, M., Soncini, M., Cantini, M., Sadr, N., Ferrario, G., and Fiore, G.B., „Design and functional testing of a multichamber perfusion platform for three-dimensional scaffolds,“ *ScientificWorldJournal* 2013, p. Article ID 123974, 2013.
- [93] Timmins, N.E., Scherberich, A., Früh, J.A., Heberer, M., Martin, I., and Jakob, M., „Three-dimensional cell culture and tissue engineering in a T-CUP (tissue culture under perfusion),“ *Tissue Eng* 13, pp. 2021 - 2028, 2007.
- [94] Pörtner, R., Nagel-Heyer, S., Goepfert, C., Adamietz, P., and Meenen, N.M., „Bioreactor design for tissue engineering,“ *J Biosci Bioeng* 100, pp. 235 - 245, 2005.
- [95] Bancroft, G.N., Sikavitsas, V.I. and Mikos, A.G., „Design of a flow perfusion bioreactor system for bone tissue-engineering applications,“ *Tissue Eng* 9, pp. 549 - 554, 2003.

- [96] Gaspar, D.A., Gomide, V., and Monteiro, F.J., „The role of perfusion bioreactors in bone tissue engineering,” *Biomatter* 2, pp. 167 - 175, 2012.
- [97] Williams, C., Kadri, O.E., Voronov, R.S., and Sikavitsas, V.I., „Time-dependent shear stress distributions during extended flow perfusion culture of bone tissue engineered constructs,” *Fluids* 3, p. 25, 2018.
- [98] Chen, H.C., and Hu, Y.C., „Bioreactors for tissue engineering,” *Biotechnol Lett* 28, pp. 1415 - 1423, 2006.
- [99] Hambor, J.E., „Bioreactor design and bioprocess controls for industrial cell processing,” *BioProcess Int* 10, pp. 22 - 77, 2012.
- [100] Lee, P.S., Eckert, H., Hess, R., Gelinsky, M., Rancourt, D., Krawetz, R., Cuniberti, G., and Scharnweber, D., „Developing a customized perfusion bioreactor prototype with controlled positional variability in oxygen partial pressure for bone and cartilage tissue engineering,” *Tissue Eng Part C Methods* 23, pp. 286 - 297, 2017.
- [101] Janssen, F.W., Oostra, J., Oorschot, A., and van Blitterswijk, C.A., „A perfusion bioreactor system capable of producing clinically relevant volumes of tissue-engineered bone: in vivo bone formation showing proof of concept,” *Biomaterials* 27, pp. 315 - 323, 2006.
- [102] Selden, C., and Fuller, B., „Role of Bioreactor Technology in Tissue Engineering for Clinical Use and Therapeutic Target Design,” *Bioengineering* 5, p. 32, 2018.
- [103] Place, T.L., Domann, F.E., and Case, A.J., „Limitations of oxygen delivery to cells in culture: An underappreciated problem in basic and translational research,” *Free Rad Biol Med* 113, pp. 311 - 322, 2017.
- [104] Bhumiratana, S., Bernhard, J.C., Alfi, D.M., Yeager, K., Eton, R.E., Bova, J., Shah, F., Gimble, J.M., Lopez, M.J., Eisig, S.B., and Vunjak-Novakovic, G., „Tissue-Engineered Autologous Grafts for Facial Bone Reconstruction,” *Sci Transl Med* 8, p. 343ra83, 2016.
- [105] Guarino, R.D., Dike, L.E., Haq, T.A., Rowley, J.A., Pitner, J.B., and Timmins, M.R., „Method for determining oxygen consumption rates of static cultures from microplate measurements of pericellular dissolved oxygen concentration,” *Biotechnol Bioeng* 86, pp. 775 - 787, 2004 .
- [106] Rowley, J.A., Timmins, M., Galbraith, W., Garwin, J., Kosovsky, M., and Heidaran, M., „Oxygen consumption as a predictor of MC3T3-E1 osteoblast growth and differentiation on 3D biodegradable scaffolds,” *Mol Biol Cell* 13, p. 345a, 2002.
- [107] Salter, E., Goh, B., Hung, B., Hutton, D., Ghone, N., and Grayson, W.D., „Bone Tissue Engineering Bioreactors: A Role in the Clinic?,” *Tissue Eng Part B Rev* 18, pp. 62 - 75, 2012.
- [108] Egger, D., Fischer, M., Clementi, A., Ribitsch, V., Hansmann, J., and Kasper, C., „Development and characterization of a parallelizable perfusion bioreactor for 3D cell culture,” *Bioengineering* 4, p. 51, 2017.

- [109] Dias, M.R., Fernandes, P.R., Guedes, J.M., and Hollister, S.J., „Permeability analysis of scaffolds for bone tissue engineering,“ *J Biomech* 45, pp. 938 - 944, 2012.
- [110] Cantini, M., Fiore, G.B., Redaelli, A., and Soncini, M., „Numerical fluid-dynamic optimization of microchannel-provided porous scaffolds for the co-culture of adherent and non-adherent cells,“ *Tissue Eng Part A* 15, pp. 615 - 623, 2009.
- [111] Starly, B., and Choubey, A., „Enabling sensor technologies for the quantitative evaluation of engineered tissue,“ *Ann Biomed Eng* 36, pp. 30 - 40, 2008.
- [112] Papkovsky, D.B., and Dmitriev, R.I., „Biological detection by optical oxygen sensing,“ *Chem Soc Rev* 42, pp. 8700 - 8732, 2013.
- [113] Hansmann, J., Groeber, F., Kahlig, A., Kleinhans, C., and Walles, H., „Bioreactors in tissue engineering - principles, applications and commercial constraints,“ *Biotechnol J* 8, pp. 298 - 307, 2013.
- [114] European Committee on Organ Transplantation, Guide to the quality and safety of tissues and cells for human application 3rd Edition, Strasbourg: European Directorate for the Quality of Medicines & HealthCare (EDQM), 2017.
- [115] Moll, G., Alm, J.J., Davies, L.C., von Bahr, L., Heldring, N., and Stenbeck-Funke, L., „Do cryopreserved mesenchymal stromal cells display impaired immunomodulatory and therapeutic properties?,“ *Stem Cells* 32, pp. 2430 - 2442, 2014.

PAPER I

A Perfusion Bioreactor System for Cell Seeding and Oxygen-Controlled Cultivation of Three-Dimensional Cell Cultures

METHODS ARTICLE

A Perfusion Bioreactor System for Cell Seeding and Oxygen-Controlled Cultivation of Three-Dimensional Cell Cultures

Jakob Schmid, MS,¹⁻³ Sascha Schwarz, ME,^{1,4} Robert Meier-Staude, PhD,³ Stefanie Sudhop, PhD,^{1,5} Hauke Clausen-Schaumann, PhD,^{1,5} Matthias Schieker, MD,² and Robert Huber, PhD^{1,3}

Bioreactor systems facilitate three-dimensional (3D) cell culture by coping with limitations of static cultivation techniques. To allow for the investigation of proper cultivation conditions and the reproducible generation of tissue-engineered grafts, a bioreactor system, which comprises the control of crucial cultivation parameters in independent-operating parallel bioreactors, is beneficial. Furthermore, the use of a bioreactor as an automated cell seeding tool enables even cell distributions on stable scaffolds. In this study, we developed a perfusion microbioreactor system, which enables the cultivation of 3D cell cultures in an oxygen-controlled environment in up to four independent-operating bioreactors. Therefore, perfusion microbioreactors were designed with the help of computer-aided design, and manufactured using the 3D printing technologies stereolithography and fused deposition modeling. A uniform flow distribution in the microbioreactor was shown using a computational fluid dynamics model. For oxygen measurements, microsensors were integrated in the bioreactors to measure the oxygen concentration (OC) in the geometric center of the 3D cell cultures. To control the OC in each bioreactor independently, an automated feedback loop was developed, which adjusts the perfusion velocity according to the oxygen sensor signal. Furthermore, an automated cell seeding protocol was implemented to facilitate the even distribution of cells within a stable scaffold in a reproducible way. As proof of concept, the human mesenchymal stem cell line SCP-1 was seeded on bovine cancellous bone matrix of 1 cm³ and cultivated in the developed microbioreactor system at different oxygen levels. The oxygen control was capable to maintain preset oxygen levels $\pm 0.5\%$ over a cultivation period of several days. Using the automated cell seeding procedure resulted in evenly distributed cells within a stable scaffold. In summary, the developed microbioreactor system enables the cultivation of 3D cell cultures in an automated and thus reproducible way by providing up to four independently operating, oxygen-controlled bioreactors. In combination with the automated cell seeding procedure, the bioreactor system opens up new possibilities to conduct more reproducible experiments to investigate optimal cultivation parameters and to generate tissue-engineering grafts in an oxygen-controlled environment.

Keywords: oxygen measurement, feedback control, cell seeding, perfusion microbioreactor, 3D cell culture

Impact Statement

The article describes a novel parallelized perfusion microbioreactor system, which is manufactured using three-dimensional printing technology. The microbioreactor system enables the cultivation in up to four independently operating, oxygen-controlled microbioreactors. This is achieved by a feedback loop, which adjusts the perfusion velocity to keep the oxygen

¹Center for Applied Tissue Engineering and Regenerative Medicine (CANTER), University of Applied Sciences Munich, Munich, Germany.

²Laboratory of Experimental Surgery and Regenerative Medicine (ExperiMed), Ludwig-Maximilians University Munich, Munich, Germany.

³Department of Industrial Engineering and Management, University of Applied Sciences Munich, Munich, Germany.

⁴Department of Mechanical Engineering, Technical University Munich, Garching, Germany.

⁵Center for Nanoscience (CeNS), Ludwig-Maximilians University Munich, Munich, Germany.

© Jakob Schmid et al. 2018; Published by Mary Ann Liebert, Inc. This Open Access article is distributed under the terms of the Creative Commons License (<http://creativecommons.org/licenses/by/4.0>), which permits unrestricted use, distribution, and reproduction in any medium, provided the original work is properly cited.

concentration at a preset level in each bioreactor individually. Furthermore, an implemented automated cell seeding procedure facilitates to distribute cells evenly in a stable scaffold before cultivation. The microbioreactor system can contribute to systematic investigations of crucial cultivation parameters in an oxygen-controlled environment and to more reproducible cultivation processes in tissue engineering.

Introduction

THE PRODUCTION OF SYNTHETIC tissue constructs, which resemble native tissue, has great potential for regenerative medicine.¹ For the cultivation of cells in a three-dimensional (3D) environment, bioreactor systems are mandatory to receive tissue-engineered grafts with uniform cell distribution, growth, and viability in a reproducible way.^{2–5} The application of bioreactor systems allows for the improvement of tissue quality by coping with limitations of static cultivation and by providing proper cultivation conditions for instance to mimic an *in vivo*-like environment.^{3,6}

Several dynamic cultivation systems^{7–11} have been developed to overcome the limitations of static cultivation of 3D cell cultures, which are foremost linked to poor mass transfer. In static conditions, the distribution of nutrients and oxygen as well as the removal of waste products is solely dependent on diffusion, and thus limited to distances ~ 100 – $200 \mu\text{m}$.^{12,13} Using a microbioreactor, the supply with oxygen and nutrients can be significantly improved, especially when large tissue-engineered grafts are cultivated,^{14–16} with perfusion bioreactors having the highest potential to mitigate diffusional limitations.^{17–19}

One of the most crucial cultivation parameters, which has to be considered for 3D cell culture, is the oxygen concentration (OC). Since every cell type demands a different OC for optimal cell growth and differentiation,^{12,20,21} the ability to ascertain optimal conditions is decisive for successful tissue engineering. Furthermore, the interpretation of oxygen data can provide information about cell growth and metabolic behavior in real time.^{22–24} To maintain OCs at an optimal level during a cultivation process, not only real-time sensing but also an automated feedback mechanism is needed.^{3,6,25} Nonetheless, many bioreactor systems lack integrated oxygen sensor technology^{9–11} or use sensor signals solely to observe present culture conditions.^{26–28}

Besides integrated measurement instrumentation, the parallelization of bioreactors improves the functionality of a system significantly; not only because parallel experimental setups are much more time effective than subsequent approaches but also because the conduction of several parallel experiments allows for the investigation of several parameters in one run.^{3,6,29} Most bioreactor systems include the option of multiplexing.^{9,10,30–32} However, to display variations in an oxygen-controlled environment, bioreactors within a system have to be operating independently. Whereas the independent operation of parallel running bioreactors is described for mechanical stimuli,³³ no such design is available for oxygen-controlled 3D cell culture.

If stable scaffolds are used for 3D cell culture, bioreactors can facilitate the generation of tissue-engineered grafts by not only maintaining optimal conditions but also by enabling uniform cell distributions during cell seeding before cultivation. Dynamic cell seeding procedures—conducted by bioreactors in an automated way—seem to have the highest potential for resulting in even cell distributions throughout stable scaffolds.^{34–36} This has to be considered,

since varying cell distributions are leading to spatial nutrient and oxygen differences within a 3D cell culture, resulting in inhomogeneous growth.³⁷

All these cultivation systems aim at the production of artificial tissue of high quality. However, for the fast and reproducible investigation of optimal culture conditions, cultivation systems need measurement instrumentation, the ability to control cultivation parameters as well as parallel and independent-operating bioreactors.^{3,6} However, currently available bioreactor systems lack at least one of these features. In addition, poorly controllable factors such as homogeneous cell seeding into 3D scaffolds are often not considered in bioreactor designs, and thus impeding the generation of comparable results.

Consequently, we developed a perfusion microbioreactor system for the oxygen-controlled cultivation of scaffold-based 3D cell cultures. The system is parallelizable up to four bioreactors, which are operated independently. Integrated needle-type microsensors (NTHs) are used to measure the OC in the geometric center of the 3D cell culture. The oxygen signals are processed in an automated feedback control to maintain OCs at a preset level by adjusting the perfusion speed for each bioreactor separately. In addition, an automated cell seeding procedure was implemented to facilitate the reproducible generation of homogeneous tissue. The bioreactors were optimized concerning a minimized dead volume, bubble-free operation, and a homogeneous flow distribution. Bioreactors were manufactured using stereolithography (SLA) and fused deposition modeling (FDM) 3D printing technology to provide a flexible and fast production process.

Materials and Methods

Microbioreactor

The perfusion microbioreactor was designed with the help of computer-aided design (CAD; SolidWorks 2016) and fabricated using the 3D printing technologies FDM (Ultimaker 2+) and SLA (FormLabs Form 2). Poly-L-Lactic acid (Innofil3D) was used for FDM, and DentalSG resin (FormLabs) for SLA. Gasket and 3D cell culture housing (3D-CCH) were molded using two-component silicone (Smooth-On MoldStar 15). To offer connectivity through luer-lock, hollow needles were glued into inlet, outlet, and sensor ports. The used materials were selected based on biocompatibility and the ability to be sterilized by autoclaving.

The microbioreactor design consists of five components (Fig. 1A). The bottom component contains the medium inlet and the housing for the 3D-CCH. The upper component contains the medium outlet and the sensor port. A silicone gasket between both components is used to seal the microbioreactor. The assembled components are kept in place using a threaded fixation ring, ensuring the long-term tightness of microbioreactors (Fig. 1B). The sensor port is designed to be used with syringe-guided NTHs allowing for measurements directly in the geometric center of the scaffold (Fig. 1C).

Due to the fabrication process through molding, the shape of the 3D-CCH can be varied and thus customized for

BIOREACTOR SYSTEM FOR CONTROLLED CULTIVATION OF 3D CELL CULTURES

587

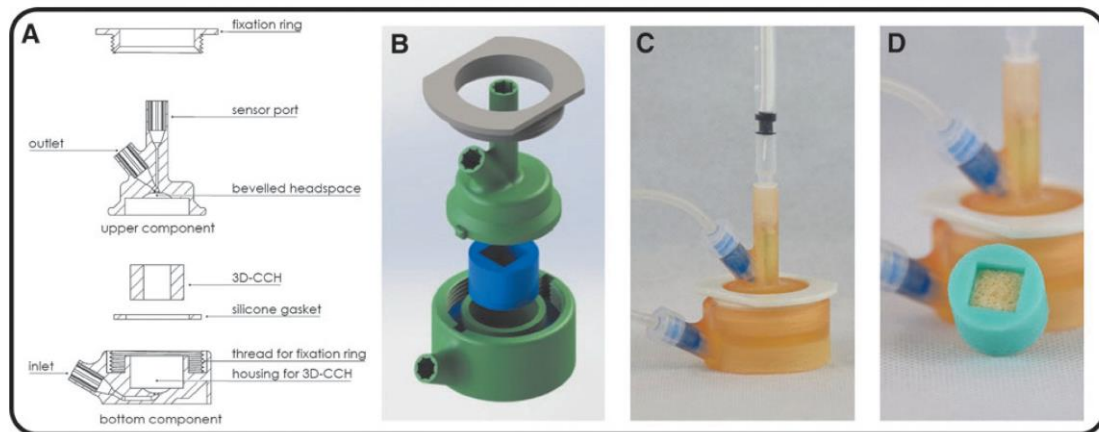


FIG. 1. 3D-printed microreactor for 3D cell culture. (A) Sectional drawing. (B) Explosion drawing. (C) Assembled with inlet/outlet/sensor. (D) Cubic bovine bone matrix scaffold in 3D-CCH. 3D, three dimensional; CCH, cell culture housing.

different scaffolds. Consequently, scaffolds can be inserted press-fit in the microreactor—preventing leakage flow around the scaffolds—regardless of their shape. For the development of the microreactor, cubic scaffolds with edge lengths of 10 mm (as described in section “Cell culture”) were used (Fig. 1D).

Inlet and outlet are designed to avoid both dead spaces and entrapped air. The former is realized by opening up the inlet to the full diameter of the 3D-CCH, also resulting in a more uniform flow through the scaffold. The latter by a beveled head space in the upper component, which effectively transports air bubbles out of the microreactor.

Parallelized microreactor system

The developed microreactor system consists of up to four microreactors, a peristaltic pump, and oxygen mea-

surement instrumentation, which is assembled into one system (Fig. 2). In addition, software to display, log, and control the OC in each microreactor independently is provided (see section “OC control”). All bioreactors receive the cell culture medium from one medium reservoir. Used medium is collected in one waste reservoir. Each bioreactor is connected to the medium reservoir by gas-permeable tubes (PharMed Ismaprene; Ismatec), to allow for gas exchange with the surrounding atmosphere to keep O_2 and CO_2 concentrations in the medium at a constant level.

A peristaltic pump with low pulsation and four independently movable channels (Reglo ICC; Ismatec) is used for cell culture medium transport. For oxygen measurement, sensors are connected to electro-optical modules (EOMs) through ST/ST couplers (PreSens). To prevent false oxygen measurements due to temperature changes, the temperature of the cell culture medium is measured in the inlet of the

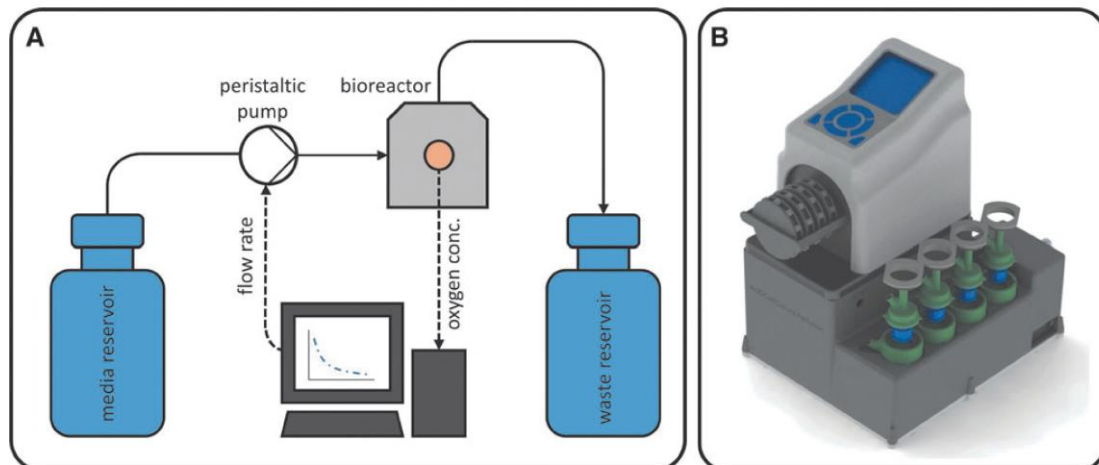


FIG. 2. Parallelized microreactor system. (A) Process flow diagram of one bioreactor. Up to four microreactors (gray) can be used simultaneously. (B) Set up microreactor system with pump and four parallel microreactors.

bioreactor using a PT100 thermocouple (PreSens) in a flow-through cell. The PT100 is connected to the EOMs to be able to measure OCs while considering the current media temperature. RS232 serial port to USB adapters is used to connect EOMs and the pump to a PC. The system is set up in an incubator, which takes over the tasks of temperature control and setting up a CO₂ atmosphere.

Computation fluid dynamics

To show the microbioreactors' ability to provide a homogeneous flow through a 3D cell culture, a flow profile was simulated with and without an inserted scaffold by

$$FR_{new} \left(\frac{\mu\text{L}}{\text{min}} \right) = FR \left(\frac{\mu\text{L}}{\text{min}} \right) + 11 \left(\frac{\text{min}}{\mu\text{L} \cdot \%O_2} \right) \cdot (OC_{current} - OC_{setpoint}).$$

computational fluid dynamics (CFD) analysis using ANSYS CFX 17.0 through the ANSYS Workbench. Calculations were performed within a half model in the symmetric plane of the microbioreactor using a fine mesh (48,518 nodes, 123,979 elements) with tetrahedral structures for the main flow and prismatic elements for the sidewall areas.

A laminar incompressible flow with flow rates (FRs) between 10 and 250 μL/min was simulated with regard to impulse, mass, and energy conservation. The flow through inserted scaffolds was simulated using Darcy's law with scaffolds of 10×10×10 mm—according to scaffolds used for 3D cell culture in this study (see section "Cell culture")—as a porous medium with pore sizes of 450 μm and 68% porosity (data provided by RTI Surgical for Tutobone scaffolds). The Darcian permeability (K) was estimated with $K = 10^{-9} \text{ m}^2$.^{38–40} Since the flow through the microbioreactor was found to be highly laminar in the considered range of FRs ($Re < 1$), the quadratic loss coefficient was not taken into account for the simulations.

Oxygen measurement

Needle-type oxygen microsensors (NTH-PSt1; PreSens) connected to EOMs (EOM-o2-micro; PreSens) were used for the oxygen measurements. A hollow needle of 0.4 mm diameter and 20 mm length was used to connect the NTH to the microbioreactor through luer-lock, to protect the optic fiber and to avoid deflection. Due to the bioreactors' design, the sensor tip of the mounted NTH is located directly in the geometric center of the 3D-CCH if the NTH is fully extended. A hole with a diameter of 0.5 and 5 mm length was drilled into the scaffold to ensure the correct positioning of the sensor tip in the 3D cell culture. OCs were measured every 120 s. According to the NTH-PSt1 manual, a two-point calibration was performed before each. Ambient air was used as the 21% oxygen reference and 100% CO₂ as the 0% oxygen reference.

OC control

Coding was performed with the visual programming language "G" using LabView 15 (National Instruments). The feedback mechanism allows for the independent control of OC by adjusting the FR of each channel of the peristaltic

pump according to the oxygen sensor signal of the associated microbioreactor.

FRs between 10 and 250 μL/min were used for this approach. A proportional controller was coded to readjust the FR according to the oxygen signal. In accordance with the equation commonly used for proportional controllers, the proportional value (KP) was calculated by dividing the range of the regulating variable "FR" by the range of the control variable "OC." The control deviation (*e*) was calculated by subtracting the OC-setpoint from the current OC:

$$FR_{new} = FR + KP \cdot e$$

To address the inertia of the system three checkpoints were integrated into the feedback loop to avoid high FR fluctuations. These comprise the control deviation, the trend of the OC during the last 10 iterations (ΔOC), and an OC-control time-out interval, which has to be defined before cultivation. After a FR adjustment the controller will remain inactive until the OC-control time-out interval elapsed. A FR adjustment is only possible if all the requirements listed in Table 1 are met. Otherwise, the FR will be kept constant.

The OC-control is embedded in an iterative loop (while loop), which is started after the initialization of the pump and the EOMs. For each iteration, data are requested from the EOMs, processed for the control, and (if necessary) written to the pump. In addition, a log-file is created to save the data hourly for further analysis. The following data are logged: cultivation time, OC, current flow rate, and whether the OC-control is active.

To demonstrate the functionality of the OC-control, oxygen levels were adjusted to 5%, 10%, and 15%, while one reactor remained uncontrolled.

Cell culture

The human telomerase reverse transcriptase immortalized human mesenchymal cell (hMSC) line SCP-1⁴¹ modified to express green fluorescence protein (GFP) constitutively was used for the experiments. Cells were cultured at 37°C in a humidified 90% air and 10% CO₂ atmosphere using Dulbecco's modified Eagle's medium (Merck) with 200 mM Glutamax (Gibco), 100 U/mL Penicillin/Streptomycin (Biochrom), and 10% fetal bovine serum (Biochrom). Decellularized cancellous bone matrix (Tutobone; RTI Surgical) of 10×10×10 mm was used as a scaffold for 3D cell culture.

TABLE 1. OXYGEN CONTROL, CRITERIA FOR FLOW RATE ADJUSTMENTS

| Possible adjustments | Control deviation | ΔOC | OC-control time-out interval |
|----------------------|-------------------|-----------------|------------------------------|
| Flow rate increase | $e < 0$ | $\Delta OC < 0$ | Elapsed |
| Flow rate decrease | $e < 0.5$ | $\Delta OC < 0$ | |

OC, oxygen concentration.

BIOREACTOR SYSTEM FOR CONTROLLED CULTIVATION OF 3D CELL CULTURES

589

Perfusion was performed using a multichannel peristaltic pump (RegloICC; Ismatec). Flow velocities were adjusted between 10 and 250 $\mu\text{L}/\text{min}$ to keep the OC in the 3D culture at a preset level. After the cultivation, cell nuclei were stained with 4',6-diamidino-2-phenylindole (DAPI; Thermo Fisher). Cells were analyzed at 475 nm (GFP) and 461 nm (DAPI) using a Zeiss Axio Observer.Z1 microscope and the associated Zen software.

Cell seeding

Cells were cultivated in T-flasks until a sufficient cell count was reached. Cells were trypsinized and counted using a hemocytometer (Brandt).

For static cell seeding, cells were resuspended in the medium to reach a concentration of 1×10^7 cells/mL. The scaffolds were centrifuged (500 g, 5 min, room temperature) in cell culture medium to remove air bubbles. Subsequently, 250 μL of the cell suspension was seeded on the scaffolds as described elsewhere.¹⁴ After 1 h static incubation, scaffolds were placed into the bioreactors for dynamic cultivation.

For dynamic cell seeding, the loading volume had to be increased due to pumpability. To keep the number of seeded cells equal, cells were resuspended in a medium at a lower concentration of 1.25×10^6 cells/mL. The scaffolds were placed into the microbioreactors and flushed with cell culture medium to remove air bubbles.

Subsequently, 2 mL of the cell suspension was seeded on the scaffolds using an oscillating flow at 1 mL/min. Oscillation was performed by changing the flow direction after every 200 μL inward and 100 μL outward directed flow. After reaching the total load volume of 2 mL, cells were cultivated statically for 1 h to allow the cells to adhere to the scaffold. Subsequently, dynamic cultivation was started. The dynamic cell seeding procedure was implemented in the bioreactor systems software and conducted automatically before cultivation, and thus referred to as "automated cell seeding."

To evaluate whether OC and FR data of parallel runs can give information about the uniformity of cell distribution on the scaffolds, mean values and relative standard deviations of OCs and FRs were calculated every 5 h.

Sterilization

The sterilization of thermostable materials was performed by autoclaving. For thermoplastic materials and oxygen sensors, a peroxide-based methodology was established, using 20% EtOH and 0.1% peroxyacetic acid for 45 min. Subsequently, the material was rinsed with demineralized water ($3 \times$ for 1 h) to remove residual peroxide and EtOH.^{42,43}

Results

Microbioreactor and parallelized microbioreactor system

The bioreactors were manufactured using SLA and FDM. Gaskets and 3D-CHH were molded using two-component silicone. Rapid prototyping technologies offered a highly flexible design. The sterilization protocol and the functional sealing mechanism prevented contaminations reliably.

The microbioreactor system allows for the measurement and control of oxygen in up to four independent-operating microbioreactors. In combination with the implemented cell seeding procedure, a highly automated cultivation process could be performed. Due to the compact size of the system, it is suitable to fit in a bench-top incubator (for temperature control and setting up a CO_2 atmosphere).

Computation fluid dynamics

A CFD analysis with and without scaffold was done for various flow conditions. The calculated CFD model was used to investigate whether the designed microbioreactor is able to provide a homogeneous flow profile through an inserted 3D cell culture using FRs between 10 and 250 $\mu\text{L}/\text{min}$.

At 250 $\mu\text{L}/\text{min}$, the flow profile of an empty microbioreactor shows high inhomogeneity with higher flow velocities in the center and areas with velocities close to 0 in the outer areas (Fig. 3A). The positive effect on the distribution of the media in the microbioreactor by opening the inlet to the full diameter of the 3D-CCH is already slightly visible though. If a scaffold is added to the model, a very homogeneous flow profile can be observed at 250 $\mu\text{L}/\text{min}$.

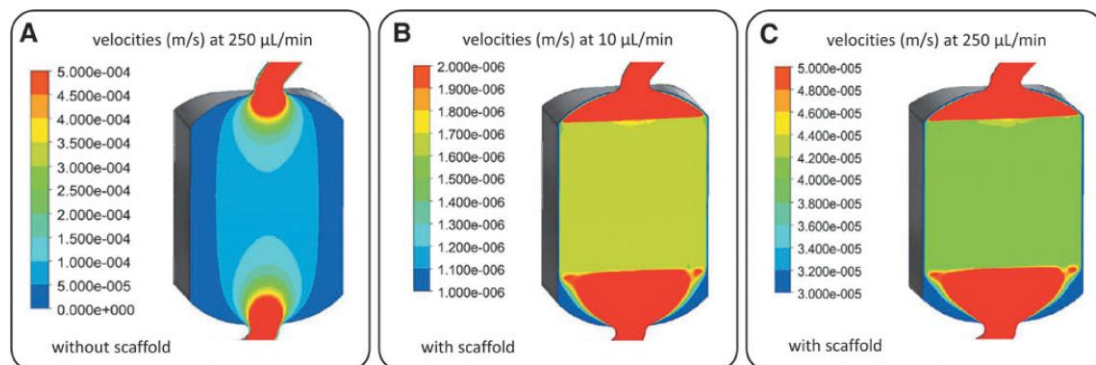


FIG. 3. Computation fluid dynamics analysis of flow distributions in the developed microbioreactor. (A) Flow distribution and velocities at 250 $\mu\text{L}/\text{min}$ without inserted scaffold. (B) Flow distribution and velocities at 10 $\mu\text{L}/\text{min}$. (C) Flow distribution and velocities at 250 $\mu\text{L}/\text{min}$.

(Fig. 3C) as well as at $10 \mu\text{L}/\text{min}$ (Fig. 3B). At the given FRs, the observed flow velocities in the inserted scaffolds vary between $4 \times 10^{-4} \text{ m/s}$ at $250 \mu\text{L}/\text{min}$ and $1.6 \times 10^{-6} \text{ m/s}$ at $10 \mu\text{L}/\text{min}$, respectively.

OC control

To demonstrate the systems' capability of controlling the OC in a reliable and reproducible way, two OC-controlled runs were conducted. For each run, 2.5×10^6 SCP-1 cells were seeded on Tutobone scaffolds statically and subsequently cultivated in four parallel microbioreactors. During the cultivation, oxygen levels of three microbioreactors were adjusted to 5%, 10%, and 15%, respectively, using the LabView-coded OC-control. The fourth microbioreactor remained uncontrolled.

Before reaching the OC-setpoint, the FR was kept constant at the minimal FR of $10 \mu\text{L}/\text{min}$. Once the OC fell below the OC-setpoint, the OC-control was triggered. Subsequently, the FR was adjusted according to the OC signal, to keep OCs at a preset level. Before OC-control activation, the oxygen consumption of the cells caused a decrease of OC levels in the center of the scaffolds. After OC-control activation, the controller was capable of adequately adjusting the FR to keep the OC constant during the whole cul-

tivation period (Fig. 4A, C). An OC-time-out interval (see "OC control") of 20 min was found to be suitable to minimize overshoot. As a result, the OC constantly remained in the range of "OC-setpoint $\pm 0.5\%$ " over a period of several days without great fluctuations. If OC levels were uncontrolled during the cultivation, OC levels dropped to anoxic conditions at $\sim 0\%$ (Fig. 4A, C).

When comparing OC (prior OC-control) and FR progressions, it is noticeable that the slopes differ significantly in both runs (Fig. 4). This is most likely a consequence of the static cell seeding procedure, which was used for this approach. Both uneven cell distribution and different cell seeding efficiencies could be the reason for the differences in the observed OC and FR slopes. Consequently, an automated cell seeding procedure was developed to aim for higher homogeneity and thus reproducibility.

Automated cell seeding

An automated (dynamic) cell seeding protocol was developed to distribute cells uniformly on a stable scaffold inserted into the developed microbioreactor. To demonstrate the functionality of the cell seeding protocol, SCP-1 cells were seeded on Tutobone scaffolds using different methods; first, the developed automated protocol and second, a static

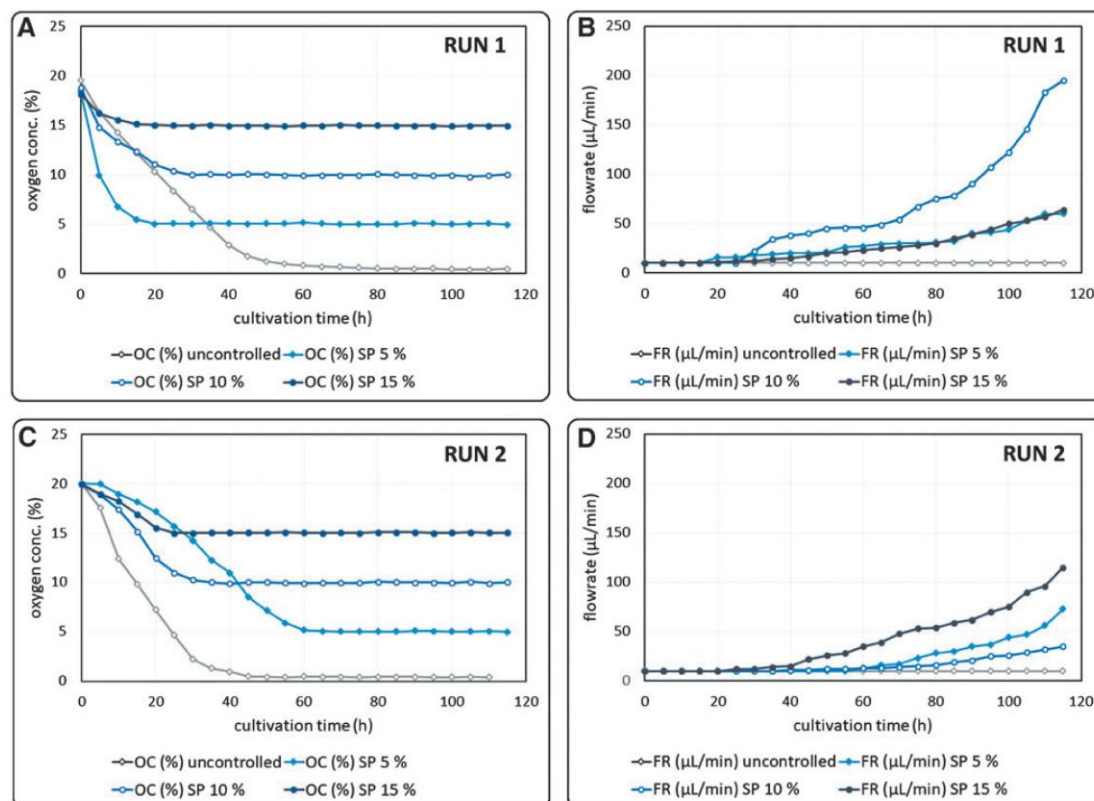


FIG. 4. Cultivation of SCP-1 cells on Tutobone scaffolds, four parallel bioreactors, OC-control at different levels. OC and FR progressions of two runs of four parallel bioreactors, controlled at different oxygen levels (uncontrolled, 5%, 10%, and 15%). (A) OCs of Run 1. (B) FRs of Run 1. (C) OCs of Run 2. (D) FRs of Run 2. OC, oxygen concentration; FR, flow rate.

cell seeding approach. For each approach, three scaffolds were seeded with 2.5×10^6 cells and subsequently cultivated in the developed microbioreactor system for 5 days. OCs were controlled at 15% O_2 . The progression of the OC and FR data was analyzed to evaluate the reproducibility of the developed automated and the static cell seeding procedure. After the cultivation, scaffolds were cut in half. Subsequently, the cell distribution was evaluated using fluorescence microscopy.

The capability of the developed automated cell seeding protocol is clearly visible both in the OC and FR signals, and in the evaluated 3D cell cultures. The automated protocol resulted in a homogeneous cell distribution within the whole scaffold (Fig. 5B, C), whereas several cell-free spots could be observed when cells were seeded statically (Fig. 5E–G). Statically seeded cultures showed relative standard deviations up to 8.8% for OC slopes before OC-control (0–30 h) and up to 40% for FRs (30–120 h) (Fig. 5D). In contrast, relative standard deviations for OC slopes and FRs were mostly <2% (OCs) and 20% (FRs), respectively, when the developed automated cell seeding procedure was used (Fig. 5A).

Discussion

Microbioreactor and parallelized microbioreactor system

To facilitate the investigation of scaffold-based 3D cell cultures, we developed a microbioreactor system, which includes three important features to improve reproducibility: OC measurement and control, an automated cell seeding procedure, and parallelization. In this study, we assessed whether the implementation of these features in one cultivation system enables the generation of homogeneous 3D cell cultures in a reproducible way. In contrast to commercially available^{31,32,35} and tailor-made (micro)bioreactor systems,^{9,10,25,30,44} the developed microbioreactor system is able to monitor and control one of the most critical cultivation parameters, the OC, while offering the possibility of multiplexing (up to four bioreactors). In combination with the implemented automated cell seeding system, the developed microbioreactor system allows for fast and reproducible investigation of 3D cell cultures, which is a considerable need for TE.^{3,6}

For the manufacture of the microbioreactors, rapid prototyping technologies such as SLA and FDM were used. The use of SLA and FDM allows for the fast production of microbioreactors and flexibility toward modifications for specific needs (e.g., different scaffold geometries). With the rapid advance of 3D printing technology and the general availability of 3D printers and materials, the fast production of smaller batches could make the system easily accessible for research facilities. Thus, the developed microbioreactor system represents a flexible and cost-efficient tool for the optimization and investigation of 3D cell cultures.

Computation fluid dynamics

The use of a perfused bioreactor allows for an optimal supply with nutrients, while toxic metabolites are effectively removed from the cell culture.^{4,17,18} However, this is only the case if the flow is evenly distributed throughout the scaffold. Consequently, we investigated whether the devel-

oped microbioreactor is capable of providing a homogeneous flow profile throughout an inserted 3D cell culture by CFD.

It was found that the pressure drop over the scaffold is sufficient to distribute fluids uniformly throughout the 3D cell culture. When compared with other microbioreactor systems, which are already used for tissue-engineering approaches,⁴⁵ the flow profile of the developed microbioreactor shows comparable characteristics. Consequently, the developed microbioreactor is capable of supplying even relatively large scaffolds/3D cell cultures with nutrients and oxygen in a homogeneous way.

OC control

OC measurement instrumentation was integrated into the developed microbioreactor. Furthermore, a functional OC-control was developed in LabView 15. The control was able to keep the OC at a preset level with high accuracy (setpoint $\pm 0.5\%$) and was able to reduce oxygen gradients in the 3D cell culture, which would result in inhomogeneous tissue quality.^{14,46} The proliferation potential of hMSCs, such as SCP-1 cells, is known to be unaffected by the present OC as long as the cells are cultivated at normoxic or hypoxic conditions. Some findings indicate even higher proliferation rates at hypoxic conditions, whereas the lack of oxygen at anoxic conditions leads to cell death of hMSCs and hence inhomogeneous 3D cell cultures.^{12,25,47,48}

In accordance with these findings, the viability of the 3D cell cultures was found to be comparable when the OC was adjusted to 5%, 10%, or 15%, respectively, while the effect of the anoxic conditions on the cells in uncontrolled 3D cell culture resulted in high amounts of dead cells (data not shown). Regarding the progress of the FRs (Fig. 4B, D), their exponential shape suggests exponential cell growth, but apparently the slopes differ significantly. Since cell growth of SCP-1 cells is not affected by the present OCs at normoxic or hypoxic conditions,⁴⁷ other effects have to be responsible for the differently increasing FRs at 15%, 10%, or 5%, respectively.

Since the number of cells, which were used for cell seeding, was equal, the different slopes are most likely a result of inhomogeneous cell distributions on the scaffold and different cell seeding efficiencies. Uneven cell distributions are most likely responsible for the differences in which the OCs drop before OC-control activation, too (Fig. 4A, C). The amount of metabolic active cells on a scaffold can be directly linked to the oxygen uptake rate (OUR) within a 3D cell culture.⁴⁹ The measurement by a needle-type oxygen sensor solely displays the amount of oxygen-consuming cells surrounding the sensors, which offers the opportunity to compare cell distributions by comparing OUR signals of equally treated scaffolds.

Inhomogeneity is also noticeable by analyzing OC and FR progressions, for example, in the 3D cell culture, which was adjusted to 5% in run 1. Whereas the rapid OC decrease indicates a high amount of growing cells in the scaffold, the slow increase of the FR after OC-control activation is rather an evidence for a lower cell count. It is most likely that a high amount of cells had adhered in the surrounding of the oxygen probe, while significant areas of the scaffold remained cell free after cell seeding.

This leads to the conclusion that a functional OC-control is able to reduce oxygen gradients to maintain high cell

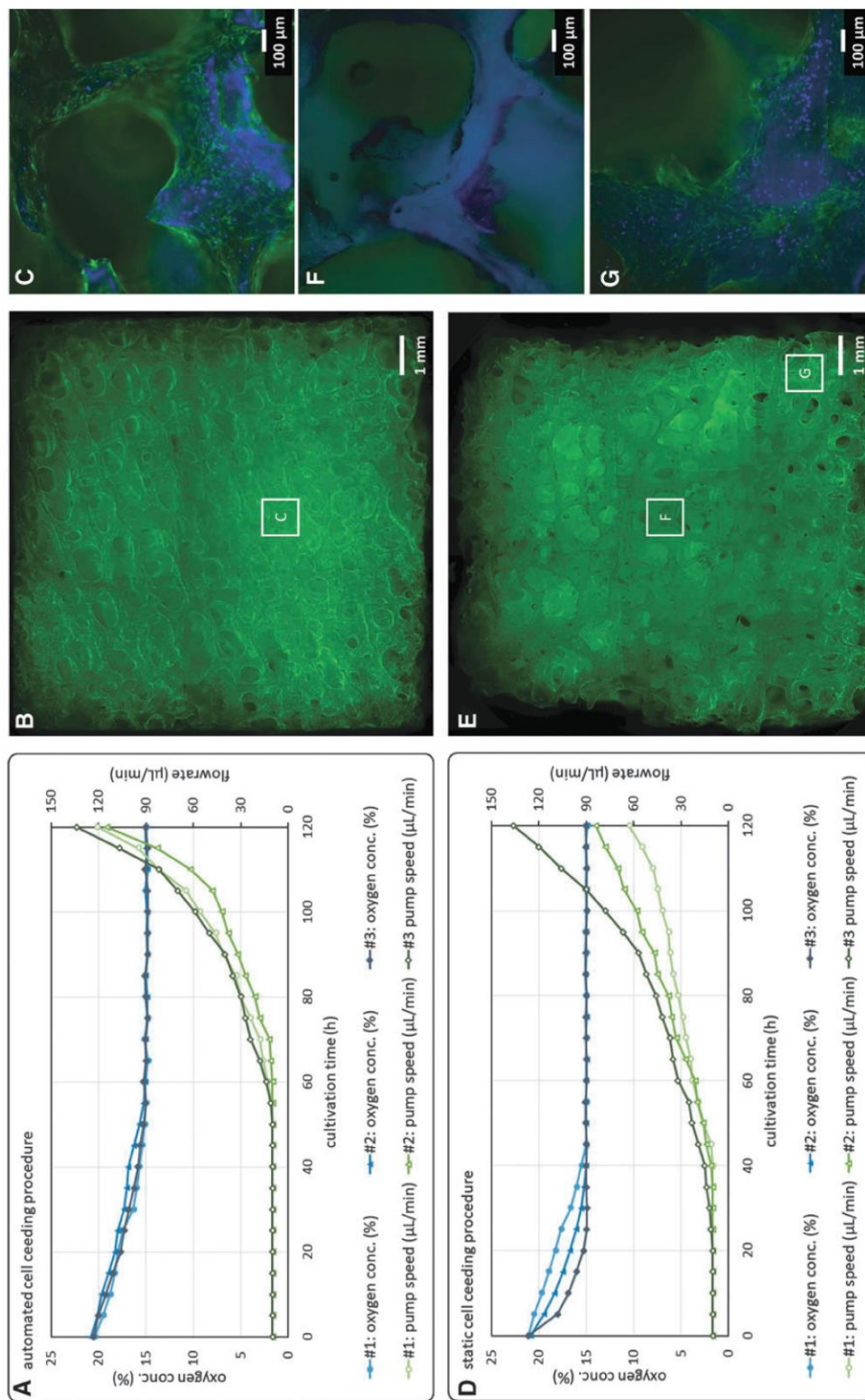


FIG. 5. Cultivation of SCP-1 cells on Tubone scaffolds, three parallel bioreactors, automated versus static cell seeding, OC- and FR progressions and evaluation of homogeneity. (A) Progression of OCs and FRs for an automated cell seeding approach ($n = 3$). (B) Homogeneous cell distribution after 120 h cultivation after automated cell seeding (GFP, DAPI, 2.5× magnification). (C) Automated cell seeding, overgrown scaffold section (GFP, DAPI, 10× magnification). (D) Progression of OCs and FRs for a static cell seeding approach ($n = 3$). (E) Inhomogeneous cell distribution after 120 h cultivation after static cell seeding (GFP, DAPI, 2.5× magnification). (F) Static cell seeding, cell-free scaffold section. (GFP, DAPI, 10× magnification). (G) Static cell seeding, overgrown scaffold section (GFP, DAPI, 10× magnification). GFP, green fluorescent protein; DAPI, 4',6-diamidino-2-phenylindole.

viabilities in the 3D cell culture, but the OC-control alone is not sufficient to guarantee for homogeneous tissue quality. This is especially the case for 3D cell cultures with uneven cell distributions after cell seeding. Besides OC-control, a protocol for homogeneous cell seeding is hence mandatory for the generation of tissue of high quality in a reproducible way.

The OC-control allows for many different applications. First of all, it is possible to avoid the OC to drop below levels that would impede the viability of the 3D cell culture due to lack of oxygen. For the cell line used in this study (SCP-1), OCs <1% should be avoided to obtain a 3D cell culture of high viability. Critical OCs for optimal cell growth or cell differentiation could be easily determined by adjusting the OC to different levels in each bioreactor, and subsequently analyzing the viabilities of cultures or degree of differentiation.

The OC-control is implemented by a feedback loop, which adjusts the perfusion speed according to the OC in the associated bioreactor. One drawback of that mechanism is the variation of shear forces, which are applied to the cells. This is due to the variation in the FR during the cultivation process. This factor was not considered in this study. Nevertheless, since shear stress is known to affect the differentiation potential of hMSCs^{45,50,51} and is well considered in recent bioreactor studies,^{45,51} the decoupling of OC-control and FR is recently under investigation. This would make it possible to investigate whether the control of OCs could be combined with the control of shear forces in the developed micro-bioreactor system.

Furthermore, the OC has to drop from the initial to the preset OC before the control is activated, which requires a high amount of oxygen-consuming cells on the scaffold. This issue is highly linked to the pore size of the used scaffold. Large pore sizes and high porosities facilitate the oxygen supply of growing cells. Furthermore, large pores result in a smaller total surface area, and thus a lower amount of oxygen-consuming cells on an overgrown scaffold.⁵² Consequently, it is possible that the OC will not drop to the desired level, if scaffolds with large pore sizes are used, which naturally impedes the functionality of the OC-control.²⁵

Automated cell seeding

An automated cell seeding procedure was developed to facilitate uniform cell seeding in solid scaffolds. The use of a dynamic cell seeding procedure was shown to be much more efficient compared with static cell seeding approaches.^{35,34} These findings were confirmed in this work (Fig. 5). The concept of an oscillating flow profile, which was applied in other studies,³⁵ was suitable to distribute cells throughout the whole scaffold homogeneously, with no visible cell-free spots.

However, even though the cell number used for the different protocols was equal, it must be considered that the seeding volume for the automated cell seeding had to be increased due to pumpability. The potential effect of different seeding volumes on the initial cell distribution was not further investigated though, since the main focus of the study was to implement the automated cell seeding protocol, and to investigate if unequal cell distributions can be observed in OC and FR progressions.

In addition, cell distribution is dependent on the pore size and geometry of the used scaffold. Consequently, the au-

tomated cell seeding procedure has to be optimized for different scaffolds before application. The integrated OC sensors and the OC-control of the developed system can be used for these optimization procedures efficiently. It was shown that cell seeding homogeneity is directly observable in OC and FR signals, since it is most likely that uneven cell distributions are the reason for differing OC- and FR progressions in parallel runs (Fig. 5A, D). Consequently, the developed system is also usable for the optimization and validation of dynamic cell seeding protocols.

Conclusions

The developed micro-bioreactor system offers a novel option for the investigation of 3D cell cultures on solid scaffolds. The system is parallelizable up to four micro-bioreactors, whereas each micro-bioreactor can be adjusted to a preset OC individually. This is achieved by integrated OC measurement instrumentation and a developed OC-control, which adjusts the perfusion rate according to the present OC in an automated feedback loop. The OC-controlled cultivation of 3D cell cultures prevents OCs to drop below levels that could impede the viability of the cells. In addition, it enables optimization of cell growth and cell differentiation as a function of OC.

The implementation of an automated cell seeding system in combination with the functional OC-control and the parallelized setup facilitates the investigation and generation of tissue-engineered constructs with high homogeneity and viability in a reproducible way.

Acknowledgments

The authors thank Conny Hasselberg-Christoph and Benedikt Kaufmann for their technical assistance. This work was supported by the Bavarian Research Foundation (Project No. AZ-1222-16), and the Bavarian State Ministry for Science and Arts (research focus "Generation and characterization of three-dimensional tissue [Herstellung und Charakterisierung dreidimensionaler Gewebe]"—CANTER) as well as by Pre-Sens GmbH, Regensburg, Germany. Prof. Matthias Schieker is currently an employee of the Novartis Institutes of Biomedical Research, Basel, Switzerland.

Disclosure Statement

No competing financial interests exist.

References

1. Drosse, I., Volkmer, E., Capanna, R., De Biase, P., Mutschler, W., and Schieker, M. Tissue engineering for bone defect healing: an update on a multi-component approach. *Injury* **39**, S9, 2008.
2. Carvalho, J.L., de Carvalho, P.H., and de Goes, A.M. Advances in biomaterials science and biomaterials applications. In: Pignatello, R., ed. *Innovative Strategies for Tissue Engineering*. London: InTECH Open Limited, 2013, pp. 295–313.
3. Ravichandran, A., Liu, Y., and Teoh, S.H. Review: bioreactor design toward generation of relevant engineered tissues: focus on clinical translation. *J Tissue Eng Regen Med* **12**, e7, 2018.
4. Kasper, G., van Griensven, M., and Pörtner, R. *Bioreactor Systems for Tissue Engineering*. Berlin, Germany: Springer, 2009.

5. Amini, A.R., Laurencin, C.T., and Nukavarapu, S.P. Bone tissue engineering: recent advances and challenges. *Crit Rev Biomed Eng* **40**, 363, 2012.
6. Hansmann, J., Groeber, F., Kahlig, A., Kleinhans, C., and Walles, H. Bioreactor in tissue engineering - principles, applications and commercial constraints. *Biotechnol J* **8**, 298, 2013.
7. Sikavitsas, V.I., Bancroft, G.N., and Mikos, A.G. Formation of three-dimensional cell/polymer constructs for bone tissue engineering in a spinner flask and a rotating wall vessel bioreactor. *J Biomed Mater Res* **62**, 136, 2002.
8. Nishi, M., Matsumoto, R., Dong, J., and Uemura, T. Engineered bone tissue associated with vascularization utilizing a rotating wall vessel bioreactor. *J Biomed Mater Res A* **101**, 421, 2013.
9. Bouet, G., Cruel, M., Laurent, C., Vico, L., Malaval, L., and Marchat, D. Validation of an in vitro 3D bone culture model with perfused and mechanically stressed ceramic scaffold. *Eur Cell Mater* **29**, 250, 2009.
10. Piola, M., Soncini, M., Cantini, M., Sadr, N., Ferrario, G., and Fiore, G.B. Design and functional testing of a multichamber perfusion platform for tree-dimensional scaffolds. *ScientificWorldJournal* **2013**, Article ID 123974, 2013.
11. Timmins, N.E., Scherberich, A., Früh, J.A., Heberer, M., Martin, I., and Jakob, M. Three-dimensional cell culture and tissue engineering in a T-CUP (tissue culture under perfusion). *Tissue Eng* **13**, 2021, 2007.
12. Volkmer, E., Kallukalam, B.C., Maertz, J., *et al.* Hypoxia preconditioning of human mesenchymal stem cells overcomes hypoxia-induced inhibition of osteogenic differentiation. *Tissue Eng Part A* **16**, 153, 2010.
13. Lovett, M., Lee, K., Edwards, A., and Kaplan, D.L. Vascularization strategies for tissue engineering. *Tissue Eng Part B Rev* **15**, 353, 2009.
14. Volkmer, E., Drosse, I., Otto, S., *et al.* Hypoxia in static and dynamic 3D culture systems for tissue engineering of bone. *Tissue Eng Part A* **14**, 1331, 2008.
15. Carrier, R.L., Rupnick, M., Langer, R., Schoen, F.J., Freed, L.E., and Vunjak-Novakovic, G. Effects of oxygen on engineered cardiac muscle. *Biotechnol Bioeng* **78**, 617, 2002.
16. Rouwkema, J., Rivron, N.C., and van Blitterswijk, C.A. Vascularization in tissue engineering. *Trends Biotechnol* **26**, 434, 2008.
17. Pörtner, R., Nagel-Heyer, S., Goepfert, C., Adamietz, P., and Meeßen, N.M. Bioreactor design for tissue engineering. *J Biosci Bioeng* **100**, 235, 2005.
18. Bancroft, G.N., Sikavitsas, V.I., and Mikos, A.G. Design of a flow perfusion bioreactor system for bone tissue-engineering applications. *Tissue Eng* **9**, 549, 2003.
19. Gaspar, D.A., Gomide, V., and Monteiro, F.J. The role of perfusion bioreactors in bone tissue engineering. *Biomater* **2**, 167, 2012.
20. Fehrer, C., Brunauer, R., Laschober, G., *et al.* Reduced oxygen tension attenuates differentiation capacity of human mesenchymal stem cells and prolongs their lifespan. *Aging Cell* **6**, 745, 2007.
21. Holzwarth, C., Vaegler, M., Gieseke, F., *et al.* Low physiologic oxygen tension reduce proliferation and differentiation of human multipotent mesenchymal stromal cells. *BMC Cell Biol* **11**, 11, 2010.
22. Super, A., Jaccard, N., Cardoso Marques, M.P.C., *et al.* Real-time monitoring of specific oxygen uptake rates of embryonic stem cells in a microfluidic cell culture device. *Biotechnol J* **11**, 1179, 2016.
23. Weyand, B., Nöhre, M., Schmälzlin, E., *et al.* Noninvasive oxygen monitoring in three-dimensional tissue cultures under static and dynamic culture conditions. *Biores Open Access* **4**, 266, 2015.
24. Streeter, I., and Cheema, U. Oxygen consumption rate of cells in 3D culture: the use of experiment and simulation to measure kinetic parameters and optimise culture conditions. *Analyst* **136**, 4013, 2011.
25. Volkmer, E., Otto, S., Polzer, H., *et al.* Overcoming hypoxia in 3D culture systems for tissue engineering of bone in vitro using an automated, oxygen-triggered feedback loop. *J Mater Sci Mater Med* **23**, 2793, 2012.
26. Lee, P.S., Eckert, H., Hess, R., *et al.* Developing a customized perfusion bioreactor prototype with controlled positional variability in oxygen partial pressure for bone and cartilage tissue engineering. *Tissue Eng Part C Methods* **23**, 286, 2017.
27. Chan, W.Y., and Chong, C.K. Perfusion bioreactors improve oxygen transport and cell distribution in esophageal smooth muscle construct. *IFMBE Proceedings*. Berlin, Germany: Springer, 2009, p. **23**.
28. Janssen, F.W., Oostra, J., van Oorschot, Av, and van Blitterswijk, C.A. A perfusion bioreactor system capable of producing clinically relevant volumes of tissue-engineered bone: in vivo bone formation showing proof of concept. *Biomaterials* **27**, 315, 2006.
29. Meyvatson, I., and Beebe, D.J. Cell culture models in microfluidic systems. *Annu Rev Anal Chem* **1**, 423, 2008.
30. Sailon, A.M., Allori, A.C., Davidson, E.H., Reformat, D.D., Allen, R.J., and Warren, S.M. A novel flow-perfusion bioreactor supports 3D dynamic cell culture. *J Biomed Biotechnol* **2009**, Article ID: 873816, 2009.
31. 3D Biotek. 3D Biotec perfusion bioreactor. [Online]. Available at: http://3dbiotek.com/Documents/Bioreactor_Brochure.pdf (Accessed May 7, 2018).
32. SKE Research Equipment. SKE inflow perfusion bioreactor. [Online]. Available at: <http://ske.it/products/inflow-modular-perfusion-bioreactor> (Accessed May 7, 2018).
33. Brady, M.A., Vaze, R., Amin, H.D., Overby, D.R., and Ethier, C.R. The design and development of a high-throughput magneto-mechanostimulation device for cartilage tissue engineering. *Tissue Eng Part C Methods* **20**, 149, 2014.
34. van den Dolder, J.V.D., Spauwen, P.H.M., and Jansen, J.A. Evaluation of various seeding techniques for culturing osteogenic cells on titanium fiber mesh. *Tissue Eng* **9**, 315, 2003.
35. Wendt, D., Marsano, A., Jakob, M., Heberer, M., and Martin, I. Oscillating perfusion of cell suspensions through three-dimensional scaffolds enhances cell seeding efficiency and uniformity. *Biotechnol Bioeng* **84**, 205, 2003.
36. Koch, M.A., Vrij, E.J., Engel, E., Planell, J.A., and Lacroix, D. Perfusion cell seeding on large porous PLA/calcium phosphate composite scaffolds in a perfusion bioreactor system under varying perfusion parameters. *J Biomed Mater Res A* **95**, 1011, 2010.
37. Galban, C.J., and Locke, B.R. Effects of spatial variation of cells and nutrient and product concentrations coupled with product inhibition on cell growth in a polymer scaffold. *Biotechnol Bioeng* **64**, 633, 1999.

38. Innocentini, M.D.M., Faleiros, R.K., Pisani, R., Thijs, I., Luyten, J., and Mullens, S. Permeability of porous gelcast scaffolds for bone tissue engineering. *J Porous Mater* **17**, 615, 2010.
39. Truscello, S., Kerckhofs, G., Van Bael, S., Pyka, G., Schrooten, J., and Van Oosterwyck, H. Prediction of permeability of regular scaffolds for skeletal tissue engineering: a combined computational and experimental study. *Acta Biomater* **8**, 1648, 2012.
40. Sanz-Herrera, J.A., Kasper, C., van Griensven, M., Garcia-Aznar, J.M., Ochoa, I., and Doblare, M. Mechanical and flow characterization of sponceram carriers: evaluation by homogenization theory and experimental validation. *J Biomed Mater Res B Appl Biomater* **87**, 42, 2008.
41. Böcker, W., Yin, Z., Drosse, I., *et al.* Introducing a single-cell-derived human mesenchymal stem cell line expressing hTERT after lentiviral gene transfer. *J Cell Mol Med* **12**, 1347, 2008.
42. Shearer, H., Ellis, M.J., Perera, S.P., and Chaudhuri, J.B. Effects of common sterilization methods on the structure and properties of poly(D,L lactic-co-glycolic acid) scaffolds. *Tissue Eng* **12**, 2717, 2006.
43. Yoganarasimha, S., Trahan, W.R., Best, A.M., *et al.* Peracetic acid: a practical agent for sterilizing heat-labile polymeric tissue-engineering scaffolds. *Tissue Eng Part C Methods* **20**, 714, 2014.
44. Bhaskar, B., Owen, R., Bahmaee, H., Rao, P.S., and Reilly, G.C. Design and assessment of a dynamic perfusion bioreactor for large bone tissue engineering scaffolds. *Appl Biochem Biotechnol* **185**, 555, 2018.
45. Egger, D., Fischer, M., Clementi, A., Ribitsch, V., Hansmann, J., and Kasper, C. Development and characterization of a parallelizable perfusion bioreactor for 3D cell culture. *Bioengineering* **4**, 51, 2017.
46. Malda, J., Klein, T.J., and Upton, Z. The roles of hypoxia in the in vitro engineering of tissues. *Tissue Eng* **13**, 2153, 2007.
47. Maertz, J., Saller, M., Kallakukalam, B.C., Docheva, D., Schieker, M., and Volkmer, E. Hypoxia and HIF-1 α regulation do not affect proliferation of human mesenchymal stem cells but inhibit osteogenic differentiation in vitro. *JSM Regen Med Bio Eng* **3**, 1019, 2015.
48. Carrancio, S., López-Holgado, N., Sánchez-Guijo, F.M., *et al.* Optimization of mesenchymal stem cell expansion procedures by cell separation and culture conditions modification. *Exp Hematol* **36**, 1014, 2008.
49. Lambrechts, T., Papantoniou, I., Sannaert, M., Schrooten, J., and Aerts, J.M. Model-based cell number quantification using online single-oxygen sensor data for tissue engineered perfusion bioreactors. *Biotechnol Bioeng* **111**, 1982, 2014.
50. Chen, H.C., and Hu, Y.C. Bioreactors for tissue engineering. *Biotechnol Lett* **28**, 1415, 2006.
51. Williams, C., Kadri, O.E., Voronov, R.S., and Sikavitsas, V.I. Time-dependent shear stress distributions during extended flow perfusion culture of bone tissue engineered constructs. *Fluids* **3**, 25, 2018.
52. Loh, Q.L., and Choong, C. Three-dimensional scaffolds for tissue engineering applications: role of porosity and pore size. *Tissue Eng B Rev* **19**, 485, 2013.

Address correspondence to:

Robert Huber
Department of Industrial Engineering and Management
University of Applied Sciences Munich
Lothstr. 34
Munich 80335
Germany

E-mail: robert.huber@hm.edu

Received: July 24, 2018


Accepted: September 17, 2018

Online Publication Date: October 17, 2018

PAPER II

A Laser-Cutting based Manufacturing Process for the Generation of Three-Dimensional Scaffolds for Tissue Engineering using Polycaprolactone/Hydroxyapatite Composite Polymer

A laser-cutting-based manufacturing process for the generation of three-dimensional scaffolds for tissue engineering using Polycaprolactone/Hydroxyapatite composite polymer

Journal of Tissue Engineering
Volume 10: 1–11
© The Author(s) 2019
Article reuse guidelines:
sagepub.com/journals-permissions
DOI: 10.1177/2041731419859157
journals.sagepub.com/home/tej


Jakob Schmid^{1,2,3}, Sascha Schwarz^{1,4}, Martina Fischer³,
Stefanie Sudhop^{1,5}, Hauke Clausen-Schaumann^{1,5},
Matthias Schieker² and Robert Huber^{1,3} 

Abstract

A manufacturing process for sheet-based stacked scaffolds (SSCs) based on laser-cutting (LC) was developed. The sheets consist of Polycaprolactone/Hydroxyapatite (PCL/HA) composite material. Single sheets were cut from a PCL/HA foil and stacked to scaffolds with interconnecting pores of defined sizes. HA quantities up to 50% were processable with high reproducibility, while the accuracy was dependent on the applied laser power. The smallest achievable pore sizes were about 40 µm, while the smallest stable solid structures were about 125 µm. The human mesenchymal stem cell line SCP-1 was cultured on the manufactured PCL/HA scaffolds. The cells developed a natural morphology and were able to differentiate to functional osteoblasts. The generation of PCL/HA SSCs via LC offers new possibilities for tissue engineering (TE) approaches. It is reliable and fast, with high resolution. The SSC approach allows for facile cell seeding and analysis of cell fate within the three-dimensional cell culture, thus allowing for the generation of functional tissue constructs.

Keywords

Tissue engineering, scaffold, laser-cutting

Received: 28 March 2019; accepted: 4 June 2019

Introduction

Scaffolds are commonly used in bone tissue engineering (TE) as a support for cell adhesion and to guide three-dimensional (3D) growth.¹ To generate functional tissue equivalents, the scaffolds should provide a suitable pore size, porosity, and an interconnecting pore structure.^{2,3} Furthermore, biocompatibility, resorbability, and osteoinductivity are important for successful bone TE approaches.^{4–6}

In general, these requirements are met by natural scaffolds such as decellularized bone grafts (e.g. from bovine femur spongiosa). However, these materials inherit the potential of pathogen transfer and immune rejection, as well as high variation in pore size and porosity.^{7,8}

Consequently, in recent years, synthetic materials have been investigated and evaluated in their potential

¹Center for Applied Tissue Engineering and Regenerative Medicine (CANTER), University of Applied Sciences Munich, Munich, Germany

²Laboratory of Experimental Surgery and Regenerative Medicine (ExperiMed), Ludwig-Maximilians University Munich, Munich, Germany

³Department of Industrial Engineering and Management, University of Applied Sciences Munich, Munich, Germany

⁴Department of Mechanical Engineering, Technical University of Munich, Garching, Germany

⁵Center for Nanoscience (CeNS), Ludwig Maximilian University of Munich, Munich, Germany

Corresponding author:

Robert Huber, Center for Applied Tissue Engineering and Regenerative Medicine (CANTER), University of Applied Sciences Munich, Lothstr. 34, 80335 Munich, Germany.
Email: robert.huber@hm.edu



Creative Commons Non Commercial CC BY-NC: This article is distributed under the terms of the Creative Commons Attribution-NonCommercial 4.0 License (<http://www.creativecommons.org/licenses/by-nc/4.0/>) which permits non-commercial use, reproduction and distribution of the work without further permission provided the original work is attributed as specified on the SAGE and Open Access pages (<https://us.sagepub.com/en-us/nam/open-access-at-sage>).

to replace natural scaffolds, to provide equally potent matrices for cell adhesion, growth, and differentiation. Synthetic thermoplastic polymers like Polycaprolactone (PCL), Polylactide (PLA), Polyglycolide (PGA), or their corresponding copolymers show suitable properties for the generation of scaffolds for bone TE. Besides being biocompatible, resorbable, and Food and Drug Administration (FDA)-approved, PCL has been shown to be both osteoconductive and osteoinductive, which is both mandatory to ensure cell growth and differentiation on the scaffold. Furthermore, PCL is soluble in common organic solvents, which makes it accessible for rapid prototyping manufacturing techniques.^{4,5,9,10}

To further improve the properties of PCL, composite materials can be created by adding bioactive materials, for instance, bioceramics, to the polymer. A broadly used bioceramic material for creating PCL-based composite materials is hydroxyapatite (HA, $\text{Ca}_{10}(\text{PO}_4)_6(\text{OH})_2$), since it is of the same chemical composition as the inorganic phase of natural bone.^{4,9,11}

The use of a PCL/HA composite material results in enhanced osteoconductivity and osteoinductivity, as well as in improved mechanical properties compared to PCL only. Furthermore, alkaline metabolic waste products are released during the resorption of HA. These can effectively neutralize acidic metabolic waste products, which occur during natural hydrolysis of PCL. Thus, critically low pH values can be avoided in degrading PCL/HA-based implants.^{4,12} These characteristics make PCL/HA composite materials a promising material for the generation of scaffolds for bone TE.

For bone TE applications, most scaffolds are designed as solid structures, since these are beneficial for mimicking the mechanical properties of bone and retaining the desired geometry.^{4,5,13} However, achieving spatially uniform cell distributions after cell seeding is difficult in solid scaffolds. Therefore, dynamic cell seeding procedures have to be developed, which have to be optimized for each scaffold design individually.^{14–16} In addition, the investigation of cell fate in a solid 3D-cell culture (3DCC) can only be performed by cutting or sawing the tissue-engineered construct (TEC). As a consequence, the TEC cannot be used for further applications.

A sheet-based scaffold concept offers a solution to these drawbacks of scaffold-based TE. Hereby, single sheets are manufactured and stacked to form a 3D scaffold (referred to as stacked scaffold, SSC).^{6,17} The advantages of SSCs are that single sheets can be seeded with cells individually and investigated with regard to cell distribution before the seeded sheets are stacked to an SSC. Moreover, cell distributions can be investigated after cultivation, by disassembling the SSC into single sheets. Furthermore, a sheet-based design can be used to combine both, solid structures and hydrogels for instance for vascularization approaches.^{5,17}

Many manufacturing techniques—such as fused deposition modeling (FDM) and electrospinning—have been

applied for the generation of scaffolds from PCL/HA composite materials.^{6,9,18,19} With the help of those techniques, scaffolds can be created in a highly reproducible way, while pore size and porosity can be controlled to allow for cell ingrowth and migration as well as for nutrient supply during dynamic cultivation. However, the generation of PCL/HA sheets via FDM requires non-standard 3D printing devices and sophisticated techniques to obtain a printable mixture that remains stable after printing.^{18,20} Furthermore, the process is prone to clogging of the printing nozzle due to HA particles. Bigger printing nozzles can prevent clogging, but only at the expense of printing resolution. Due to the relatively low melting temperature of PCL, the resolution can be further impaired by the heated nozzle. When a new layer is added to the printed construct, the heat of the nozzle can deform fine structure in subjacent layers.²¹ In electrospinning, the pore size of the resulting scaffolds is not easily controllable and limited to smaller pore sizes. Therefore, electrospinning is not an option for applications where larger pore sizes and geometries are desired.^{6,10,22,23} Techniques like porogen leaching are also limited to thin scaffold constructs since porogens have to be removed entirely from the generated scaffold, which is difficult especially for larger structures. Furthermore, interconnecting pore structures are hard to achieve in a controlled way.^{22,24}

Laser-cutting (LC) is a manufacturing technique, which has not been investigated for the generation of sheet-based scaffolds so far. In LC devices, a continuous wave laser is used to process materials with very high precision.^{25,26} Templates for the cutting process can be generated by computer-aided design (CAD). Thus, the manufacturing process is highly flexible with respect to the final design of a generated sheet and the resulting 3D scaffold.

Consequently, we developed a new manufacturing procedure based on LC, for the generation of PCL/HA sheets for 3DCC, which is shown in the present study. LC offers the possibility for a fast and reproducible generation of sheets and scaffolds. By using LC, certain drawbacks of common manufacturing techniques, like FDM or electrospinning, can be circumvented. Furthermore, the sheet-based scaffold approach enables for facile and easy cell seeding and investigation of cell growth and distribution.

Materials and methods

Generation of a PCL/HA foil

To produce a PCL/HA foil of 200 μm thickness, a 25×35 cm mold with a 200 μm recess was used. The mold was milled out of an aluminum block, to guarantee a fast removal of thermal energy after the cutting process, which is mandatory for the generation of fine structures. To generate the PCL/HA composite material, HA nanopowder (Sigma Aldrich) was dispersed in chloroform (Sigma Aldrich). Subsequently, PCL pellets (Sigma Aldrich) were

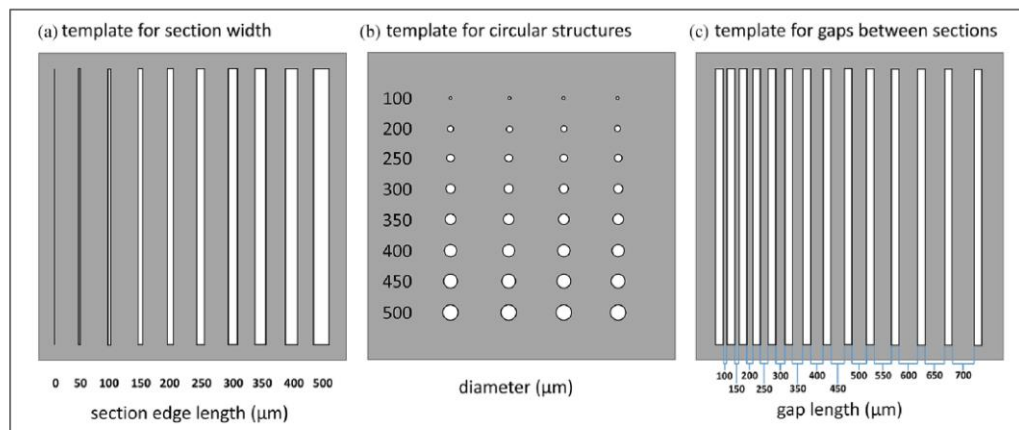


Figure 1. Test templates for the evaluation of the accuracy and the limits of the laser-cutting process: (a) test template for section width, varying from 0 to 500 μm (0 equals only a straight line, no rectangular shape in the designed template); (b) test template for circular structures with varying diameters from 100 to 500 μm ; and (c) test template for gaps between sections, varying between 100 and 700 μm .

solubilized in the chloroform solution with continuous stirring. After the PCL pellets dissolved completely, the solution was heated to 60°C, until the slurry was highly viscous. The slurry was poured in the aluminum mold and heated to 80°C until the chloroform evaporated completely. Subsequently, the PCL/HA slurry was spread and smoothed in the mold using a pre-heated, round profile aluminum bar and cooled to RT prior to further processing via LC. The experiments conducted in this work were performed with a 75% PCL, 25% HA composite material.

Generation of PCL/HA sheets by LC

Adobe Illustrator CS6 (Adobe Systems) was used, to create cutting templates for the laser cutter. PCL/HA sheets were produced using a Zing 24 laser cutter (Epilog) equipped with a 30 W, continuous wave CO₂ laser. The PCL/HA foil was cut into 10 × 10 mm sheets at 6 W laser power (corresponding to 20%) and maximum laser head travel speed. Subsequently, the aluminum mold was cooled down to 4°C for easy removal of the sheets. Sheets were removed from the mold using a scalpel, sterilized in 80% EtOH for 20 minutes and stored at RT.

To evaluate the accuracy and limits of the cutting process, three different test templates were created and cut out of a 75% PCL, 25% HA (75PCL25HA) foil. For the generation of test templates, the width of cut sections (section width), the gap between cut sections (section gap), and the diameter of circular structures (circle diameter) were varied (Figure 1). To evaluate the effect of different applied laser power levels on the accuracy, the templates were cut at levels between 0.3 and 12 W (1%–40%). For each laser power level, five equal test templates were manufactured.

To investigate the robustness of the cutting process, the deviations between equal structures (e.g. the widths of cut sections) on the created sheets were measured using a Zeiss Axio Observer.Z1 (Carl Zeiss) equipped with a 2.5× objective and analyzed using the Zen V2.6 software (Carl Zeiss). Subsequently, mean values (MVs) and standard deviations (SDs) were calculated. To investigate the accuracy of the cutting process, deviations between the manufactured sheets and the corresponding templates were calculated. For each laser power value used, MVs and SDs were calculated from the determined deviations.

Mechanical properties of 75PCL25HA sheets

The ultimate tensile strength (UTS) and the Young's modulus (YM) of single 75PCL25HA sheets (geometry 2, see Figure 4) were measured using a Mach1 mechanical tester (Biomomentum) with a 75 N load cell. The mechanical properties were determined in a dry state using a head speed of 0.2 mm/second. MVs and SDs were calculated from the measurements.

Scanning electron microscopy and energy-dispersive X-ray spectroscopy

To investigate, if residual aluminum particles remain on the PCL/HA sheets after the LC process, scanning electron microscopy (SEM) and energy-dispersive X-ray spectroscopy (EDX) were performed. Therefore, manufactured sheets were sputter coated with platinum and subsequently analyzed using a Lyra 3 system (Tescan). Imaging was performed at 5 kV using a secondary electron detector and the associated LycaTC software (Tescan). EDX was performed

at 10 kV using an X-Max silicon drift detector (Oxford Instruments) and the associated Aztec software (Oxford Instruments).

Cell culture

The human mesenchymal stem cell (hMSC) line SCP-1, modified to express green fluorescent protein (GFP) constitutively,²⁷ was used for the experiments. Cells were cultured at 37°C using Dulbecco's Modified Eagle Medium (DMEM, Merck) with 200 mM Glutamax (Gibco), 100 U/mL Penicillin/Streptomycin (Biochrom), and 10% fetal bovine serum (FBS, Biochrom) in a humidified 90% air, 10% CO₂ atmosphere. Quadratic 75PCL25HA sheets with edge lengths of 10 mm and a grid of 19 rectangular sections with 300 μm section width were used for the experiments (see Figure 4(a)).

To analyze cell growth and distribution, 50,000 SCP-1 cells were seeded by pipetting 100 μL of a 5×10^5 cells/mL suspension on each sheet. Subsequently, the cells were cultivated statically for 5 days, while the medium was changed every 48 hours. Cells cultivated on unprocessed PCL/HA foil and on cell culture dishes were used as a control, to investigate if the processing of PCL/HA by LC affects cell adherence and growth, for example, by structural alterations of the polymer in the heat affected zone (HAZ) of the laser. GFP producing cells were analyzed at 475 nm using a Zeiss Axio Observer.Z1 (Carl Zeiss) microscope and the associated Zen V2.6 software (Carl Zeiss).

Cell differentiation

To investigate cellular responses to differentiation factors, SCP-1 cells growing on manufactured PCL/HA sheets were differentiated to osteoblasts using the StemPro Osteogenesis Differentiation Kit (Thermo Fisher). Cells were seeded on single 75PCL25HA sheets (see "Cell culture" section) and cultivated statically in DMEM until 60%–80% confluency was reached. Subsequently, the cells growing on the sheets were cultivated in osteogenic differentiation medium (ODM) for a minimum of 21 days. The medium was changed every 2 days to provide a sufficient nutrient supply. Cells growing on unprocessed PCL/HA and on cell culture dishes, as well as cells cultivated in DMEM were used as a control.

The differentiation of hMSCs to osteoblasts was verified by staining calcium depositions in the mineralized extracellular matrix of mature osteoblasts, using Alizarin-Red S staining (ARS, Merck). Therefore, single sheets were incubated in ARS for 2 minutes and subsequently rinsed with PBS solution (Merck). Overgrown sheets, which were cultivated in DMEM were used as a negative control. ARS stained sheets were analyzed at 405 nm, using a Zeiss Axio Observer.Z1 microscope and the associated Zen V2.6 software.

3D cell culture

For 3D cell culture, circular 75PCL25HA sheets with 10 mm diameter and a grid of 19 rectangular sections were used (see Figure 4(b)). Fifty sheets were seeded with 50,000 SCP-1 cells each, by pipetting 100 μL of a 5×10^5 cells/mL suspension on each sheet. After 1 hour of static incubation, sheets were stacked in an alternating way (consecutive sheets rotated by 90°), to form a scaffold with interconnecting pores (referred to as SSC) (Figure 2).

Subsequently, the SSC was placed in a perfusion micro-bioreactor system and cultivated dynamically for 5 days. During the cultivation, oxygen levels were controlled at 15% to guarantee sufficient oxygen and nutrient supply as described elsewhere.²⁸ To investigate cell growth and distribution and to investigate if the SSC offers a coherent structure with interconnecting pores, the SSC was taken out of the bioreactor and disassembled after the cultivation. Subsequently, the cells growing on the sheets were analyzed at 475 nm (GFP) using a Zeiss Axio Observer.Z1 microscope and the associated Zen V2.6 software.

Results

Generation of PCL/HA sheets

Sheets were generated from PCL/HA foil by LC. PCL/HA slurries with HA-quantities of up to 50% were suitable for the production process. When higher amounts of HA were used, slurries could not be smoothed sufficiently, resulting in a PCL/HA foil of insufficient quality for the subsequent LC; 25% HA slurries gave the best results with regard to processability and sheet stability. Consequently, sheets containing 75% PCL and 25% HA (75PCL25HA) were used for the subsequent experiments.

Laser powers below 3 W (10% of the maximum power) were not sufficient for cutting the PCL/HA foil and are thus not suitable for processing the PCL/HA foil. For laser power values between 3 and 12 W (10%–40%), the variation between cut structures was constantly ≤ 20 μm for all applied power settings. For laser powers above 3 W (10%), the removal of material during the LC process affected the accuracy of the procedure, with deviations between designed templates and resulting sheets increasing linearly with increasing laser power (Figure 3). Material removal led to both larger sections and diameters as well as thinner gaps between sections—except for 100 μm circular structures when cutting with 4.5 W laser power or lower, which resulted in smaller diameters.

Resulting structures, which were thinner than 125 μm, were not reliably stable. These structures were easily damaged during removal from the aluminum mold or removed entirely by the lasers' power input during the cutting process.

Using 6 W laser power (20% of maximum power) resulted in a well controllable process and was used for the production of 75PCL25HA sheets for all subsequent

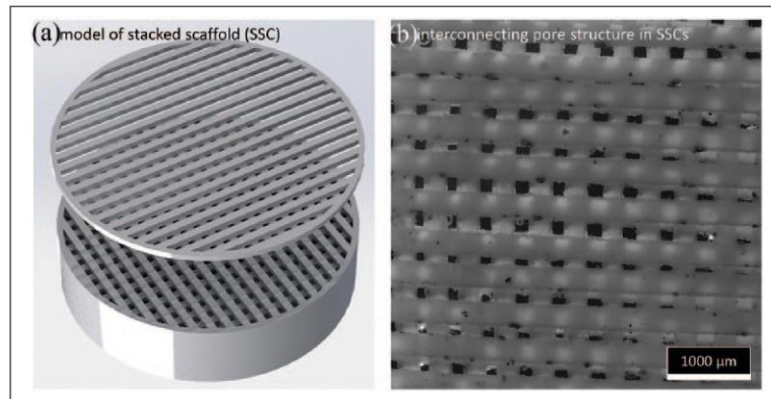


Figure 2. Model and structure of a stacked scaffold (SSC): (a) model of a stacked scaffold, illustrating the alternating way, how sheets are stacked and (b) resulting interconnecting pore structure of SSCs.

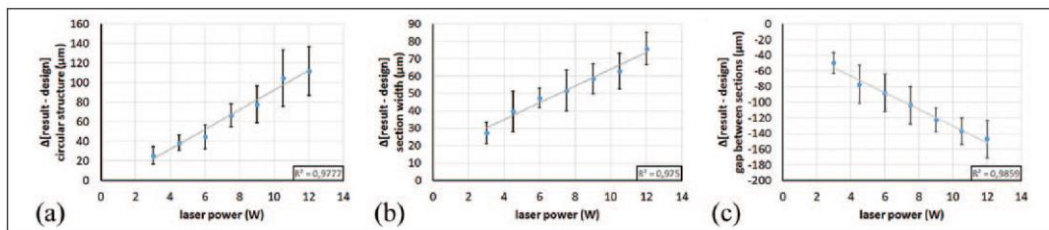


Figure 3. Evaluation of the cutting accuracy depending on the applied laser power for 75PCL25HA sheets: Mean values and standard deviations ($MV \pm SD$, $n = 5$) calculated from differences between manufactured sheets and designed cutting templates: (a) deviations for diameters of circular structures, (b) deviations for section widths, and (c) deviations for gaps between sections.

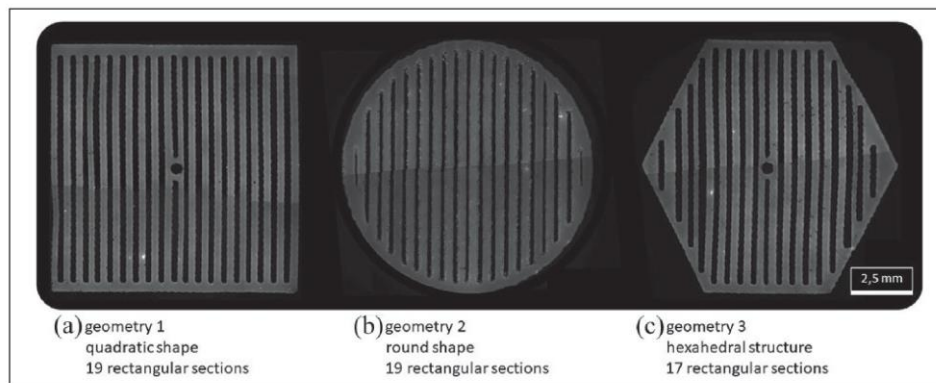


Figure 4. Different geometries cut from 75PCL25HA foil at 6 W laser power: (a) quadratic shape (10×10 mm), 19 rectangular sections ($9.5 \text{ mm} \times 0.3 \text{ mm}$), central circular section, for example, for sensor placement within the scaffold; (b) circular shape (10 mm diameter), 19 rectangular sections (varying length $\times 0.3 \text{ mm}$); and (c) hexahedral shape (10×10 mm), 17 rectangular sections (varying length $\times 0.3 \text{ mm}$), central circular section, for example, for sensor placement within the scaffold.

experiments. The cutting templates were adjusted to account for the determined deviation accordingly. To demonstrate the flexibility of the LC process, quadratic (geometry 1), circular (geometry 2), and hexahedral (geometry 3)

shaped sheets were cut from a 75PCL25HA foil (Figure 4). All geometries shared the same diameter of 10 mm with equally distributed sections. Section widths were designed to be 250 μm (resulting in section widths of approximately

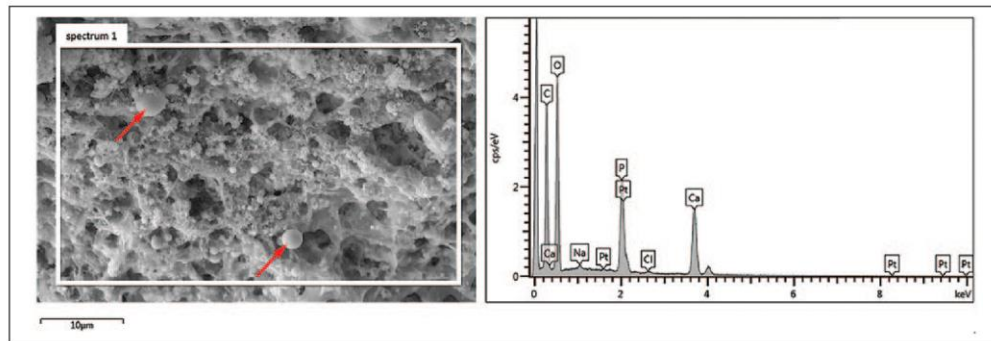


Figure 5. SEM image and EDX analysis of 75PCL25HA sheet.

SEM image and EDX analysis of the cut edge of a manufactured 75PCL25HA sheet. HA nanoparticles embedded in PCL are visible in the SEM image (2 nanoparticles are indicated exemplarily by arrows). EDX analysis was performed in the area of the white box.

300 µm). A central circular hole was added in geometry 1 and 3, to accommodate for the insertion of a sensor into the scaffold, for instance, for pO₂ or pH measurements inside of the 3DCC. Using the developed manufacturing process, five sheets could be generated per minute, whereas the manufacturing speed varied slightly depending on the geometry.

Mechanical properties of 75PCL25HA sheets. The mechanical properties of 75PCL25HA sheets (geometry 2, see Figure 4) were determined using a Mach1 mechanical tester. To determine the YM and the UTS, the force-affected cross-section area was calculated from a CAD model while having regard to the deviations of the manufacturing process (Figure 3). The YM was determined at 110 ± 18 MPa, and the UTS at 3.05 ± 0.80 MPa ($n = 5$).

SEM and EDX. Since an aluminum mold is used in the manufacturing process of PCL/HA sheets, the sheets were examined by SEM and EDX, to investigate if residual aluminum particles remain on the manufactured sheets. Several surfaces, including cut edges, were imaged and examined. HA nanoparticles embedded in PCL were clearly visible in the SEM image. In the EDX analysis, the following elements were found: Carbon (C), oxygen (O), calcium (Ca), phosphorous (P), and platinum (Pt), which are the main components of PCL ($(C_6H_{10}O_2)_n$) and HA ($Ca_{10}(PO_4)_6(OH)_2$). Furthermore, traces of sodium (Na) and chlorine (Cl) could be detected. However, no traces of aluminum were found on the manufactured sheets (Figure 5).

Cell growth and differentiation on PCL/HA sheets

To investigate cell growth and adhesion on 75PCL25HA sheets, 50,000 eGFP-labeled SCP-1 cells were seeded per sheet (sheet geometry 1, see Figure 4) and cultivated statically in DMEM for 5 days. Cells growing on cell culture

dishes and on unprocessed PCL/HA were used as a control.

Cells adhered and grew homogeneously on the 75PCL25HA sheets (Figure 6(a)) as well as on unprocessed PCL/HA. The cell morphology was comparable to the cells growing on a cell culture dish (Figure 6(b) and (c)).

To investigate the cellular response of SCP-1 cells to differentiation factors, cells were cultivated in ODM for 21 days. Staining of calcium depositions in the extracellular matrix of mature osteoblasts was used to determine if the differentiation was successful.

In contrast to cells cultivated in DMEM (Figure 7(a)), the staining with ARS revealed high amounts of calcium depositions in the extracellular matrix of cells which were cultivated in ODM while growing on LC processed PCL/HA (Figure 7(b) and (c)) as well as on unprocessed PCL/HA and on cell culture dishes. The differentiation of SCP-1 cells to mature osteoblasts is thus possible with cells growing on 75PCL25HA sheets.

Cell growth on stacked PCL/HA scaffolds

To investigate cell growth on SSCs made of 50 circular 75PCL25HA sheets (Figure 4(b)), single sheets were seeded with 50,000 SCP-1 cells and cultivated in DMEM for 1 hour separately. Subsequently, the sheets were stacked with alternating orientation (Figure 2) to form an SSC with interconnecting pore structure and placed in an oxygen controlled perfusion microbioreactor to ensure a proper nutrient and oxygen supply of the 3DCC. The circular sheet shape was chosen for 3DCC, to facilitate a homogeneous nutrient and oxygen supply in the SSC.

SCP-1 cells were cultivated in the SSC for a minimum of 5 days. Subsequently, the distribution of the cells in the SSC was investigated. The distribution of cells throughout the scaffold was easily assessable by disassembling the SSC and analyzing the scaffold sheet by sheet. The SSC

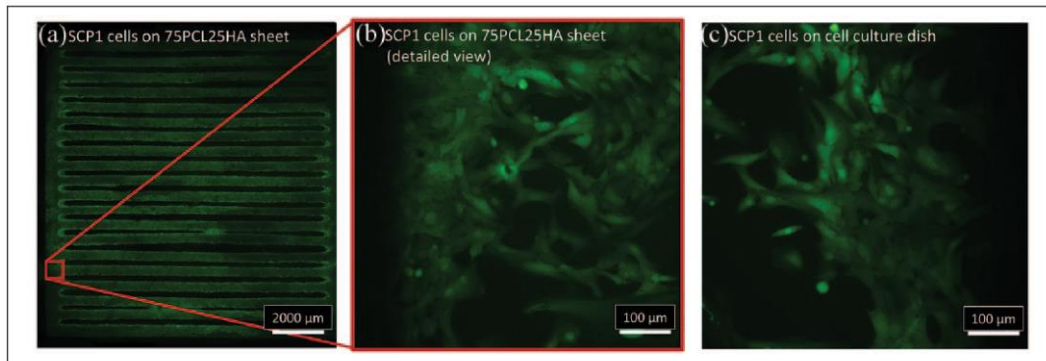


Figure 6. Fluorescence images showing growth and morphology of eGFP-labeled SCP-1 cells on 75PCL25HA sheets, after 5 days of cultivation: (a) SCP-1 cell growing homogeneously on a 75PCL25HA sheet, stacked from 9 frames, 2.5× magnification; (b) SCP-1 cell morphology on 75PCL25HA sheet, GFP, 20× magnification; and (c) SCP-1 cell morphology on a cell culture dish, GFP, 20× magnification.

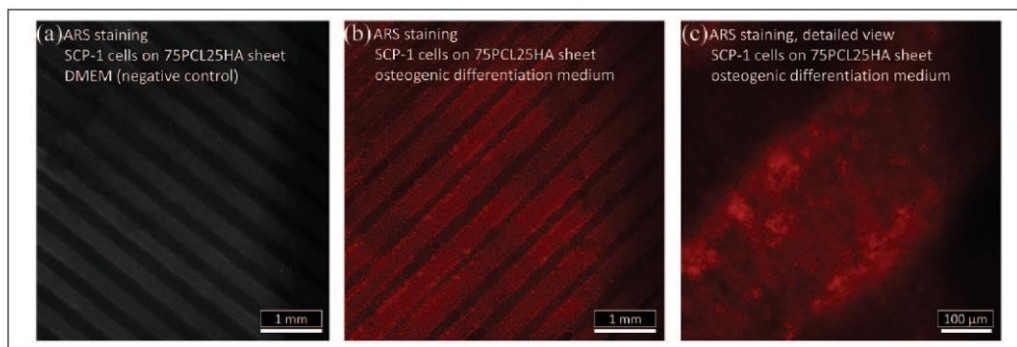


Figure 7. Investigation of differentiation of SCP-1 cells on PCL/HA sheets to osteoblasts after 21 days of cultivation, ARS-staining. Fluorescence images of Alizarin Red-S (ARS) stained SCP-1 cell cultures on 75PCL25HA sheets after 21 days of cultivation: (a) control, cultivation in DMEM, 2.5× magnification; (b) cultivation in ODM, 2.5× magnification; and (c) cultivation in ODM, 20× magnification.

was homogeneously overgrown, thus cells and sheets formed a coherent TE graft. The areas where the single sheets were in contact with each other were clearly visible in the fluorescence images of the SCP-1 cells (Figure 8).

Discussion

Generation of PCL/HA sheets

The generation of sheet-based scaffolds made of PCL/HA composite materials via LC was shown to be feasible. The developed method is easy to carry out, fast, and reproducible. Compared to other manufacturing methods, the sheet generation via LC does not require specific equipment but a standard commercially available LC device.

Prior to LC, a PCL/HA foil has to be created. For this purpose, an aluminum mold was used, since the great thermal conductivity of aluminum allows for both homogeneous

heating during the casting process and fast dissipation of the laser energy during the cutting process. Even though lasers operating in the kilowatt range are needed to cut aluminum,²⁹ it was investigated if traces of aluminum can be found on the cut edges of manufactured sheets. Therefore, SEM and EDX analyses were performed. Besides the main components of HA and PCL, platinum (sheets were sputtered with Pt prior to the measurement) and traces of sodium and chlorine (most likely transferred on the sheets during handling) were detected. Consequently, the use of an aluminum mold is unproblematic for the generation of the PCL/HA foil.

The LC process is suitable for PCL/HA ratios between 0% and 50% HA, which is comparable to other manufacturing methods like FDM, electrospinning and porogen leaching.^{6,9,18,24,30,31} However, PCL/HA foils with 25% HA were found to have the best properties regarding processability and sheet stability. If lower quantities of HA are used, the processing of the composite material is

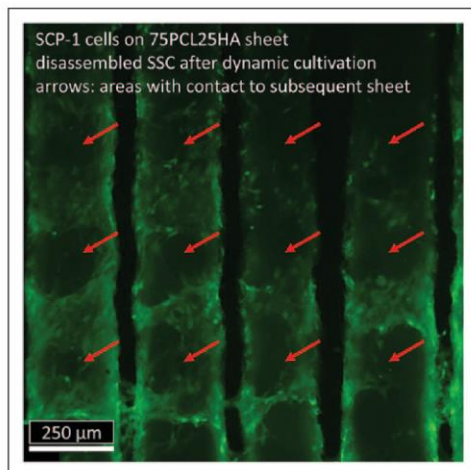


Figure 8. SCP-1 cells on a 75PCL25HA sheet after cultivation for 5 days as SSC in an oxygen controlled perfusion microbioreactor.

Fluorescence image (GFP) of SCP-1 cells growing on a 75PCL25HA sheet after cultivation of 5 days as SSC in an oxygen controlled micro-bioreactor and subsequent disassembling to single sheets. Areas, where single sheets were in contact with each other are indicated with red arrows, GFP, 10 \times magnification.

facilitated, but the resulting sheets are less stable and are damaged easily when they get removed from the aluminum mold. Also, the cut edges of manufactured sheets are not as smooth when lower HA quantities are used. The use of high HA quantities results in more stable sheets, but a less processable material, which impedes the creation of the PCL/HA foil.

The LC process itself is very robust and renders a well controllable manufacturing process, with variations between equally cut structures (e.g. diameters of circular structures) being lower than 20 μm . The design of different sheets is limited with respect to two structural features. First, structures between cut sections should be larger than 125 μm to be reliably stable and second, the width of the smallest possible section is about 40 μm (4.5 W laser power, designed section width 0 μm).

The energy input by the laser leads to material removal, which results in both larger sections and smaller gaps between sections, and thus in deviations between the designed cutting template and the resulting sheet. Naturally, higher laser powers result in higher material removal and thus in higher deviations of the resulting sheets to the CAD designed templates (Figure 3). Thus, lower laser powers are favorable for the manufacturing process.

Furthermore, the use of lower laser powers can lessen undesirable effects in the HAZ, like the alteration of the semi-crystalline structure of the processed polymer.³² A higher crystallinity percentage can be observed in the HAZ

of polymers, which were processed at high laser powers. Naturally, these changes in crystallinity can have an effect on the degradation of the material.^{33,34} Even though a relatively low laser power and a high laser head travel speed were applied in the developed manufacturing process, to minimize effects in the HAZ,³² the effect of LC on the biodegradation of the manufactured sheets has to be further investigated.

The mechanical properties of 75PCL25HA sheets were investigated using a Mach1 mechanical tester. A YM of 110 ± 18 MPa and an UTS of 3.05 ± 0.80 MPa were calculated from tensile tests of five single sheets. These values are well in the expected range for PCL/HA composite materials.³⁵ However, these values only represent single sheets. If sheets are stacked to form a scaffold, the compression modulus should be determined, to investigate the shape-persistency and durability of the created scaffold. However, this value is not only dependent on the used material but also on the scaffold's architecture.^{36,37} Consequently, the compressive modulus has to be investigated for each SSC design individually.

Compared to FDM printing, the LC process circumvents drawbacks like nozzle clogging and instability of subjacent layers during the printing process, while offering comparable flexibility and reproducibility. Furthermore, FDM printing requires slurries with exact viscosities, for proper printing,^{18,21,22} which is not the case for the LC process, which therefore facilitates the production process substantially. Compared to other scaffold fabrication methods, pore interconnectivity—which can be problematic, for instance, for porogen leaching—is guaranteed, when sheets are stacked to a scaffold (SSC). In addition, the size of the SSC is not limited to smaller sizes, since there is no risk of residual solvents or porogens which could remain in larger scaffolds and hamper cell growth and viability (porogen leaching) or poor mechanical integrity (electrospinning).^{22,38}

Cell growth and differentiation on PCL/HA sheets

Besides the physical properties like pore size and porosity, TE scaffolds have to allow cells to adhere, grow, and differentiate to form functional tissue. PCL/HA is known to be a highly functional composite material for bone TE applications.^{9,39–41} However, LC is prone to generate a HAZ when thermoplastic materials are cut.³² Beside the executed cut, the material in the HAZ can alter its properties due to heat exposure and subsequent cooling.^{42,43} Consequently, we investigated the adherence and growth of hMSCs on the manufactured PCL/HA sheets and the differentiation potential of hMSCs when exposed to osteogenic differentiation factors.

The hMSC cell line SCP-1 was adhering and growing homogeneously on PCL/HA sheets, including HAZs,

while the cells maintained their typical morphology²⁷ (Figure 6). Furthermore, no differences in cell growth, adherence, or morphology were observed, when cells were cultivated on non-processed PCL/HA foil.

The testing of the differentiation potential of SCP-1 cells growing on the manufactured sheets was equally conclusive. Cells differentiated into osteoblasts within a cultivation period of 21 days in ODM, which was verified by staining calcium depositions in the extracellular matrix using ARS (Figure 7). The same results were found for SCP-1 cells growing on non-processed PCL/HA foil or cell culture dishes. Consequently, the processing via LC did not alter the properties of the material in a significant way with regard to cell growth, adherence, and cellular response to osteogenic differentiation factors. It has to be noted that calcium is a main component of HA. Thus, ARS could also stain exposed HA particles on the surface of the sheets,⁴⁴ possibly leading to false positive results. However, no staining was visible, if the sheets were fully overgrown with non-differentiated cells (Figure 7(a)).

Cell growth on stacked PCL/HA sheet scaffolds

Important properties of a functional scaffold are pore size, porosity, and the presence of an interconnecting pore network.^{1,4,5} These parameters can be controlled precisely and reproducibly using the LC process. By stacking 50 circular sheets to an SSC, cylindrical scaffolds of 10 mm diameter and 10 mm height, with theoretical pore sizes of 300 μm , an interconnecting pore network, and porosities of 60% (approximated from the CAD model according to Loh and Choong⁴⁵) can be created. It has to be considered that these porosity values can differ slightly from values obtained by, for instance, a gravimetric porosity determination.⁴⁶ However, scaffold and pore size, as well as the porosity, are variable and dependent on the initial sheet design.

The advantage of the SSC in contrast to solid scaffolds is the possibility to assemble and disassemble the scaffold. Thus, cell seeding and the investigation of cell fate after cultivation is considerably facilitated. However, single sheets can be welded together to form a solid scaffold structure, if desired.⁶ On the contrary, the need to assemble the scaffold prior to cultivation can also be considered as a drawback of the SSC approach. The stacking of single sheets is time-consuming and the risk of contamination is higher when inoculated sheets are stacked to a 3D scaffold.

Prior cultivation, single sheets were inoculated with cells separately. Thus, the cell distribution could be assessed before the single sheets were stacked to a scaffold. Consequently, a homogeneous cell distribution is easier to achieve in the SSC. In contrast, solid scaffolds require complex dynamic cell seeding procedures to avoid inhomogeneous cell distributions and low initial cell densities.^{14–16,47} To further speed up the cell seeding procedure, and to maximize seeding efficiencies on the PCL/HA

sheets, the use of cell sheets^{48,49} is recently under investigation. Cell sheets can be produced by using cell culture dishes with temperature responsive surfaces. As a result, PCL/HA sheets could be inoculated with contiguous, confluent cells with intact ECM prior assembly to an SSC.

After inoculation with SCP-1 cells and stacking to an SSC, the construct was cultivated for 5 days in an oxygen controlled perfusion bioreactor²⁸ to provide sufficient oxygen and nutrient supply. Subsequently, the SSC was disassembled and cell fate was analyzed. After a cultivation period of 5 days, the SSC was overgrown with cells and formed a coherent structure. The areas where the single sheets were in contact with each other were clearly visible in the fluorescence image of GFP-labeled cells (Figure 8). The possibility to disassemble the scaffold after cultivation is advantageous when homogeneity of, for instance, cell growth or differentiation has to be assessed. Compared to solid scaffolds, which would have to be cut prior analysis,^{47,50} a much simpler workflow is possible using SSCs.

Laser-cut sheets could not only be used for the generation of SSCs but also for the generation of synergetic TECs by adding hydrogel layers in between laser-cut sheets, to provide both mechanical stability of the solid scaffold as well as the highly biomimetic environment of the hydrogel. Over recent years, different manufacturing techniques were used to develop different scaffold/hydrogel hybrid systems.^{51–53} However, the feasibility of using laser-cut sheets for the generation of a hydrogel/scaffold hybrid system will be investigated in further studies.

Conclusion

A novel method for the generation of sheet-based scaffolds via LC has been introduced. The LC process is fast, reproducible, and highly flexible, and allows for the generation of sheets out of PCL/HA composite material in the range of 0%–50% HA. Single sheets can be stacked together to form a coherent scaffold structure with interconnecting pores. Cell adherence, growth, and osteogenic differentiation were shown to be feasible on the manufactured PCL/HA sheets. Calcium depositions were clearly present in the samples which were cultivated in ODM (Figure 6), indicating that the developed manufacturing method is suitable for the generation of functional PCL/HA scaffolds for TE applications. The use of SSCs can simplify both investigation of cell distribution after cultivation and cell seeding prior to cultivation. Also, the generation of scaffold/hydrogel hybrid systems, for instance, for vascularization approaches could be possible. Consequently, the generation of SSCs by LC offers new possibilities for TE research.

Acknowledgements

The authors would like to thank Dr. Constanze Eulenkamp, Conny Hasselberg-Christoph, Benedikt Kaufmann, and Joseph Thaler for technical assistance. Prof. Matthias Schieker is

currently an employee of the Novartis Institutes of Biomedical Research, Basel, Switzerland.

Declaration of conflicting interests

The author(s) declared no potential conflicts of interest with respect to the research, authorship, and/or publication of this article.

Funding

The author(s) disclosed receipt of the following financial support for the research, authorship, and/or publication of this article: This work was supported by the Bavarian Research Foundation (project no. AZ-1222-16) and the Bavarian State Ministry for Science and Arts (research focus "Generation and characterization of three-dimensional tissue (Herstellung und Charakterisierung dreidimensionaler Gewebe)"—CANTER") as well as by PreSens GmbH, Regensburg, Germany.

ORCID iD

Robert Huber  <https://orcid.org/0000-0003-1008-7405>

References

- Ikada Y. Challenges in tissue engineering. *J R Soc Interface* 2006; 3: 589–601.
- Loh QL and Choong C. Three-dimensional scaffolds for tissue engineering applications: role of porosity and pore size. *Tissue Eng Part B Rev* 2013; 19(6): 485–502.
- Mikos AG, Bao Y, Cima LG, et al. Preparation of poly(glycolic acid) bonded fiber structures for cell attachment and transplantation. *J Biomed Mater Res* 1993; 27(2): 183–189.
- Hutmacher DW. Scaffolds in tissue engineering bone and cartilage. *Biomater* 2000; 21: 2529–2543.
- An J, Teoh JEM, Sutmornnod R, et al. Design and 3D printing of scaffolds and tissues. *Engineering* 2015; 1: 261–268.
- He F-L, Li D-W, He J, et al. A novel layer-structured scaffold with large pore sizes suitable for 3D cell culture prepared by near-field electrospinning. *Mat Sci Eng C* 2017; 86: 18–27.
- Naughton GK, Tolbert WR and Grillot TM. Emerging developments in tissue engineering and cell technology. *Tissue Eng* 1995; 1(2): 211–219.
- Badylak SF and Gilbert TW. Immune response to biologic scaffold materials. *Semin Immunol* 2008; 20(2): 109–116.
- Chuenjitkuntaworn B, Inrung W, Damrongsri D, et al. Polycaprolactone/hydroxyapatite composite scaffolds: preparation, characterization, and in vitro and in vivo biological responses of human primary bone cells. *J Biomed Mater Res A* 2010; 94(1): 241–251.
- Do A-V, Smith R, Acri TM, et al. 3D printing technologies for 3D scaffold engineering. In: Deng Y and Kuiper J (eds) *Functional 3D tissue engineering scaffolds: materials, technologies and applications*. Amsterdam: Elsevier Ltd., 2018, pp. 203–234.
- Wutticharonmongkol P, Sachavanakit N, Pavasant P, et al. Novel bone scaffolds of electrospun polycaprolactone fibers filled with nanoparticles. *J Nanosci Nanotechnol* 2006; 6: 514–522.
- Shikinami Y and Okuno M. Bioresorbable devices made of forged composites of hydroxyapatite (HA) particles and poly-L-lactide (PLLA): part I. Basic characteristics. *Biomaterials* 1998; 20: 859–877.
- Roseti L, Parisi V, Petretta M, et al. Scaffolds for bone tissue engineering: state of the art and new perspectives. *Mater Sci Eng C Mater Biol Appl* 2017; 78: 1246–1262.
- Vunjak-Novakovic G, Obradovic B, Martin I, et al. Dynamic cell seeding of polymer scaffolds for cartilage tissue engineering. *Biotechnol Prog* 1998; 14(2): 193–202.
- Melchels FP, Barradas AM, vanBlitterswijk CA, et al. Effects of the architecture of tissue engineering scaffolds on cell seeding and culturing. *Acta Biomater* 2010; 6(11): 4208–4217.
- Alvarez-Barreto JF, Linhan SM, Shambaugh RL, et al. Flow perfusion improves seeding of tissue engineering scaffolds with different architectures. *Ann Biomed Eng* 2007; 35(3): 429–442.
- Sutmornnod R, An J, Yeong WY, et al. Hybrid membrane based structure: a novel approach for tissue engineering scaffold. In: *ICAM-BM 2014*, Beijing, China, 13 November. Beijing: ICAM-BM, 2014, pp. 41–42.
- Goncalves EM, Oliveira FJ, Silva RF, et al. Three-dimensional printed PCL-hydroxyapatite scaffolds filled with CNTs for bone cell growth stimulation. *J Biomed Mater Res B Appl Biomater* 2016; 104(6): 1210–1219.
- Zhao P, Haibing GU, Mi H, et al. Fabrication of scaffolds in tissue engineering: a review. *Front Mech Eng* 2018; 13: 107–119.
- Temple JP, Hutton DL, Hung BP, et al. Engineering anatomically shaped vascularized bone grafts with hASCs and 3D-printed scaffolds. *J Biomed Mater Res A* 2014; 102: 1–9.
- Wang X, Jiang M, Zhou Z, et al. 3D printing of polymer matrix composites: a review and prospective. *Composites Part B* 2016; 110: 442–458.
- Trachtenberg JE, Kasper FK and Mikos AG. Polymer Scaffold fabrication. In: Lanza R, Langer R and Vacanti J (eds) *Principles of tissue engineering*. 4th ed. Burlington, MA: Academic Press, 2014, pp. 423–440.
- Khorshidi Solouk A, Mirzadeh H, Mazinani S, et al. A review of key challenges of electrospun scaffolds for tissue-engineering applications. *J Tissue Eng Regen Med* 2016; 10(9): 715–738.
- Tan Q, Li S, Ren J, et al. Fabrication of porous scaffolds with a controllable microstructure and mechanical properties by porogen fusion technique. *Int J Mol Sci* 2011; 12(2): 890–904.
- Todd RH, Allen DK and Alting L. *Manufacturing processes reference guide*. South Norwalk, CT: Industrial Press Inc, 1994.
- Caristan CL. *Laser cutting guide for manufacturing*. Dearborn, MI: Society of Manufacturing Engineers, 2004.
- Bocker W, Yin Z, Drosse I, et al. Introducing a single cell-derived human mesenchymal stem cell line expressing hTERT after lentiviral gene transfer. *J Cell Mol Med* 2008; 12(4): 1347–1359.
- Schmid J, Schwarz S, Meier-Staude R, et al. A perfusion bioreactor system for cell seeding and oxygen-controlled

- cultivation of tree-dimensional cell cultures. *Tissue Eng Part C Methods* 2018; 24: 585–595.
29. Stourmaras A, Stavropoulos P, Salonitis K, et al. An investigation of quality in CO₂ laser cutting of aluminum. *CIRP J Manuf Sci Technol* 2009; 2: 61–69.
 30. D'Amora U, D'Este M, Eglin D, et al. Collagen density gradient on 3D printed poly(ϵ -caprolactone) scaffolds for interface tissue engineering. *J Tissue Eng Regen Med* 2018; 12: 321–329.
 31. Wang Y, Liu L and Guo S. Characterization of biodegradable and cytocompatible nano-hydroxyapatite/polycaprolactone porous scaffolds in degradation in vitro. *Polym Degrad Stab* 2010; 95: 207–213.
 32. Tamrin KF, Nukman Y, Choudhury LA, et al. Multiple-objective optimization in precision laser cutting of different thermoplastics. *Opt Lasers Eng* 2015; 67: 57–65.
 33. Guerra AJ, Farjas J and Ciurana J. Fibre laser cutting of polycaprolactone sheet for stents manufacturing: a feasibility study. *Opt Laser Technol* 2017; 95: 113–123.
 34. Passaglia E, Bertoldo M, Coiai S, et al. The effect of crystalline morphology on the degradation of polycaprolactone in a solution of phosphate buffer and lipase. *Polym Adv Technol* 2008; 19: 1901–1906.
 35. Baji A, Wong SC and Srivatsan TS. Processing methodologies for polycaprolactone-hydroxyapatite composites: a review. *Mater Manuf Process* 2006; 21: 211–218.
 36. Sabree I, Gough JE and Derby B. Mechanical properties of porous ceramic scaffolds: influence of internal dimensions. *Ceramics Int* 2015; 41: 8425–8432.
 37. Shor L, Güçeri S, Wen X, et al. Fabrication of three-dimensional polycaprolactone/hydroxyapatite tissue scaffolds and osteoblast-scaffold interactions in vivo. *Biomaterials* 2007; 28: 5291–5297.
 38. Murphy MB and Mikos AG. Polymer scaffold fabrication. In: Lanza R, Langer R and Vacanti J (eds) *Principles of tissue engineering*. 3rd ed. Burlington, MA: Academic Press, 2007, pp. 309–322.
 39. Huttmacher DW, Schantz T, Zein I, et al. Mechanical properties and cell cultural response of polycaprolactone scaffolds designed and fabricated via fused deposition modeling. *J Biomed Mater Res* 2001; 55(2): 203–216.
 40. Chuenjitkunataworn B, Osathanon T, Nowwarote N, et al. The efficacy of polycaprolactone/hydroxyapatite scaffold in combination with mesenchymal stem cells for bone tissue engineering. *J Biomed Mater Res Part A* 2015; 104: 264–271.
 41. D'Anto V, Raucci MG, Guarino V, et al. Behaviour of human mesenchymal stem cells on chemically synthesized HA-PCL scaffolds for hard tissue regeneration. *J Tissue Eng Regen Med* 2016; 10(2): E147–E154.
 42. Choudhury IA and Shirley S. Laser cutting of polymeric materials: An experimental investigation. *Opt Laser Technol* 2010; 42: 503–508.
 43. Davim JP, Barricas N, Conceicao M, et al. Some experimental studies on CO₂ laser cutting quality of polymeric materials. *J Mater Proc Technol* 2008; 198: 99–104.
 44. Moriguchi T, Yano K, Nakagawa S, et al. Elucidation of adsorption mechanism of bone-staining agent alizarin red S on hydroxyapatite by FT-IR microspectroscopy. *J Colloid Interface Sci* 2003; 260(1): 19–25.
 45. Loh QL and Choong C. Three-dimensional scaffolds for tissue engineering applications: role of porosity and pore size. *Tissue Eng Part B Rev* 2013; 19(6): 485–502.
 46. Lee KW, Wang S, Lu L, et al. Fabrication and characterization of poly(propylene fumarate) scaffolds with controlled pore structures using 3-dimensional printing and injection molding. *Tissue Eng* 2006; 12(10): 2801–2811.
 47. Wendt D, Marsano A, Jakob M, et al. Oscillating perfusion of cell suspensions through three-dimensional scaffolds enhances cell seeding efficiency and uniformity. *Biotechnol Bioeng* 2003; 84(2): 205–214.
 48. Yamato M and Okano T. Cell sheet engineering. *Mater Today* 2004; 7: 42–47.
 49. Valmikinathan CM, Chang W, Xu J, et al. Self-assembled temperature responsive surfaces for generation of cell patches for bone tissue engineering. *Biofabrication* 2012; 4: 035006.
 50. Thevenot P, Nair A, Dey J, et al. Method to analyze three-dimensional cell distribution and infiltration in degradable scaffolds. *Tissue Eng Part C Methods* 2008; 14(4): 319–331.
 51. Ovsianikov A, Khademhosseini A and Mironov V. The synergy of scaffold-based and scaffold-free tissue engineering strategies. *Trends Biotechnol* 2018; 36(4): 348–357.
 52. Shim JH, Kim JY, Park M, et al. Development of a hybrid scaffold with synthetic biomaterials and hydrogel using solid freeform fabrication technology. *Biofabrication* 2011; 3(3): 034102–034109.
 53. Igwe JC, Mikael PE and Nukavarapu SP. Design, fabrication and in vitro evaluation of a novel polymer-hydrogel hybrid scaffold for bone tissue engineering. *J Tissue Eng Regen Med* 2014; 8(2): 131–142.

Acknowledgment

In the first place, I would like to thank my direct supervisor Prof. Dr. Robert Huber for providing any possible support. His encouragement, guidance, and expertise enabled me to write this dissertation and to gain a foothold in the scientific world.

I would like to thank Prof. Dr. Matthias Schieker for giving me the opportunity to work in his lab, and for accepting to be the first referee of my thesis.

Sascha Schwarz for introducing me in the world of 3D printing and for providing valuable input.

Dr. Stefanie Sudhop and Prof. Dr. Hauke Clausen-Schaumann for their support in organizational matters and their input to improve the scientific papers.

Special thanks to Stefanie Bauer and my family for taking care of my physical (and mental) health, enduring my moods and supporting me in any respect.

And of course, thanks to my colleagues for making my everyday work enjoyable.